United States
Environmental Protection
Agency

Office of Air Quality
Planning and Standards
Research Triangle Park NC 27711

EPA-450/4-89-020
NOVEMBER 1989

Air

EPA

REVIEW AND EVALUATION OF AREA SOURCE DISPERSION ALGORITHMS FOR EMISSION SOURCES AT SUPERFUND SITES

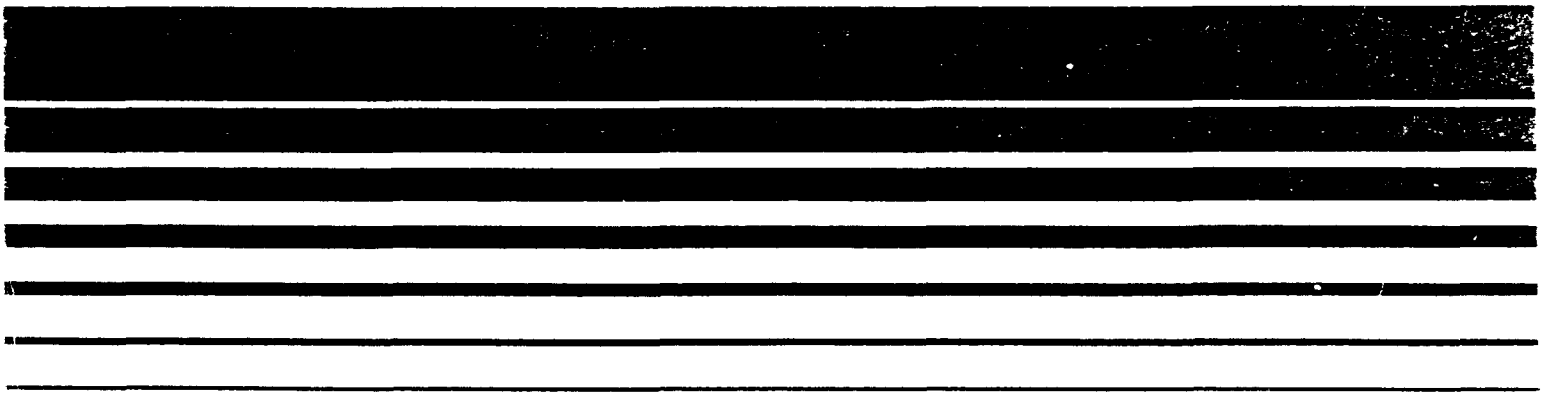

EPA-450/4-89-020

REVIEW AND EVALUATION OF AREA SOURCE DISPERSION ALGORITHMS FOR EMISSION SOURCES AT SUPERFUND SITES

By
TRC Environmental Consultants, Inc.
East Hartford, CT 06108

EPA Contract No. 68-02-4399

EPA Project Officer: Jawad S. Touma

Office Of Air Quality Planning And Standards
Office Of Air And Radiation
U. S. Environmental Protection Agency
Research Triangle Park, NC 27711

November 1989

This report has been reviewed by the Office Of Air Quality Planning And Standards, U. S. Environmental Protection Agency, and has been approved for publication as received from the contractor. Approval does not signify that the contents necessarily reflect the views and policies of the Agency, neither does mention of trade names or commercial products constitute endorsement or recommendation for use.

EPA-450/4-89-020

ACKNOWLEDGEMENTS

The authors wish to acknowledge the contributions of numerous individuals, without whose assistance this study could not have been successfully completed. The Project Officer, Mr. Jawad Touma, provided guidance and review comments throughout the course of the project, including numerous constructive suggestions regarding the draft report. Mr. Joseph Tikvart, Chief of the Source Receptor Analysis Branch, also provided a critical review of the report. A large number of investigators were contacted during the review of technical literature and recent modeling developments. Dan Reible of Louisiana State University, Jim Bowers of U.S. Army-Dugway, and Richard Schultz of Trinity Consultants were particularly helpful in providing information to aid this effort. Dr. Brian Lamb of Washington State University provided valuable information concerning the forest canopy area source experiments. The sensitivity analysis plots presented in Section 3 were produced through the diligent efforts of Ms. Maureen Hess.

TABLE OF CONTENTS

SECTION			PAGE
		ACKNOWLEDGEMENTS	ii
1.0		INTRODUCTION	1-1
	1.1	Approach	1-1
	1.2	Identify Superfund Site Area Source Characteristics	1-2
	1.2.1	Source Site and Shape Considerations	1-3
	1.2.2	Environmental Influences	1-7
	1.2.3	Human Activity	1-7
	1.2.4	Summary of Findings	1-8
2.0		REVIEW OF AREA SOURCE DISPERSION ALGORITHMS	2-1
	2.1	Introduction	2-1
	2.2	Overview of Area Source Algorithms	2-2
	2.2.1	Virtual Point Source	2-2
	2.2.2	Point Source Array	2-3
	2.2.3	Line Source Segment(s)	2-3
	2.2.4	Line Source Integration	2-4
	2.3	Existing Area Source Models	2-6
	2.3.1	Industrial Source Complex Short-Term Model	2-7
	2.3.2	Fugitive Dust Model	2-7
	2.3.3	Point, Area, Line-Source Model	2-10
	2.3.4	Gaussian-Plume, Multiple Source Air Quality Algorithm	2-10
	2.3.5	SHORTZ Model	2-12
	2.3.6	TEM/PEM	2-13
	2.3.7	ISCLT	2-13
	2.3.8	Climatological Dispersion Model	2-14
	2.3.9	LONGZ Model	2-16
	2.3.10	VALLEY Model	2-16
	2.3.11	Air Quality Dispersion Model	2-18
	2.3.12	Area Source Screening Techniques	2-18
	2.3.13	Toxic Release Models	2-19
	2.3.14	Other Existing Models	2-21
	2.4	Overview of Area Source Dispersion Literature	2-21
	2.5	Limitations of Existing Models	2-24
3.0		ANALYSIS OF MODEL PREDICTIONS FOR EXAMPLE APPLICATIONS	3-1
	3.1	Approach	3-1
	3.2	Tests of Mathematical and Physical Principles	3-3
	3.3	Predicted Concentrations for Base Case	3-8
	3.3.1	Short-Term Models	3-8
	3.3.2	Long-Term Models	3-10
	3.4	Tests of Mathematical and Physical Properties	3-11
	3.4.1	ISCST	3-11
	3.4.2	FDM	3-13
	3.4.3	PAL	3-14
	3.4.4	RAM	3-14
	3.4.5	SHORTZ	3-15
	3.4.6	ISCLT	3-17

TABLE OF CONTENTS
(CONTINUED)

SECTION			PAGE
	3.4.7	CDM	3-17
	3.4.8	VALLEY	3-18
3.5		Discussion of Results	3-19
	3.5.1	Short-Term Results	3-20
	3.5.2	Sector Average Models	3-22
4.0		COMPARISON OF MODEL PREDICTIONS WITH EXPERIMENTAL DATA	4-1
4.1		Database Description	4-1
4.2		Results	4-5
	4.2.1	Unpaired Comparisons	4-6
	4.2.2	Paired Comparisons	4-6
5.0		CONCLUSIONS AND RECOMMENDATIONS	5-1
5.1		Conclusions	5-1
		REFERENCES	R-1

LIST OF FIGURES

FIGURE		PAGE
2-1	SUBDIVISION OF A SQUARE AREA SOURCE INTO FIVE LINE SOURCE SEGMENTS NORMAL TO THE WIND DIRECTION	2-5
2-2	SUBDIVISION OF RECTANGULAR AREA SOURCE INTO LINE SEGMENTS BY PAL	2-11
2-3	ILLUSTRATION OF SECTOR INTEGRATION USED IN CDM	2-15
2-4	SCHEMATIC OF THE VIRTUAL POINT SOURCE AS PROJECTED FROM AN AREA SOURCE	2-17
3-1	AREA SOURCE AND RECEPTOR CONFIGURATION FOR BASE CASE SCENARIO	3-2
3-2(a)	ILLUSTRATION OF INFLUENCE ZONE FOR NEAR-FIELD RECEPTORS	3-5
3-2(b)	SUBDIVISION OF BASE CASE AREA SOURCE	3-6
3-2(c)	SOURCE-RECEPTOR CONFIGURATION FOR DIAGONAL WIND DIRECTION	3-7
3-3 to 3-47	GRAPHS OF CENTERLINE CONCENTRATION VS. DOWNWIND DISTANCE FOR SELECTED MODELS, METEOROLOGICAL CONDITIONS AND SOURCE CONFIGURATIONS	3-23 to 3-67
4-1	ISOPRENE FLUX EXPERIMENT SAMPLING GRID, RELEASE POINTS AND WOODLOT	4-3
4-2	RANGE OF MAXIMUM PREDICTED AND OBSERVED CONCENTRATIONS FOR TRACER RELEASE EXPERIMENTS	4-7

LIST OF TABLES

TABLE		PAGE
1-1	AREA SOURCE CHARACTERISTICS	1-4
2-1	CHARACTERIZATION OF AREA SOURCE ALGORITHMS IN EXISTING MODELS	2-8
3-1	SUMMARY OF SENSITIVITY TEST RESULTS FOR SHORT-TERM MODELS	3-21
4-1	METEOROLOGICAL AND EMISSION CHARACTERISTICS FOR TRACER RELEASE EXPERIMENTS IN A FOREST CANOPY	4-4
4-2	MAXIMUM OBSERVED AND PREDICTED NORMALIZED TRACER CONCENTRATION FOR EXPERIMENT	4-8
4-3	SUMMARY OF RELATIVE DIFFERENCES BETWEEN OBSERVED AND PREDICTED MAXIMUM VALUES	4-10

1.0 INTRODUCTION

An evaluation of dispersion modeling techniques available for estimating ambient concentrations produced by emissions from sites contaminated with toxic pollutants has been conducted. The focus of this study has been the application of area source dispersion algorithms to these emission sources. These sources can be characterized as low level releases with little buoyancy due to either momentum or temperature. Potential applications include both the estimation of short-term concentrations associated with site remediation activities and the calculation of long-term concentrations for estimating population exposures in the vicinity of a landfill, lagoon or waste disposal facility.

1.1 Approach

The study consisted of four tasks. The report has been organized to present the results of each task in sequence.

Task 1 - Identify Source Characteristics. The emission characteristics representative of superfund/landfill sources were examined to identify modeling requirements and related technical issues associated with estimating ambient concentrations near these sites. Task 1 findings are described in Section 1.2.

Task 2 - Review Available Area Source Models. Existing models and the technical literature were reviewed to identify available modeling techniques for estimating short-term and long-term concentrations due to area sources. Specific models were selected for further evaluation, based on their potential suitability for landfill/superfund applications. Task 2 findings are described in Section 2.

Task 3 - Analysis of Model Predictions for Example Applications. Five short-term area source models and three long-term (sector average) models were

applied to a number of example applications in order to compare the magnitude of concentration predictions and to test whether near-field and far-field concentration estimates were consistent with mathematical and physical principles. Task 3 results are presented in Section 3.

Task 4 - Comparison of Model Predictions with Observed Concentrations. The five short-term models were applied to estimate ambient concentrations for a series of tracer dispersion experiments involving low-level releases within an isolated grove of trees. These experiments simulate an area source release over an area of 15,000 square meters. Predicted and observed tracer concentrations were compared for thirteen one-hour experiments at sampler locations approximately 100 m downwind of the source region. Task 4 results are summarized in Section 4.

Conclusions and recommendations from this study are discussed in Section 5.

1.2 Identify Superfund Site Area Source Characteristics

Landfills and other large area sources have characteristics which have a substantial bearing on the air quality modeling method used to simulate pollutant dispersion from such sources. Many of the currently used pollutant dispersion models are based on a Gaussian formulation originally developed for point sources. Over time, the model formulations have been adapted for application to distributed sources (line sources, area sources, volume sources) but many of the original point source assumptions are retained in these models. The purpose of this discussion is to describe the types of emissions from superfund sites that may be modeled as area sources. Subsequent sections of this report will provide detailed descriptions of the current model formulations used to predict dispersion from these area sources.

Various types of toxic waste sources fall into the area source category. These include landfills, waste lagoons, evaporation and settling ponds,

agricultural fields which have been treated with chemicals, and regions where long-term exposure to toxic chemicals (due to manufacturing, mining, power generation, etc.) has contaminated the soil. For all of these sources, pollutants are emitted at or near ground level. The sizes of these sources can range from a few square meters in the case of settling ponds to a few square kilometers in the case of contaminated soils. The effect of these sources on the population also varies based on source size, strength and type. Many sources are located in areas remote from the general population. Others, by their nature, occur in centrally located areas where the potential for exposure is large. Emissions from many of these sources are a function of human activity. Addition of material, maintenance or disruption of the surface layer will have a bearing on emissions. Emissions may also be affected by environmental conditions such as wind speed, air temperature, ground surface temperature, and surface moisture.

1.2.1 Source Site and Shape Considerations

Estimating concentrations from surface area sources presents a number of challenges for the modeler. Available area source algorithms contain a variety of assumptions and offer different strengths and weaknesses. More reliable concentration estimates can be obtained by careful problem definition and by selection of the most appropriate model/algorithm. A summary of superfund site area source characteristics is included as Table 1-1. The location, geometry and relative elevation of a typical waste storage or landfill site are important factors in the dispersion characteristics of the site. Gaussian dispersion models generally assume an elevated source which injects pollutants into a moving air stream. Since many landfills are low-lying or in pits, the mechanisms by which pollutants enter the atmosphere are more complicated. The rate of entrainment of pollutants which exit the

TABLE 1-1

AREA SOURCE CHARACTERISTICS

- spatially continuous emissions (non-point)

- unique site geometry including depressions, piles, lagoons, etc.

- temporally variable source strength dependent on ambient atmospheric conditions (primarily temperature, wind speed, precipitation) and maintenance activity levels

- surface sources characterized by low wind speed at surface

- density flows may be important over surface area sources

- chemical type of emission may vary spatially across landfills

surface will be controlled by diffusion, mechanical (turbulent) flushing and suction effects. In the case of a surface source, the horizontal velocity at the surface is zero ("no slip" boundary condition) and the rate of emission of the pollutant is determined by the diffusive velocity, which is based on vapor pressure gradients and boundary layer resistance. The near surface layer is characterized by low mean wind speeds (often less than 1 m/s). The Gaussian models generally avoid extrapolating wind speeds down to the surface, however, because low wind speed values can cause unrealistically high concentration predictions. Most models specify a minimum 1.0 m/s wind speed for calculating concentrations.

Many modern landfills have substantial vertical extent (>10 m) and therefore may be modeled as elevated area or volume sources. Since the landfill is projecting into the flow, the ambient wind will ventilate the surface layer of the landfill. The actual height is physically limited by base area of the landfill and the angle of repose of the material. In practice, the maximum height may be dictated by regulation and/or constrained by the need for access by heavy machinery. In the case of a large elevated landfill, the source itself may be an obstacle to the flow and establish the flow field for some distance to the leeward side of the landfill. The modeler may account for this effect by using existing building wake or downwash algorithms. However, the elevated landfill is unlike a building because its sides are not vertical and its entire surface area (top and sides) may be emitting pollutants. The sloping sides of a landfill represent a more "aerodynamic" shape and are likely to produce less turbulence than a building with vertical walls. Since the landfill flanks are angled, the source strength per horizontal area of the flanks may be greater than that of the top. Elevated landfills may have a region of high concentration in the lee of

the landfill pile with dilution primarily due to wake eddies entraining uncontaminated air from windward of the landfill.

The estimation of emissions and dispersion is also complicated if the source is below the local land surface elevation. Situations in which trash, waste sludge, etc. are placed in a pit in the earth are common, and such situations may require emission and/or dispersion algorithms to treat a sunken source and a cavity flow problem. With existing algorithms, the sunken source may be approximated by a surface source of lesser strength. The rate of pollutant emissions to the ambient air will depend not only on the rate of emissions from the ground surface into the air within the pit, but also on the rate of exchange (ventilation) between the pit and the air above it.

In all of these scenarios, it may be useful to characterize mixing and surface conditions and use these characterizations in the calculation of source strength. Unlike the combustion effluents created by manufacturing and power production which are proportional to the production rate, the source strength of a landfill or other area source is more directly related to environmental conditions. Under conditions of limited mixing, the partial pressure gradient over the area source is reduced and volatilization of a given chemical decreases. When mixing is enhanced, partial pressure gradients are steep and the source strength increases. Snow cover may effectively cap an area source and rainfall greatly reduces emissions.

In the situation of a low lying or sub-surface source with emissions at ambient temperature (neutral thermal buoyancy) the worst case concentration scenario will be a surface-based inversion where a relatively shallow layer of dense, cold air sits on the surface of the source providing a thin mixing layer and high concentrations. It could be expected that this effect would be local because wind speed and transport are limited in most strong surface inversions. Conversely, the fact that the air in these inversions is denser

near the surface allows density flows to develop. In regions of complex terrain this effect could lead to anomalously high concentrations down the hill from a source. Air "draining" from a source of toxics and "pooling" over a low-lying area could lead to high exposures.

1.2.2 Environmental Influences

The source strength of an area source may be strongly correlated to source surface temperature. Chemical reactions and decay rates of the emitted pollutant may also depend on temperature. In the case of an area source such as a landfill, many gaseous emissions occur by evaporation. Evaporation rates are a function of the ground surface temperature. For many organic compounds, evaporation rate is strongly dependent on temperature across ambient ranges. After emission, some evaporated compounds undergo chemical reactions which are strongly temperature dependent. In general, algorithms to estimate evaporation rates and decay rates as a function of environmental conditions are not yet available.

1.2.3 Human Activity

The degree to which area source strength is coupled to the environment may depend on the surface characteristics of the source. In the case of an abandoned site, the source surface may be capped and/or vegetated which would lower source strength sensitivity to ambient temperature and wind. In the case of a cap, source strength would be largely determined by sub-surface diffusion. In an active landfill, material may be periodically "turned" causing source strength to be dependent on both the ambient environmental conditions and on landfill operation or clean-up schedules.

The source emissions from many large area sources will be spatially inhomogenous with respect to both strength and type. For example, at a

typical landfill, different types of waste (household trash, construction waste, industrial waste, etc.) will be dumped in different areas, and dumping will occur in one area while grading occurs in another. These differences are often important for estimating peak short-term concentrations, but are less important on an annual basis.

1.2.4 Summary of Findings

Air pollutant emission sources at sites contaminated with toxic pollutants are typically low-level, distributed sources, ranging in size from about 10 square meters to several square kilometers. Considerable spatial variation in emission rates across the source area is common, particularly for larger areas. Both short-term (one-hour) and long-term (annual) average concentration estimates are needed, depending upon the specific application. Typical source-receptor distances for short-term concentration estimates range from 10 m to 1000 m and may include "on-source" receptors (to estimate worker hazard) and "fenceline" receptors immediately adjacent to the contaminated area. For long-term average estimates, population exposure is most often the primary concern. Typical source-receptor distances for long-term estimates range from several hundred meters to about 10 km.

Source geometries encountered at some contaminated sites pose special challenges for air quality modeling. Elevated sources (e.g., elevated landfills), below-grade sources (e.g., excavated areas), and small heavily contaminated areas "nested" within larger source regions all represent difficult scenarios for many existing area-source models.

Source emission rates at contaminated sites often vary with environmental conditions and as a result of human activities. Many of the same factors which affect emissions will also influence dispersion behavior. It is therefore important to account for these variations when performing air quality modeling analyses.

2.0 REVIEW OF AREA SOURCE DISPERSION ALGORITHMS

2.1 Introduction

Accurate prediction of ambient concentrations resulting from pollutant emissions from area sources is a problem of considerable importance. Spatially distributed sources of pollution include landfills, settling ponds, lagoons, agricultural fields and storage piles. Residential and commercial urban areas may also be considered as area sources, although emissions actually originate from many small point sources.

The most widely used air quality models are those incorporating the Gaussian plume equation to describe the transport and dispersion of emissions from a point source. These models provide an efficient and easily understood calculation procedure for estimating concentrations. Area source algorithms based on the Gaussian plume equation are of primary interest for this study, since these algorithms can be easily incorporated into another existing model. Area source algorithms from non-Gaussian models are not transferable and are not as well suited for routine applications. Non-Gaussian area source algorithms were reviewed, however, in an effort to identify any approaches which might represent significant improvements in calculation accuracy or efficiency.

For a Gaussian model, the concentration from a point source at a receptor can be calculated readily, using a simple set of equations. If the emissions are spread uniformly over an area, however, the resulting concentration can be determined only by integrating over the source area. The area source contribution cannot be computed exactly using simple equations. Area source algorithms represent calculation procedures which have been designed to estimate the area source contribution in an efficient manner.

Pollutant dispersion models which are currently available to predict pollutant concentrations at user-specified receptor locations have been examined. One important consideration for this study is the availability of FORTRAN source code. Eleven of the models included in the UNAMAP6 package (EPA, 1986) contain area source algorithms. Additional models were identified by contacting researchers active in developing models for regulatory applications and by searching the recent technical literature.

2.2 Overview of Area Source Algorithms

Four basic techniques for estimating area source impacts were identified. Two of these approaches are primarily source-oriented, while two (upwind integration and point source array) are receptor-oriented. Different models employ variations on a given technique or a hybrid of two methods. The four basic techniques are described below.

2.2.1 Virtual Point Source

The virtual point source method as suggested by Turner (1970) to estimate area source impacts assumes that the pollutant plume downwind of an area source can be simulated as a point source. The initial source dimensions are accounted for by placing the point source upwind of the actual area source location, so that the lateral spread of the plume at the area source is comparable to the source width. The emissions for the replacement source are set equal to the area source emissions. Thus, the equations used to compute concentrations for an area source are the same as those used for a point source. One limitation inherent in this approach is that the point source plume does not accurately reproduce the crosswind concentration distribution on the source. The point source plume distribution is Gaussian, with higher concentrations in the center and lower concentrations at the edges, while the

actual emissions are uniform across the source. Another limitation of this method concerns the choice of a single source location for σ_z, which eliminates the effect of the along-wind source distribution. Concentration predictions are therefore distorted, particularly in the near-source region. Virtual point source algorithms are generally not utilized in short-term models. For long-term models, which incorporate a sector-averaged plume width, this technique is more commonly used. Examples include ISCLT, LONGZ and VALLEY.

2.2.2 Point Source Array

The receptor-oriented point source array provides a second method of estimating area source concentrations using the Gaussian plume equation for a point source. Using this approach, the model generates an array of point sources centered on the receptor. The total area of the region covered by the source array is apportioned among the point sources, so that each point is representative of its surrounding area. The emissions due to area sources are then apportioned to the point source array, based on the location of each point source and the size of the area it represents. Two of the models reviewed for this study calculate area source contributions using a point source array. CDM, a sector-average model, generates a radial source array around each receptor based on the 22.5° sectors which it employs for calculating concentrations. The Texas Episodic Model (TEM) and its derivative, PEM, generate a rectangular source array around each receptor.

2.2.3 Line Source Segment(s)

For a Gaussian model, the concentration calculation for an area source can be simplified if the source area is simulated as one or more line segments oriented normal to the wind direction. The computation effort required for a

line source with uniform emission density is roughly equivalent to that for two or three point sources. A schematic diagram is provided in Figure 2-1 illustrating the simulation of a square area using five line source segments. If the endpoints of each segment correspond to the boundaries of the source region, the simulated source will provide a reasonable representation of source geometry. The number of segments used by a model represents a choice between accuracy and efficiency. Depending upon the number of lines employed and the positioning of the lines within the source area, the collapsing of a two-dimensional area into a line may significantly distort the source-receptor geometry. This problem is most significant in the near-field and most pronounced with algorithms that use single line segments to represent an area. The majority of the short-term models reviewed for this study use the line source segment approach. Examples include ISCST, FDM, PAL, and SHORTZ.

2.2.4 Line Source Integration

The use of line source segments normal to the wind direction provides a convenient method for simulating area source contributions, but the computational effort can be substantial if each area source is subdivided into many line source segments. Certain simplifying assumptions can greatly enhance computational efficiency by accounting for the contributions of many line segments within a single calculation. Two techniques were identified which represent integration over many line segments.

Crosswind Integration. In urban regions, the emissions density generally does not change abruptly between adjacent area sources. If the emissions density is assumed to be constant in the crosswind direction, area source contributions can be calculated based only on the emissions from sources along a line directly upwind from the source. The RAM model incorporates this "narrow plume hypothesis" to compute area source contributions. This

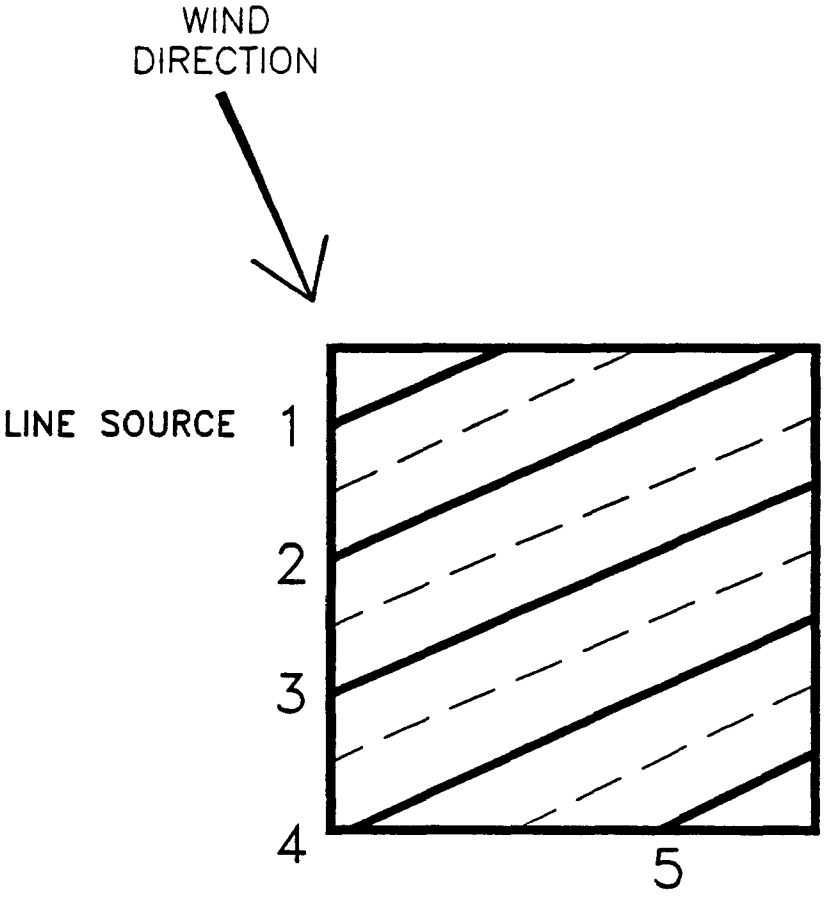

FIGURE 2-1. SUBDIVISION OF A SQUARE AREA SOURCE INTO FIVE LINE SOURCE SEGMENTS NORMAL TO THE WIND DIRECTION

technique will give accurate results only if the emissions density is relatively uniform over a crosswind distance comparable to the upwind source-receptor distance. Concentration calculations do not account accurately for source-receptor geometry for a single (isolated) area source square.

Upwind Integration. For receptors located within an area source or at near-field distances, the region upwind of a receptor is often occupied by a single area source. In this situation, the crosswind term in the Gaussian equation integrates to a constant, independent of downwind distance. For a ground-level release height, it then becomes possible to integrate over the source area in the upwind direction. This technique is only appropriate at near-field distances and only for receptors downwind of the center of the source area. Both SHORTZ and LONGZ employ upwind integration at near-field distances to calculate the vertical dispersion term in the Gaussian equation.

2.3 Existing Area Source Models

Model algorithms for area sources are contained in dispersion models designed for a wide variety of applications. The primary focus of this study is area source algorithms suitable for estimating concentrations due to routine (non-accidental) air emissions from Superfund sites and other areas contaminated with toxic materials. Models designed for regulatory applications to estimate concentrations for time periods ranging from one hour to one year over distances between 10 m and 10,000 m are most relevant. Area source algorithms in five existing short-term models designed to predict concentrations based on hourly meteorological conditions were reviewed (ISCST, FDM, PAL, RAM, SHORTZ). Six long-term (sector-average) models designed to predict concentrations based on the frequency distribution of meteorological

conditions were also reviewed (ISCLT, FDM, CDM, VALLEY, LONGZ, AQDM). A number of other models designed for air toxics or other applications were also included in the review of area source algorithms. Table 2-1 characterizes the area source algorithms in some widely used models.

2.3.1 Industrial Source Complex Short-Term Model

ISCST uses the finite line source approach to model area sources. Each square area source is modeled as a single line segment oriented normal to the wind direction. The line segment length is the diameter of a circle containing the same area as the square. For estimating lateral dispersion, the line source is located at the downwind edge of the area source. For the vertical dispersion coefficient σ_z, ISCST uses a "virtual distance" $X_v = X + X_o$, where X is the along-wind distance from the downwind edge of the area source to the receptor, and X_o is the side length of the area source square.

The ISCST algorithm predicts zero concentration for a receptor located within an area source. The ISC User's Guide recommends that receptors not be placed within a distance of one side length from any area source. If receptors are placed at closer distances, the source(s) should be subdivided.

The ISCST area source algorithm does not accurately account for source-receptor geometry. The use of a single line source segment to simulate a square area eliminates the along-wind distribution of source emissions. The length of the line segment used by ISCST is independent of wind direction, but the crosswind extent of an area source square changes with wind direction. The effect of these simplifications is greatest at near-field receptors.

2.3.2 Fugitive Dust Model

The Fugitive Dust Model (FDM) was developed to model both short-term and long-term average particulate emissions from surface mining and similar

TABLE 2-1

CHARACTERIZATION OF AREA SOURCE ALGORITHMS
IN EXISTING MODELS

Model	Area Source Algorithms
(a) Short-Term Models	
ISCST	single line segment with virtual distance for vertical dispersion
FDM	multiple line segment
PAL	multiple line segment
RAM	upwind integration (infinite line source)
SHORTZ*	line segment - near-field: upwind integration - far-field: single line segment
(b) Long-Term (Sector-Average) Models	
CDM	upwind integration (point source array)
ISCLT	virtual point source
FDM	virtual point source(s)
LONGZ*	- near-field: upwind integration - far-field: virtual point source
VALLEY	virtual point source
AQDM	virtual point source

* ground-level source height only

sources. FDM accounts for deposition losses as well as pollutant dispersion. The area source algorithm is designed for application to rectangular area sources with principal axes oriented north-south and east-west. FDM subdivides each area source into five line source segments oriented normal to the wind direction (see Figure 2-1). For short-term averages, each line source is then modeled using the CALINE line source algorithm, which has been incorporated into FDM.

CALINE is a line source model developed by the California DOT to determine the dispersion of pollutants from highways. For each line segment, FDM/CALINE predicts the concentration using the Gaussian model equations for a finite line source. Each line segment contributes based on its upwind and crosswind distance from the receptor and on σ_y and σ_z. On-source receptors are allowed, but only the line segments upwind of the receptor influence the receptor. FDM/CALINE requires a computational effort for each area source which is roughly 10 times the computational effort for one point source.

The FDM/CALINE model uses the Pasquill-Gifford dispersion coefficients, with adjustments to σ_z to account for the initial dispersion associated with vehicle-induced turbulence and the buoyancy of vehicle exhaust emissions, plus averaging-time adjustments to σ_y. Consequently, the σ_y and σ_z values used by FDM are larger than the unadjusted Pasquill-Gifford coefficients.

For long-term averages, FDM employs a sector average treatment of lateral dispersion. Each area source is again divided into five line segments normal to the wind direction. The emissions from the area source are apportioned among the five line segments in proportion to their lengths. Each segment is then modeled as a virtual point source, located at the center of the line segment. The Pasquill-Gifford σ_z coefficients are used without adjustment for long-term average calculations. For long-term averages, FDM was judged to be similar to ISCLT and was not evaluated separately.

2.3.3 Point, Area, Line-Source Model

The Point, Area, Line-Source Model (PAL) Version 2.0 is a steady-state Gaussian plume model. This model is recommended for source dimensions of tens to hundreds of meters. The area source algorithm uses multiple line sources arranged perpendicular to the wind to simulate a rectangular area source.

The program initially calculates concentrations from 9 line sources spaced equally across the source area. The Gaussian model equations for a finite line segment are used. Next, PAL computes the concentrations from 10 line segments located midway between each pair of the original nine lines and the two corners of the source area (see Figure 2-2).

PAL estimates the accuracy of the computed concentrations, based on the difference between the two concentration estimates ($C_9 - C_{10}$) divided by the average ½ ($C_9 + C_{10}$). If this relative difference exceeds a user-specified accuracy limit, PAL continues with further calculations. (The User's Guide recommends an accuracy limit of .02.) For the third iteration, 20 lines are placed midway between the 19 lines (and two corners) used previously. Iterations continue until the accuracy limit is satisfied.

PAL requires a computational effort for each area source which is at least 20 times the effort for a point source. PAL Version 2.0 uses the Pasquill-Gifford rural dispersion coefficients when the rural option is selected.

2.3.4 Gaussian-Plume, Multiple Source Air Quality Algorithm

The Gaussian-Plume Multiple Source Air Quality Algorithm (RAM) is a steady-state Gaussian plume dispersion model. RAM was developed for use in urban and rural areas with low relief.

The area source algorithm in RAM calculates concentrations for a grid of square area sources based upon contributions from sources located directly

FIGURE 2-2

Subdivision of Rectangular Area Source
Into Line Segments by PAL

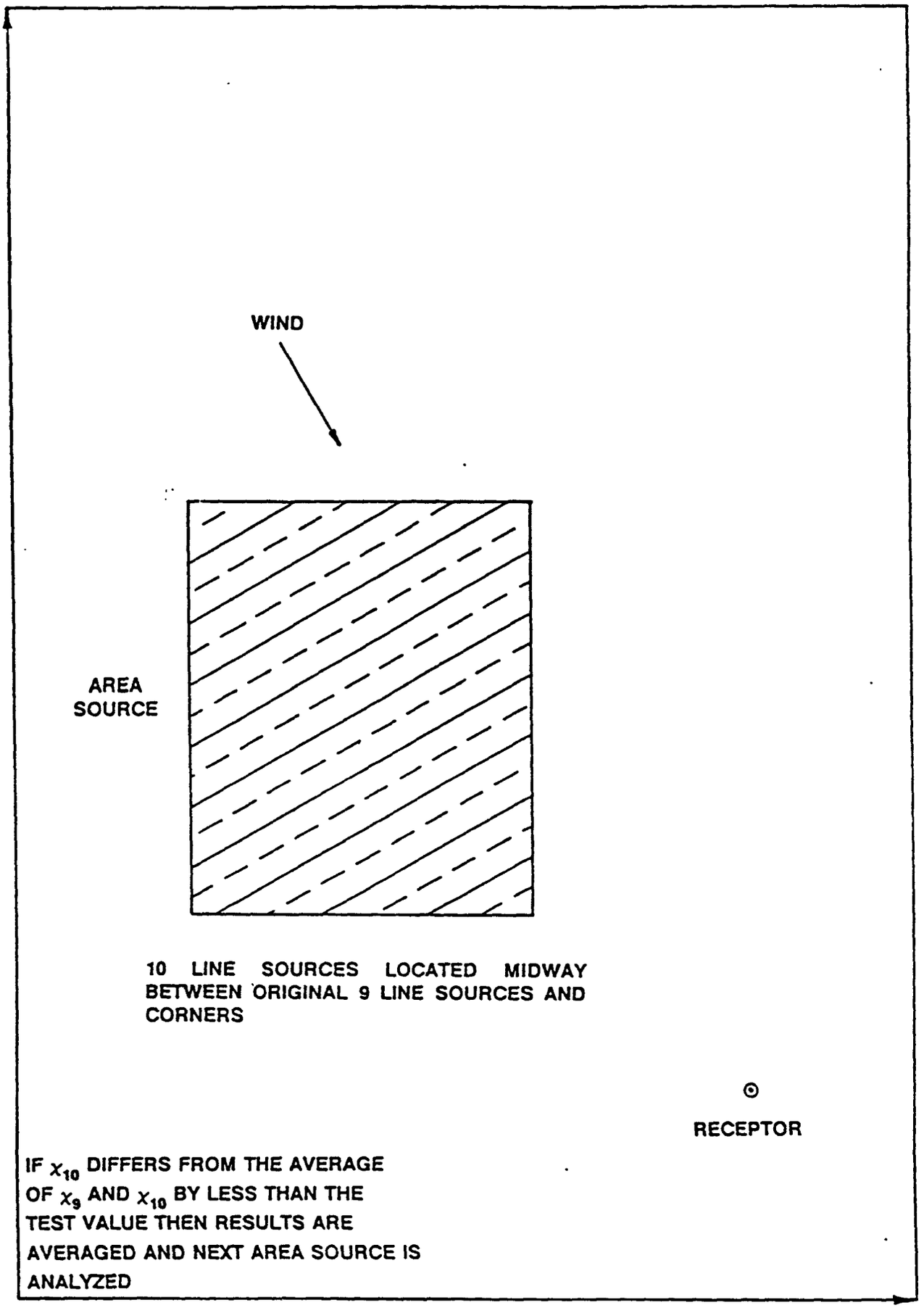

upwind of the receptor. This algorithm uses the "narrow plume simplification," which assumes that the emissions density directly upwind of the receptor is representative of emissions at all crosswind locations. This assumption allows the concentration at a receptor to be calculated using the Gaussian model equation for an infinite line source. RAM computes concentrations due to area sources along the path upwind of the receptor using a distance spacing which starts at 10 m for near-field calculations and increases in four steps to a maximum of 1,000 m at distances beyond 15 km. The narrow plume hypothesis is most suitable in situations where there is relatively little lateral variation in source strength, such as an extensive urban area. In the case of an isolated area source, this simplification is not valid, except for near-field receptors downwind of the center of the source.

2.3.5 SHORTZ Model

SHORTZ is a short-term dispersion model suitable for use in flat or complex terrain. SHORTZ calculates concentrations for ground-level area source squares utilizing a finite line source approach. Beyond a distance equal to 3 times the source width, the area source is simulated as a single line source segment oriented normal to the wind direction. The length of the segment is the crosswind projection of the source area. For near-field receptors, the vertical term is calculated as an integral from the downwind edge to the upwind edge of the source. The lateral term is calculated with the line segment located at the center of the source area. (This separation of the lateral and vertical terms in the Gaussian equation is only correct for receptors downwind of the source center.) SHORTZ accept a user-specified "source height" to produce an initial σ_z for area sources, but a ground-level release height is always assumed. The dispersion coefficients used in SHORTZ

are based on the Pasquill-Gifford dispersion curves, but they do not correspond to the Pasquill-Gifford σ_y and σ_z values used in EPA models.

2.3.6 TEM/PEM

The Pollution Episodic Model (PEM) is a Gaussian plume model which includes deposition/settling and first order chemical transformations. PEM is an urban scale model and is designed to incorporate multiple-point and area sources. It is designed to calculate short-term, ground level concentrations and deposition velocities. PEM incorporates the framework of the Texas Episodic Model (TEM) and the TEM area source treatment. PEM and TEM use a point source array to estimate area source concentrations. The emissions from area sources are apportioned among a rectangular array of points. The distance spacing of the point array is specified by the user. Area source contributions are calculated only for sources located within 8 distance increments of a receptor. This area source technique has serious limitations, and the TEM model developer does not recommend the use of this model for area sources. Based upon the initial review, neither PEM nor TEM was chosen for further evaluation in this study.

2.3.7 ISCLT

The algorithm used in ISC long-term (ISCLT) to model square area sources is a virtual point source approach. The concentration calculations in ISCLT are based on a 22.5° sector-average plume width. The distribution of concentration is smoothed between radial sectors using a smoothing function to produce a continuous distribution of concentration vs. direction. For estimating lateral dispersion, the location of the virtual point source is displaced upwind of the area source center so that the sector width at the source is equal to the diameter of a circle with the same area as the square.

For estimating vertical dispersion, the point source is located at the center of the source area.

2.3.8 Climatological Dispersion Model

The Climatological Dispersion Model (CDM) is used to model long-term average pollutant concentrations (seasonal or annual) using average emission rates and a joint frequency distribution of wind direction, wind speed and stability.

The CDM area source algorithm is designed to calculate concentrations for a grid of area source squares. CDM generates a radial array of points around each receptor based on angular and radial spacing (DINT and DELR) specified by the model user. CDM overlays the polar coordinate point array over the square area source grid and assigns emissions to each point based upon its location and the area (in the polar coordinate array) that each point represents. The process is illustrated in Figure 2-3. The point source array is then used to calculate concentrations. CDM allows a minimum angular spacing of 1.25° and a minimum radial spacing of 10 m for the point array. The radial spacing increases with distance according to the following table:

Radial Distance	Radial Spacing
≤ 2500 m	DELR
2500-5000 m	2 * DELR
>5000 m	4 * DELR

CDM computes contributions for a maximum of 100 radial increments. The size of an area source and its distance from the receptor can only be resolved in multiples of DELR. A small radial spacing provides improved spatial resolution but reduced distance range. If DELR is 25 m, the distance range is 2.5 km. Conversely, as DELR increases the spatial resolution of the point array decreases.

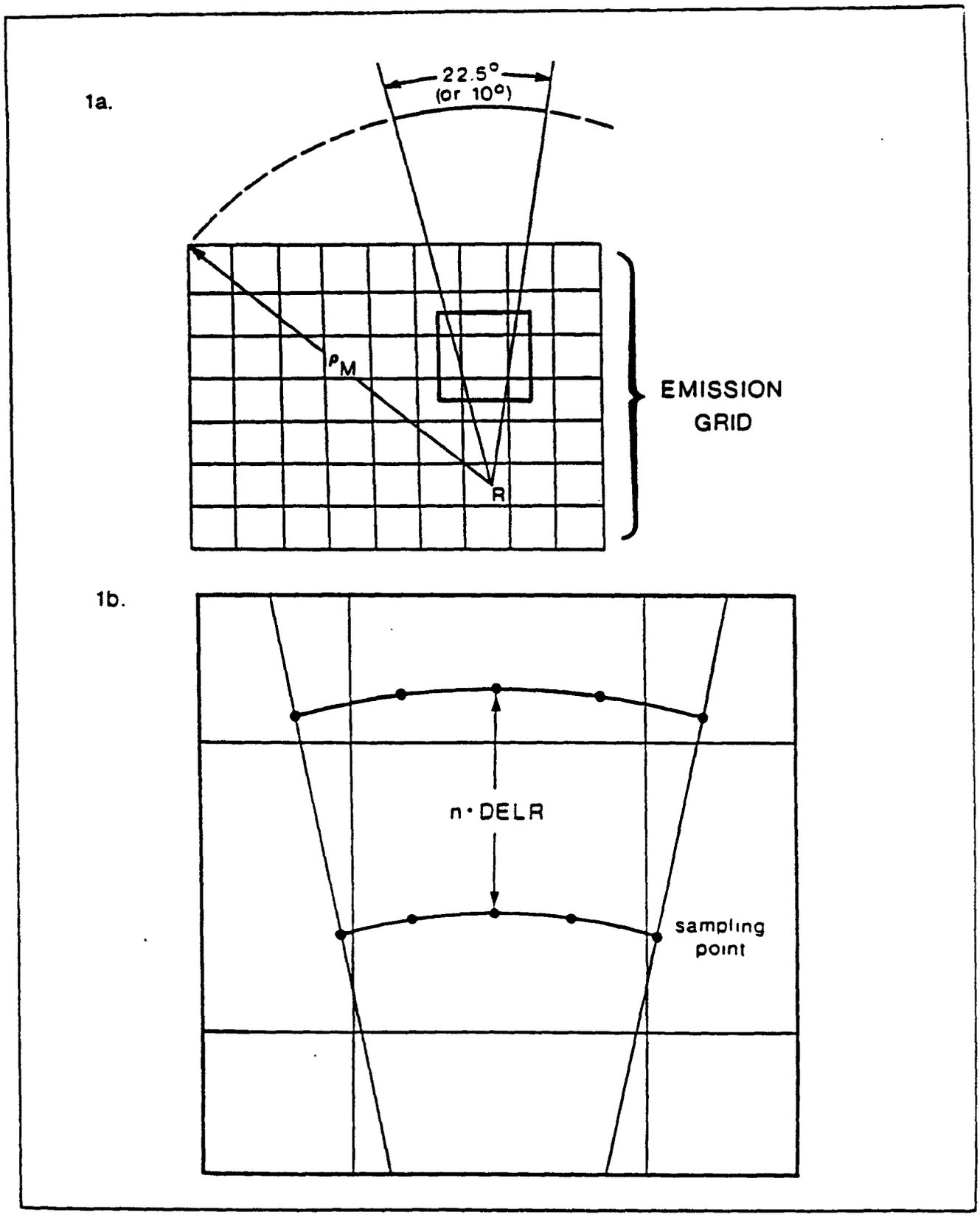

Figure 2- 3 Illustration of sector integration used in CDM. In this figure, R is receptor location, ρm is the maximum distance to the edge of the grid from the receptor, DELR is the upwind step width and n is the step number. (reproduced from Irwin et al., 1985)

2.3.9 LONGZ Model

The LONGZ model is the long-term average version of SHORTZ. The area source algorithm in LONGZ is designed for application to square, ground-level area sources. A virtual point source approach is used for distances beyond 3 source widths. The source location is displaced upwind for simulating lateral dispersion in a manner identical to ISCLT. For vertical dispersion, the point source is located at the area source center.

For near-field concentration estimates, LONGZ calculates vertical dispersion based on the integral of the vertical term in the Gaussian equation between the downwind edge and the upwind edge of the source area. The procedure for lateral dispersion is not affected. Aside from differences related to dispersion coefficients, LONGZ closely resembles ISCLT. Consequently, LONGZ was not evaluated separately in this study.

2.3.10 VALLEY Model

The VALLEY model was developed primarily to simulate dispersion from point sources in the deep valleys typical of mountainous terrain. The model employs a sector-average treatment of lateral dispersion to simulate worst-case dispersion conditions. The area source algorithm used in this model incorporates the virtual point source approach for a square area source. For vertical dispersion, the area source is modeled as if the emissions were due to a point source located at the center of the source area.

For lateral dispersion, VALLEY treats three types of source-receptor relationships: (1) far-field, where the entire source area contributes to a given receptor; (2) near-field, where only a portion of the source area affects a given receptor; and (3) the receptor is inside the source area. The first two cases are illustrated in Figure 2-4.

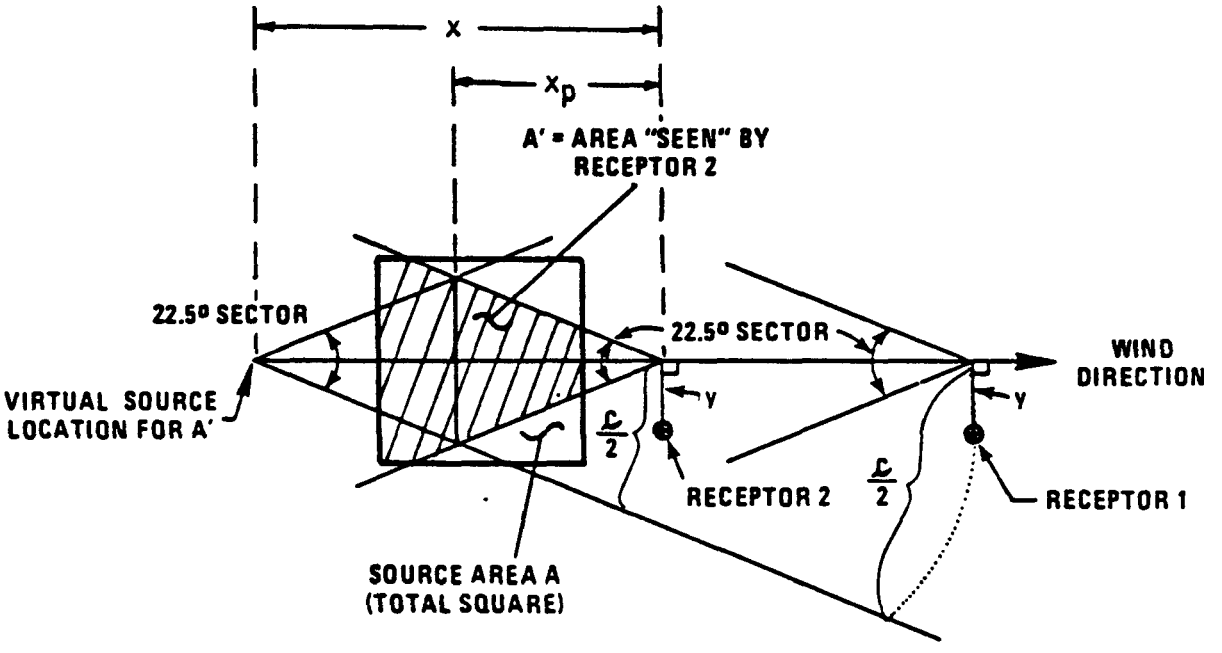

Figure 2-4 Schematic of the virtual point source as projected from an area source. (reproduced from Burt, 1977)

In the first case, Receptor 1 is sufficiently distant from the source that the entire area is encompassed by a 22.5° wedge directed from the receptor toward the source. In the far-field case, the virtual point source is displaced upwind of the source center by a distance such that the 22.5° sector width at the area source center matches the width of the area source.

In the second case, Receptor 2 is close enough to the source that a 22.5° wedge directed from the receptor toward the source does not encompass the entire source. In this case, the source emissions are reduced based on the portion of the square outside of the 22.5° sector. The upwind displacement of the virtual point source in this case is based on the area source width, reduced to account for the area outside of the sector.

In the third case, a receptor is within the boundaries of the area source and is only affected by the upwind portion of the source area. The same procedures used for case 2 are applied for this situation.

2.3.11 Air Quality Dispersion Model

The Air Quality Dispersion Model (AQDM) was designed primarily for estimating long-term averages of SO_2 and particulates in urban areas. AQDM uses a virtual point source approach to modeling area sources. The area source treatment in AQDM closely resembles that in ISCLT. AQDM was not evaluated separately.

2.3.12 Area Source Screening Techniques

A basic technique to estimate short-term pollutant concentrations due to area sources is given in the EPA document "A Workbook of Screening Techniques for Assessing Impacts of Toxic Air Pollutants" (McNaughton and Bodner, 1988) which is based on the work of Turner (1970). This approach uses the virtual point source method. Area source width is used to calculate an approximate σ_y

at the area source using properties of the Gaussian distribution. A set of curves is provided which relates σ_y to downwind distance for each Pasquill-Gifford stability class. The distance thus obtained is termed the virtual distance (x_v). The virtual distance is then added to the actual distance between the receptor and the area source. This combined distance is then used to obtain σ_y and σ_z to be used in the calculation of concentration. The concentration is calculated in a straightforward manner using emission rate, wind speed, the plume dispersion parameters and source height. The formulation avoids integration (or the numerical equivalent) making it a "calculator friendly" method.

Another screening method for estimating concentrations of pollutants from an area source is given by New York DEC, Division of Air Resources. In this treatment, an average per area emission rate and coefficient based on area size are used to calculate concentrations within the area source. A table of concentration reduction factors versus distance is presented. As a first approximation, this technique is valid for areas with sides greater than 350 feet in length and for distances closer than 3S of the source, where S is the source side length.

These techniques are intended to provide preliminary, worst-case concentration estimates to help the modeler decide whether more detailed analysis is necessary. Screening techniques are not designed to account accurately for source-receptor geometry and were not evaluated in this study.

2.3.13 Toxic Release Models

Chemical spill or accident models are of interest primarily because of the chemical libraries included in the codes and the provisions for treating evaporation, heavier-than-air gases, or other specialized problems. The spill models generally contain area source algorithms because when a liquid is

released, it forms a pool which evaporates and acts as an area source. Many of these models have relatively sophisticated algorithms to deal with chemical considerations, but most use very simple area source algorithms.

The simplest (very conservative) approach to calculating dispersion from an area source is to use the area of a pool to calculate total evaporation from the pool and then to associate the amount evaporated with a point source at the center of the pool. This approach obviously is not adequate in the near-field in the case of extensive pools. The Areal Locations of Hazardous Atmospheres Model (ALOHA) is a spill model developed by NOAA which provides graphical output of dispersion plumes due to chemical spills. ALOHA uses this point approximation of the pool source as described.

The model entitled "A Portable Computing System for Use in Toxic Gas Emergencies by the Ontario Ministry of the Environment" (known as the OME Toxic Release Model) has an extensive chemical library but also treats the pool of spilled chemicals as a point source.

The Air Force Toxic Chemical Dispersion Model (AFTOX) is a Gaussian puff/plume dispersion model which was developed to model emissions from chemical spills. AFTOX is a coupled emissions/dispersion model and uses an inventory of chemicals and corresponding chemical properties to model dispersion from instantaneous or continuous leaks or spills of any chemical in the inventory. The emission algorithm predicts whether a given spilling chemical will be in gaseous or liquid form based on an ambient temperature input. The area of the source is then calculated if the chemical is in liquid form, based on the spill rate. A source strength is then calculated based on an evaporation algorithm. The dispersion algorithm itself is non-reactive and no decay or deposition occurs. It is a Gaussian plume model under steady state, non-stable conditions and it is a Gaussian puff model otherwise. AFTOX uses a standard virtual point source algorithm to simulate an area source.

The Shell Development Company Evaporation/Air Dispersion Model for Chemical Spills on Land (SPILLS) is another model to simulate the properties of an accidental chemical release. This model also uses the virtual point source method to model area sources. An initial σ_y is assumed based on area source width and characteristics of the Gaussian distribution, a virtual distance is then calculated.

None of these models contains an area source algorithm which warrants evaluation for the present study.

2.3.14 Other Existing Models

A number of other existing models were identified which contain algorithms for treating distributed (area and volume) emission sources. These models either were designed for applications distinctly different from the air quality issues pertaining to Superfund/contaminated sites, or contain area source algorithms which were judged to be redundant with algorithms from models already chosen for evaluation. Listed below are three other models which were reviewed:

- Mesopuff - Designed for modeling long-range transport. Not appropriate for the time and distance scales of interest.
- Photochemical Box Model - Designed for modeling reactive photochemical pollutants. Employs a gridded box model equivalent to volume source. Not appropriate for near-ground emission sources or near-field concentration estimates.
- APRAC1A - Designed for modeling gridded traffic emissions based on line-source algorithm. Not appropriate for a single, isolated area source.

2.4 Overview of Area Source Dispersion Literature

A search of recent technical literature identified few published articles representing unique methods for estimating concentrations downwind of area

sources. Two published articles were identified which discussed alternative approaches to modeling area sources. Neither approach represents a computer algorithm suitable for evaluation in the present study.

The models suggested by Hwang (1987) and Chitgopekar et al. (1988) attempt to resolve some of the known shortcomings of the currently utilized area source dispersion algorithms. The discussion by Hwang is theoretical but examines both a Gaussian approach and one based on transport equations in the atmospheric boundary layer. Chitgopekar et al. (1988) attempts to resolve problems of near-field prediction through the use of a "top-hat" formulation.

Chitgopekar et al. (1988) presents an area source model developed in response to problems with virtual point models in the near-field for area sources. These authors state that "the most rigorous" treatment of Gaussian dispersion from area sources would be to model them as a dense matrix of multiple point sources. This idea can be conceptualized as increasing matrix density until, in the limit, inter-point spacing goes to zero and every point in the area is emitting. This approach is computationally intensive and is rarely used in the standard models. (The finite line segment approach in FDM or PAL is mathematically equivalent but far more efficient, if Gaussian dispersion is assumed.) Virtual point source methods do not require extensive computations and can be simplified to allow manual calculation. However, the virtual point source method should not be used if the source width is greater than 40% of the distance between the source centerpoint and the receptor (Hwang, 1986 as cited in Chitgopekar et al., 1988). This is a serious limitation due to the fact that the region of interest in many area source pollutant dispersion and exposure situations is in the near-field.

The treatment by Chitgopekar et al. is to divide the dispersion of the plume into high frequency and low frequency components. A low pass filter is used so plume meander is included but small turbulent scales are not. The

model uses a multiple line source approach. By eliminating high frequency fluctuations, the distribution immediately downwind of the area source approximates a top hat, with a region of uniform concentration in the across wind direction, downwind of the source. This treatment is equivalent to modeling the near-field region downwind of the source as if the source length was infinite. Edge effects are eliminated by filtering of the smaller (high frequency) fluctuations. These authors have developed this model so that it can be used with Pasquill-Gifford stability classes to indicate plume meander or more sophisticated boundary layer parameters obtained through eddy diffusion (diffusion analogues or similarity) equations. The authors believe that the "top hat" distribution of concentration in the near-field is more realistic that the Gaussian plume shape predicted by the virtual point source method.

Hwang (1987) gives a method for estimating on-site concentrations at toxic waste disposal sites. Gaussian dispersion models using the virtual point method perform poorly in this type of near-field application. Hwang states that when using a virtual point approximation for an area source of pollutants, the receptor should be at least the distance from source center to the property line or 100 m whichever is greater, downwind of the source center.

Hwang suggests two models for near-field (on-site) dispersion modeling. The first is a mathematical formulation of the multiple point source idea. By treating the area as being composed of differential point sources, the concentration contributions to an on-site receptor from each differential source area can be summed. This approach utilizes the standard point source Gaussian concentration equations.

The second method utilizes a partial differential equation describing atmospheric dispersion. This formulation utilizes wind speed and transfer coefficients to yield concentration. The transfer coefficients are

parameterized using the standard deviations of pollutant spreading. The equation can then be solved with the appropriate boundary conditions.

Hwang compares the results of these formulations with results obtained using a simple box method. The two formulations given in this paper agree quite closely. The box model yields values of concentration greater by a factor of two than either of the methods proposed by Hwang.

Hwang and Chitgopekar have demonstrated the advantages of alternative area source methods compared to either the virtual point source approach or a box model. Neither author, however, discussed the finite line segment approach which is widely used in short-term models. The proposed methods appear to offer few advantages when compared to the multiple line segment approach of FDM or PAL.

2.5 Limitations of Existing Models

Gaussian dispersion models have inherent limitations which are accepted for reasons of convenience and simplicity. The errors induced by simplifying Gaussian assumptions may be compounded by the treatment of area sources. General problems with many Gaussian plume models are:

1) The effects of atmospheric turbulence are not well represented by a Gaussian plume distribution. To represent dispersion of pollutants by atmospheric turbulence by a Gaussian distribution introduces error.

2) Characterization of the mixing layer as a closed surface layer may introduce error. Escape of pollutants at the top of the mixing layer and settling/deposition at the surface should both be loss terms in a correct formulation. Some of the models include simplified treatments of settling/deposition.

3) Many of the dispersion models have optional decay formulations which allow a constant chemical half-life to be entered. Many VOCs have chemical reaction rates which vary substantially as a function of solar radiation, ambient temperature, humidity, and the presence of other chemical pollutants.

4) Most of the dispersion models do not treat low wind speed scenarios adequately. Zero wind speed values cause computational

failure and very small values may cause unrealistically high concentration predictions. This problem is typically avoided by arbitrarily setting all wind speeds less than 1 m/s to be equal to 1 m/s.

The limitations noted above and uncertainties relating to emissions estimates as described in Section 1.2 contribute to a number of specific problems which might be anticipated based on the source characteristics of contaminated sites and similar area sources.

1) Since many area sources are true surface sources, low wind velocities will occur frequently at the source (from a computational standpoint, a "no-slip" or zero velocity boundary condition may force velocity to be zero at the surface).

2) Diffusion may be the dominant process in the initial stages of chemical releases from many surface area sources. A more sophisticated treatment of this process may be needed.

3) Emissions from many area sources may be dominated by VOCs which are chemically reactive and have half-lives which are strongly dependent on environmental conditions.

The dispersion models discussed here do not contain emission models. In the case of manufacturing processes, it may be reasonable to model with constant emissions. For the types of pollutant sources discussed here, steady-state emissions will not be a reasonable assumption. Ambient temperature, wind speed, moisture, and site geometry are important factors in determining source strength in many of these situations.

3.0 ANALYSIS OF MODEL PREDICTIONS FOR EXAMPLE APPLICATIONS

The analysis of model predictions for a set of hypothetical area source test cases is designed to accomplish two objectives:

- to characterize the range of concentration predictions expected from each model, and the differences between models, as a function of input meteorology, source characteristics, and receptor locations.
- to examine whether model predictions are consistent with a number of basic mathematical and physical principles.

3.1 Approach

To achieve these goals, each model was applied to a standard set of prediction scenarios which represented variations on a "base case" source/receptor configuration. The "base case" source and near-field receptors are illustrated in Figure 3-1. A single square area source with dimensions 150 m x 150 m was chosen. The wind direction is parallel to one side of the source. Six receptors were replaced at selected distances downwind of the area source center ("centerline" receptors). The receptor distances are 100 m, 125 m, 175 m, 325 m, 875 m, and 1575 m downwind of the area source center. (The first four centerline receptors, numbered R1-R4, are shown in Figure 3-1.) A second group of receptors was placed downwind of the source edge. These "edge" receptors are numbered R7-R10. In addition, model predictions were obtained at two "on-source" receptors, R11 and R12, as shown. Flat terrain was assumed.

Concentration predictions were obtained from each model for these 12 receptors, using an emission rate of 1,000 g/s. Three different stability conditions (Class B, D, and F) were modeled, with a constant wind speed value of 2 m/s and mixing height of 5000 m. For Class D stability, both a ground

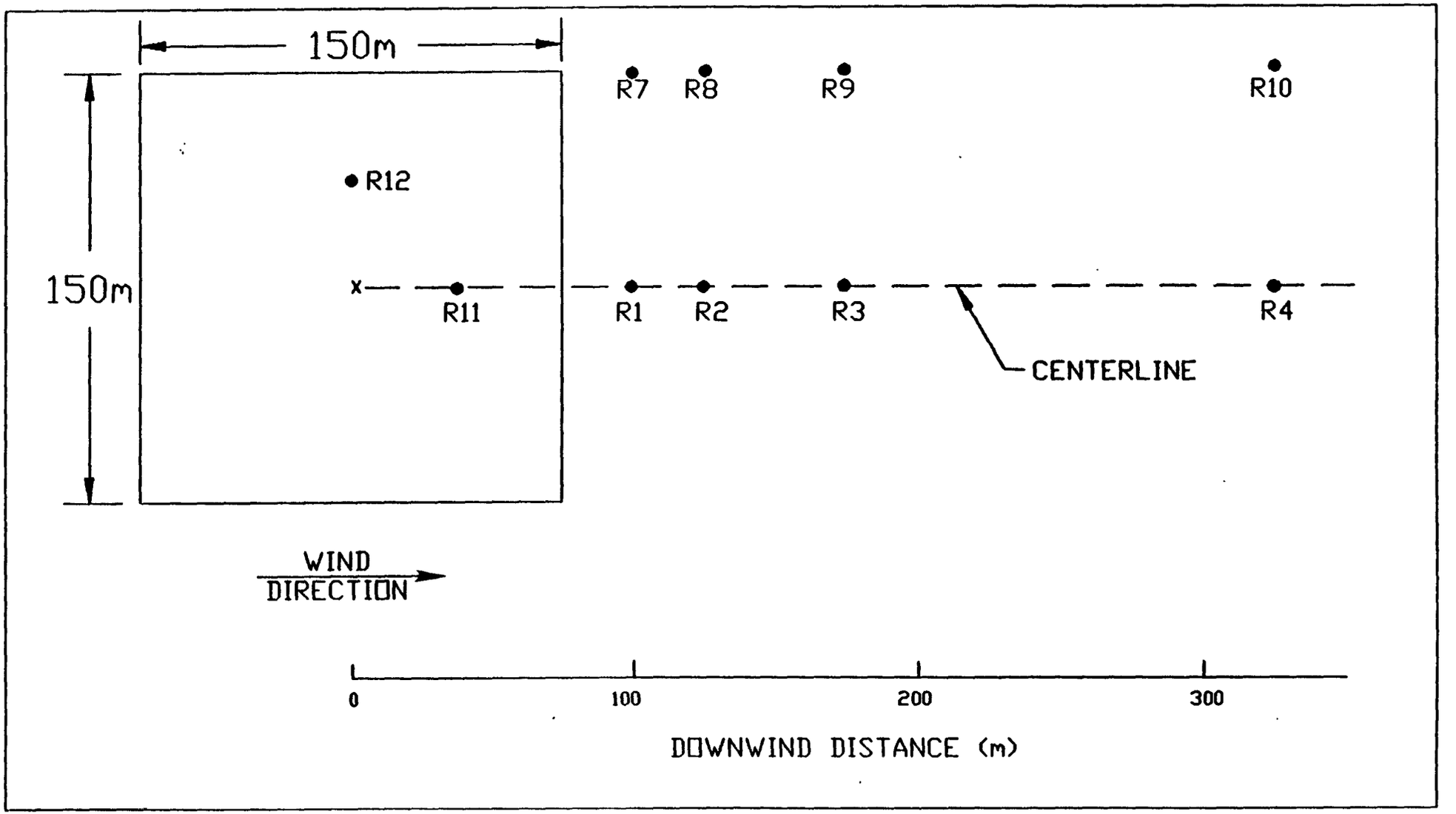

Figure 3-1. Area Source and Receptor Configuration for Base Case Scenario

level source and a 10 m source height were modeled. For Class B and Class F, only the ground level source was modeled. Rural Pasquill-Gifford (P-G) dispersion coefficients were selected for each model.

3.2 Tests of Mathematical and Physical Principles

A series of test cases representing variations on the "base case" source geometry were devised to examine whether concentration predictions from each model behave in a manner consistent with mathematical and physical principles. These tests are designed primarily to examine concentration predictions for low-level emission sources (height 10 m or less) and for area sources ranging from 50 x 50 m to 500 x 500 m. The primary focus is D stability, which represents the most common (but not the worst-case) stability condition. The following tests were applied:

Stability Comparison. For a ground level source, predicted centerline concentrations should increase with atmospheric stability (Class B = lowest, Class F = highest). The influence of stability class should be more pronounced at larger distances, since horizontal dispersion near the source is dominated by initial source dimensions.

Center Versus Edge (Near-Field). Immediately downwind of the source, predicted concentrations at edge receptors should be roughly one-half of the concentrations at corresponding centerline receptors when the wind direction is parallel to the source side. For a Gaussian model, the sources which produce significant predicted impact at a given receptor are those located upwind of the source. As the crosswind distance between source and receptor increases, the relative impact decreases according to the Gaussian equation. A source at a crosswind distance of 3.03 σ_y produces one percent of the impact of an identical source located directly upwind of the receptor. The source region which lies within ± 3 σ_y upwind of a receptor will therefore dominate

the predicted impact. At near-field distances, the "zone of influence" within ±3 σ_y upwind of the centerline receptor is entirely filled by the area source, as shown in Figure 3-2(a), while the corresponding zone upwind of the edge receptor is half empty. The empty and filled portions of the influence zone for the edge receptor are mirror images. The predicted concentration should therefore be one-half of the concentration predicted when the entire zone is filled.

Subdivision. The base case scenario is divided into four equal parts with the same total emissions, as shown in Figure 3-2(b). No significant change in predicted concentrations should result, since the overall configuration of source(s) and receptors is identical.

Far-Field Convergence. At downwind distances which are large relative to source dimensions, predicted concentrations should depend on total emissions but not on source size. (At downwind distances where σ_y is as large as the area source width, the plume from an area source will be equivalent to the plume from a point source with the same emission rate.) Centerline concentrations at distances out to 8 km were compared for three area sources with identical emissions: 150 m x 150 m (base case), 75 m x 75 m, and 450 m x 450 m. At 8 km, σ_y for D stability is roughly 450 m, so model predictions should be similar for all three sources.

Source Orientation. The orientation of the wind direction relative to the area source will influence predicted concentrations near the source. Predictions for the base case were compared to predictions for the configuration shown in Figure 3-2(c), with the wind direction at a 45° angle to the source axes. Centerline receptors were placed at the same distances downwind of the source's center. Two results are expected:

1. Predicted centerline concentrations near the source should be higher for the "diagonal" configuration, because a larger source area falls within the "zone of influence".

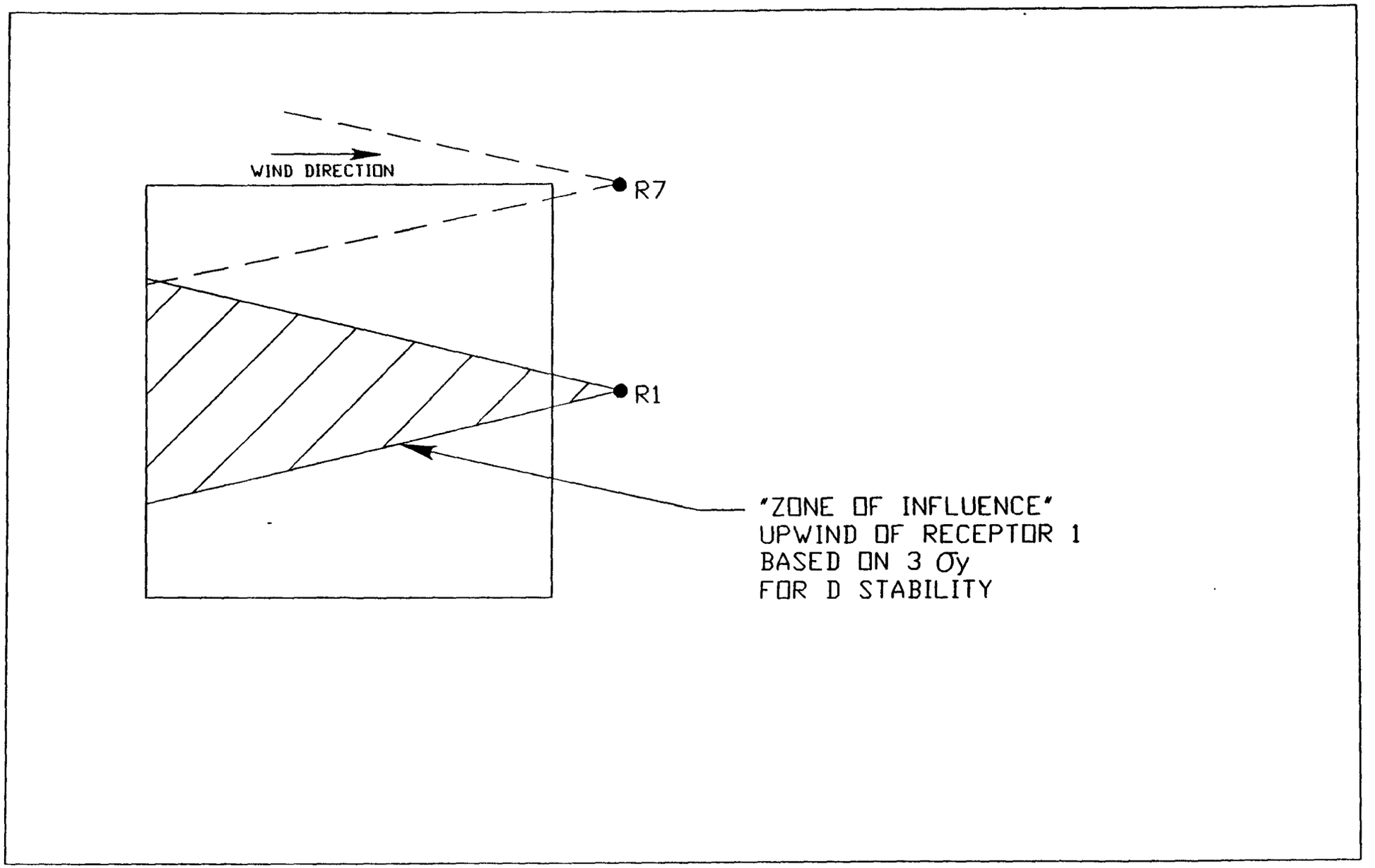

Figure 3-2 (a). Illustration of Influence Zone for Near-Field Receptors

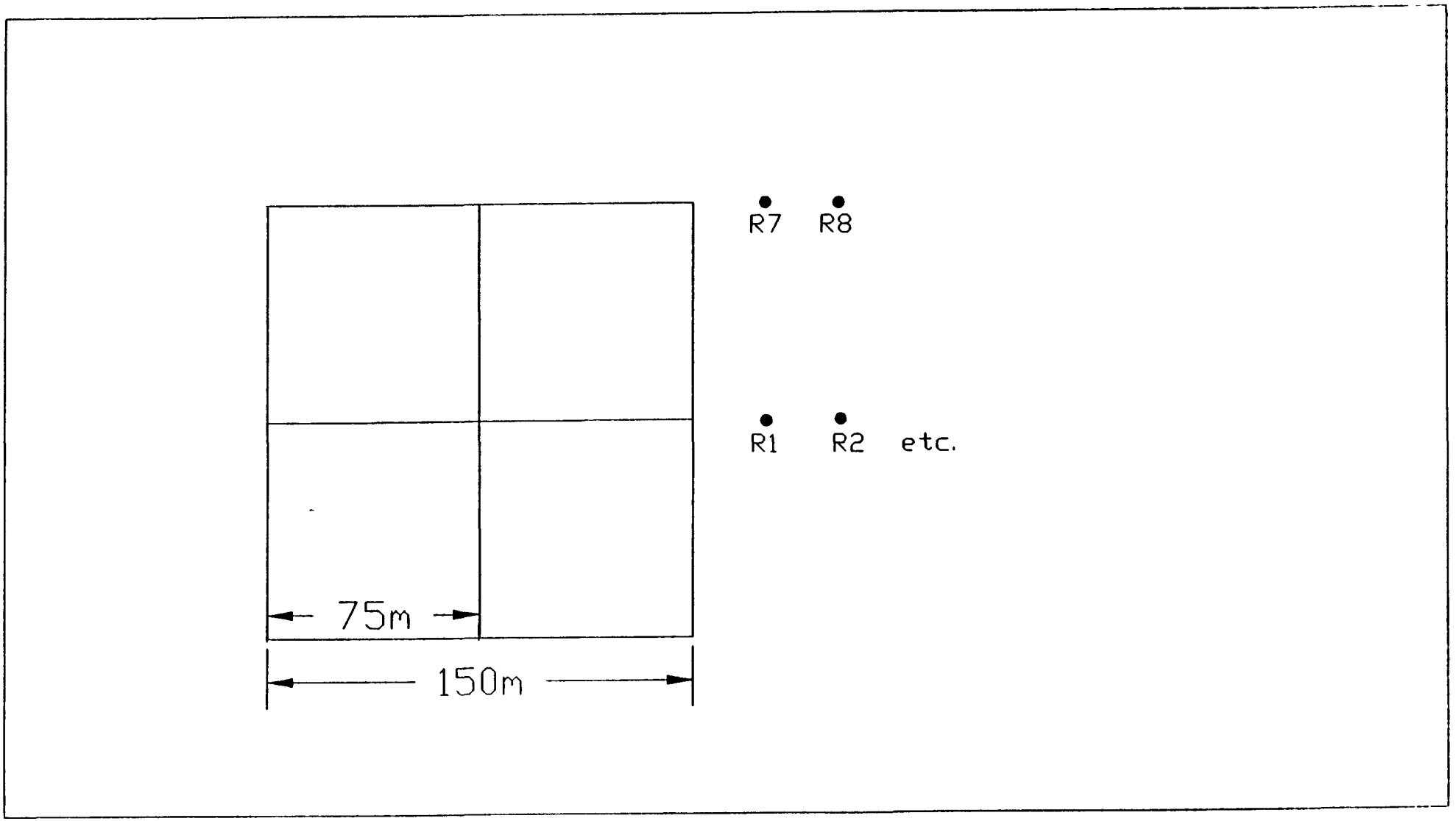

Figure 3-2 (b). Subdivision of Base Case Area Source

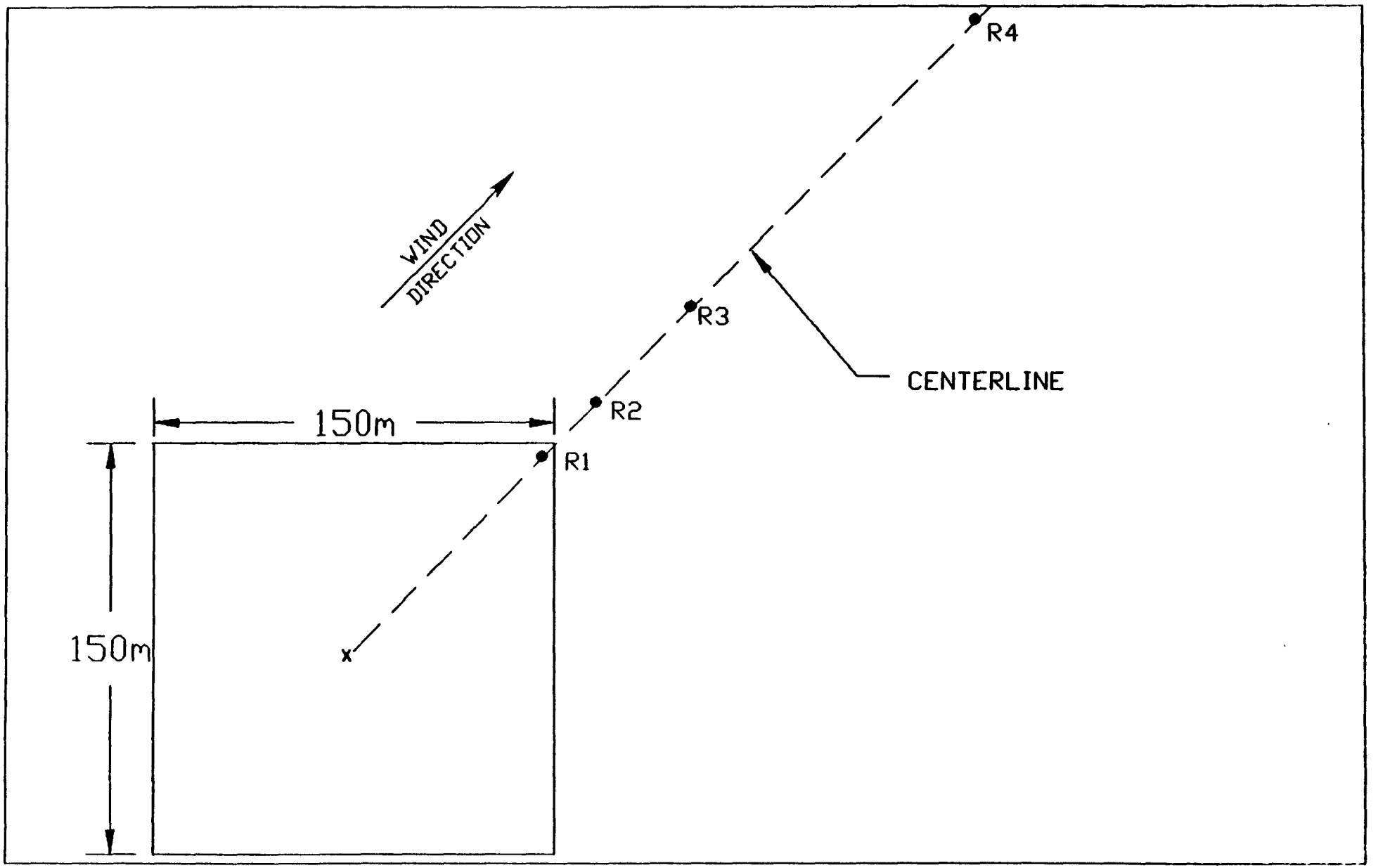

Figure 3-2 (c). Source-Receptor Configuration for Diagonal Wind Direction

2. Farther from the source, the two configurations should produce similar concentrations. (See the discussion of "far-field convergence".)

Source Height. The use of non-zero source height should produce lower predicted concentrations in the near-source region. Differences should decrease as downwind distance increases. Predictions for a 150 m x 150 m source with 10 m height were compared against the base case. At 875 m downwind distance, σ_z for D stability is roughly 28 m, and centerline concentrations predicted for a 10 m source height should be about 94 percent of predictions for a ground-level source.

All of these tests are well-suited for testing short-term (hourly) models. Some of the tests are more difficult to interpret for long-term models, which are designed to predict sector-average concentration values based on wind direction frequency. The center/edge comparison and the source orientation test were only applied to the short-term models.

3.3 Predicted Concentrations for Base Case

3.3.1 Short-Term Models

Predicted concentrations for the base case source-receptor configuration were obtained for three stability conditions (Class D, Class B, and Class F) at a constant wind speed of 2 m/s. The centerline concentrations predicted by the five short-term area source models are illustrated in Figures 3-3, 3-4, and 3-5. In these figures, the downwind distance is measured from the center of the area source. For all three stability conditions, a similar pattern is evident. FDM consistently predicts the lowest concentration values at all distances. SHORTZ generally predicts the highest concentrations within 150 m of the source, while RAM predicts the highest concentrations beyond 500 m. PAL and ISCST predict intermediate values at all distances.

At small downwind distances, the concentrations predicted by RAM are lower than those predicted by PAL and SHORTZ. (The closest distance, 37.5 m, represents receptor R11, located within the area source. See Figure 3-1. The ISCST model will not predict concentrations inside of an area source.) The gap between predictions by RAM and the other four models increases with downwind distance for all three stability conditions.

At a distance of 100 m, centerline concentration predictions for D stability (Figure 3-3) range from a low value of 2.6×10^5 $\mu g/m^3$ predicted by FDM to a maximum value of 7.5×10^5 $\mu g/m^3$ predicted by SHORTZ. At 1575 m downwind, centerline predictions range from 1.3×10^4 $\mu g/m^3$ (FDM) to 6.2×10^4 $\mu g/m^3$ (RAM). Near the source, at distances between 100 m and 175 m, PAL and SHORTZ give nearly identical centerline predictions. As distance increases, SHORTZ predictions decrease faster than PAL's. The ISCST prediction at 100 m is roughly a factor of 2 lower than PAL or SHORTZ, but ISCST and PAL predictions converge as distance increases.

For B stability (Figure 3-4), SHORTZ predicts the highest centerline concentration at 37.5 m (on the source). At distances beyond 200 m, RAM predictions are the highest and FDM predictions are lowest. Predictions by PAL and SHORTZ are very similar at all distances for B stability. Predictions by ISCST are lower in the near-field but converge with PAL and SHORTZ at 375 m. At 1575 m, the RAM concentration is a factor of 4 higher than all other models.

For F stability (Figure 3-5), SHORTZ predicts the highest centerline concentrations at 38 m and 100 m. FDM predicts the lowest concentrations at all distances. SHORTZ predictions span the largest range for F stability, since SHORTZ predicts the highest concentration at 37.5 m and matches FDM for the lowest concentration at 1575 m. PAL predictions agree with SHORTZ near

the source, while ISCST predictions are lower by about a factor of 2. At greater distances, however, PAL, RAM and ISCST predict similar values.

These base case results illustrate the effects of differences between area source algorithms and in the models' treatment of dispersion. The RAM "narrow plume simplification" apparently causes RAM predictions to diverge from the other models at large distances for B and D stability. SHORTZ and PAL generally produce similar near-field predictions, which indicates that their area source algorithms are similar (from an operational perspective). ISCST and PAL generally agree at 875 m and 1575 m, but disagree closer to the source, indicating differences in the area source algorithms, but similar dispersion treatment. FDM's treatment of both the area source (near-field) and dispersion coefficients is unique among this group of models.

The magnitude of centerline concentrations predicted by the short-term models changes significantly with source height. Predicted concentrations for a 10 m source height for D stability are illustrated in Figure 3-6. The near-field concentrations predicted by RAM and PAL decrease by more than a factor of 10 when the source height changes from zero (Figure 3-3) to 10 m (Figure 3-6). The maximum predicted concentration in Figure 3-6 is 1.9 x 10^5 $\mu g/m^3$, for SHORTZ, versus 1.8 x 10^6 $\mu g/m^3$ for SHORTZ in Figure 3-3. The relative rank of predictions by different models changes with source height at distances out to 175 m. For example, FDM predicts higher concentrations than PAL or RAM for the 10 m source height.

3.3.2 Long-Term Models

The concentrations predicted by the three long-term (sector average) models for the base case are illustrated in Figures 3-7 through 3-10. For a ground-level 150 x 150 m source and D stability (Figure 3-7) ISCLT predicts the highest centerline concentrations near the source, and CDM predicts the

highest values beyond 200 m. VALLEY predicts the lowest near-field concentrations. Beyond 500 m, ISCLT and VALLEY predict similar values.

For B stability (Figure 3-8), CDM predicts the highest near-field concentrations. Beyond 500 m, CDM and VALLEY predict similar values. ISCLT predicts higher near-field values than VALLEY, but predicts the lowest concentrations beyond 300 m.

For F stability (Figure 3-9), VALLEY predicts the highest concentrations, CDM predicts the lowest near-field concentrations, and ISCLT predicts the lowest concentrations beyond 800 m.

For a 10 m source height and D stability (Figure 3-10), ISCLT predicts the highest concentrations at 100 m and 125 m, while CDM predicts the highest values beyond 200 m. Predictions for these long-term models were less sensitive to the change in source height than predictions from several of the short-term models.

3.4 Tests of Mathematical and Physical Principles

The results obtained for the tests of physical principles defined in Section 3.2.1 are described below for each area source model.

3.4.1 ISCST

Stability Comparison. The centerline concentrations predicted by ISCST for the base case configuration for Class B, D, and F stability are compared in Figure 3-11. As expected, predictions increase as stability increases. The relative difference in predicted concentrations also increases with distance from the source. Concentrations for B and F stability differ by a factor of 5 at 100 m and a factor of 30 at 1575 m.

Near-Field (Center Versus Edge). Predicted concentrations at receptors R1 and R7 are identical. Similar results were obtained at other near-field

receptors. (If ISCST correctly accounted for source geometry, the concentration at R7 would be one-half the value predicted at R1.)

Subdivision. Predicted centerline concentrations are shown in Figure 3-12 for the single 150 m x 150 m source and the subdivided source (four 75 m x 75 m sources, as shown in Figure 3-2a). At 100 m distance (25 m from the downwind edge of the source area), ISCST predicts concentrations different by a factor of 2 for these equivalent source configurations. At 325 m, concentrations differ by 25 percent. Higher concentrations are predicted for the subdivided source. These results are not physically reasonable.

Source Orientation (Figure 3-13). Centerline concentrations predicted by ISCST are nearly identical for normal and diagonal wind directions. ISCST predictions do not reflect the difference in source-receptor geometry between these two cases.

Source Height. Centerline concentrations predicted by ISCST for a 10 m source height are lower than those predicted for a ground level source, as shown in Figure 3-14. Differences are largest near the source, exceeding a factor of 2 at 100 m, and diminish as distance increases. These results are physically reasonable and consistent with P-G dispersion coefficients.

Far-Field Convergence. Centerline concentrations predicted by ISCST are shown in Figure 3-15 for three area sources with equivalent total emissions but different areas (75 x 75 m; 150 x 150 m; and 450 x 450 m). Differences are largest near the source and diminish as distance increases. The smallest area source produces the highest predicted concentrations. At 100 m distance, the centerline value for the 75 x 75 m source is more than 5 times the corresponding value for the 450 x 450 m source. These results are consistent with source-receptor geometry and Gaussian dispersion.

Summary - ISCST. Results obtained for ISCST are reasonable for the tests based on sensitivity to stability class and source height. ISCST did not

correctly account for source-receptor geometry in the center/edge, subdivision, and source orientation tests.

3.4.2 FDM

Stability Comparison (Figure 3-16). Predicted centerline concentrations increase with stability, as expected. At 100 m distance, concentrations for B and F stability differ by only a factor of 2. At 1575 m, the difference is a factor of 20.

Center Versus Edge. Predicted concentrations at receptors downwind of the source edge (R7, R8) are one-half of the corresponding values at centerline receptors. This result is consistent with source-receptor geometry.

Subdivision (Figure 3-17). Predicted centerline concentrations are approximately 20 percent lower at 100 m distance for the subdivided source, and 10 percent lower beyond 500 m. These differences represent an inaccurate treatment of source geometry.

Source Orientation (Figure 3-18). Predicted centerline concentrations are higher near the source for the diagonal orientation, consistent with the source-receptor geometry. Results converge at greater distances.

Source Height (Figure 3-19). Predicted centerline concentrations at 100 m from the source are a factor of 2 lower for the 10 m source height than a ground level release. At 325 m and 875 m, the differences are smaller than values estimated using P-G dispersion coefficients.

Far-Field Convergence (Figure 3-20). In the near-field region, predicted centerline concentrations decrease as source area increases. As distance increases, results for all three source sizes converge.

Summary - FDM. FDM provides physically reasonable results for all but one of the tests, indicating that the treatment of source-receptor geometry is generally accurate. The subdivision test results suggest some room for improvement.

3.4.3 PAL

Stability Comparison (Figure 3-21). Centerline concentrations increase with increasing stability. Differences become larger as distance increases, growing from a factor of 5 at 100 m to a factor of 50 at 1575 m.

Center Versus Edge (Near-Field). Predicted concentrations at edge receptors near the source (R7, R8) are one-half the corresponding centerline concentrations. This result is consistent with source-receptor geometry.

Subdivision (Figure 3-22). Predicted centerline concentrations for the subdivided source are almost exactly equal to the corresponding values predicted for the single source at all distances. These results are physically reasonable.

Source Orientation (Figure 3-23). Predicted centerline concentrations for the diagonal source orientation are higher than the values for a normal wind direction. Differences become insignificant as distance increases.

Source Height (Figure 3-24). Predictions in the near-source region are very sensitive to source height. With a 10 m release height, the concentration at 100 m is lower by a factor of 10. Predictions converge as distance increases.

Far-Field Convergence (Figure 3-25). Predictions for three area source sizes converge at 8000 m from the source. In the near-field, concentrations decrease as source size increases. These are the expected results for a properly functioning model.

Summary - PAL. The results for PAL are physically reasonable for all tests. Predictions are very sensitive to source height.

3.4.4 RAM

Stability Comparison (Figure 3-26). Centerline predictions by RAM increase with stability. The difference between B and F stability increases from a factor of 4 at 100 m to a factor of 10 at 1575 m.

Center Versus Edge (Near-Field). RAM predicts identical concentrations for centerline receptors (R1, R2) and for edge receptors (R7, R8). For this test, RAM did not correctly account for source-receptor geometry.

Subdivision (Figure 3-27). RAM correctly predicts identical centerline concentrations for the single source 150 x 150 m base case and the subdivided (identical) source.

Source Orientation (Figure 3-28). RAM predicts higher centerline concentrations for the diagonal wind direction than for the normal direction. The results are reasonable near the source. At larger distances, predictions are 25 percent higher for the diagonal orientation. These results are not consistent with conservation of mass.

Source Height (Figure 3-29). RAM predictions are extremely sensitive to source height. Centerline predictions for 10 m source height are lower than predictions for a ground level source by a factor of 10 at 100 m. Predictions for these two cases converge as distance increases.

Far-Field Convergence (Figure 3-30). RAM predictions for three different area source sizes do not show convergence even at distances beyond 2000 m. In fact, the relative differences remain constant between 800 m and 8000 m.

Summary - RAM. RAM predictions are not reasonable for a single, isolated area source. (The "narrow plume hypothesis" employed by RAM is designed for application to a large area source grid, and assumes that emissions vary slowly between adjacent grid squares.) RAM does not produce physically reasonable results for the center-edge, source orientation, and far-field convergence tests.

3.4.5 SHORTZ

Stability Comparison (Figure 3-31). Predicted centerline concentrations increase with stability at all distances. The difference between Class B and

Class F predictions is a factor of 5 at 100 m but increases to a factor of 20 at 1575 m. These results are physically reasonable.

Center/Edge Comparison. Near-field concentrations predicted by SHORTZ at "edge" receptors (R7,R8) are one-half of the corresponding centerline predictions, consistent with the source-receptor geometry.

Subdivision (Figure 3-32). Predicted centerline concentrations for the 150 x 150 m source and the equivalent four 75 x 75 m sources are identical at all off-source receptors. For the on-source receptor R11, a higher concentration is predicted for the subdivided source. The results indicate that source geometry is correctly accounted for.

Source Orientation (Figure 3-33). SHORTZ predicts identical centerline concentrations for diagonal and normal wind directions. SHORTZ does not account for the different source-receptor geometry and its effect on near-field concentrations.

Source Height (Figure 3-34). Predicted centerline concentrations near the source are lower for the 10 m source height than for the ground level source, as expected. Differences of 20 and 10 percent remain at 875 m and 1575 m, respectively. These differences, while small, are larger than expected based upon the Pasquill-Gifford vertical dispersion coefficients for D stability.

Far-Field Convergence (Figure 3-35). Predicted centerline concentrations within 1000 m of the source are significantly different for the three source sizes (75 x 75, 150 x 150, 450 x 450 m). The larger source areas produce lower predictions. Centerline predictions converge at greater distances. These results are physically reasonable.

Summary - SHORTZ. Results indicate that the SHORTZ area source algorithm predicts reasonable concentration patterns for most scenarios, but does not always respond to details of source-receptor geometry.

3.4.6 ISCLT

Stability Comparison (Figure 3-36). Predicted centerline concentrations for B, D, and F stability increase with increasing stability. Differences between B and F stability are a factor of 5 at 100 m and a factor of 10 at 1500 m.

Subdivision (Figure 3-37). ISCLT predicted higher concentrations for the subdivided source area (four 75 x 75 m sources), compared to the single (150 x 150 m) source. The difference is approximately a factor of 1.5 at 100 m, and a small difference (10 percent) remains at 1575 m.

Source Height Comparison (Figure 3-38). Centerline predictions by ISCLT are not strongly affected by source height. Differences between predictions for a 10 m source height versus a ground level source are less than a factor of 2 at 100 m and decrease as distance increases.

Far-Field Convergence (Figure 3-39). Predictions for the 75 x 75 m and 150 x 150 m area sources converge gradually with increasing distance. At 8000 m, the centerline concentration for these sources is 20 percent higher than the corresponding value for the 450 x 450 m source.

Summary - ISCLT. The area source predictions by ISCLT show differences for the subdivision and far-field convergence test which are not consistent with source geometry and Gaussian plume dispersion behavior.

3.4.7 CDM

Stability Comparison (Figure 3-40). Centerline concentration predictions by CDM increase with increasing stability. The difference between B and F stability is less than a factor of 2 at 100 m and increases to a factor of 6 at 1500 m.

Subdivision (Figure 3-41). CDM's predictions for the subdivided source are indistinguishable from the base case concentrations at all distances.

Source Height (Figure 3-42). CDM predictions are not strongly sensitive to source height. The difference between predictions for 150 x 150 m ground-level and 10 m sources is only 25 percent at 100 m. Using P-G vertical dispersion coefficients (σ_z) for D stability, a larger difference was estimated at 100 m, but a much smaller difference was estimated at 1500 m.

Far-Field Convergence (Figure 3-43). The differences between concentrations predicted for three area source sizes are relatively small at near-field distances. The predictions appear to converge at 3km downwind, but large differences are predicted by CDM at 8 km. For the 75 x 75m source, the predicted concentration at 8km is higher than at 3km.

Summary - CDM. CDM predictions for the stability comparison and subdivision tests are physically reasonable. For the source height and far-field convergence tests, CDM predictions were not consistent with source-receptor geometry and Gaussian plume dispersion behavior. Inaccuracies may be related to the spatial resolution of the array used by CDM for upwind integration.

3.4.8 VALLEY

Stability Comparison (Figure 3-44). Predicted centerline concentrations for F stability are distinctly different from, and much higher than, those predicted for B and D stability. Near the source, concentrations for B and D stability are very similar, and differences increase with distance. The near-field concentrations for F stability are greater by more than a factor of 10. No physical basis for these differences is apparent.

Subdivision (Figure 3-45). Predicted centerline concentrations increase when the base case source is subdivided. VALLEY predicts concentrations 50 percent higher at 100 m and 5 percent higher at 1500 m.

Source Height (Figure 3-46). Predicted concentrations for an elevated area source are only 5 percent lower than corresponding predictions for a ground level source. Much larger differences were estimated at distances of 100-200 m using the P-G dispersion coefficients. Larger differences were also predicted by the other models.

Far-Field Convergence (Figure 3-47). Concentrations predicted by VALLEY for three area source sizes converge gradually at distances beyond 800 m from the source. At a distance of 8000 m, the predicted concentration for the 450 x 450 m source is 20 percent lower than values for the 75 x 75 m and 150 x 150 m sources.

Summary - VALLEY. The differences in concentrations predicted by VALLEY as a function of stability, source geometry and source height are not consistent with predictions by other models and do not correspond to Gaussian plume dispersion behavior. Inaccuracy of 20 to 50 percent was found in several cases.

3.5 Discussion of Results

Predicted concentrations were compared and analyzed for eight air quality models applicable to area source emissions. The model scenarios used for this analysis represent variations on a base case with a single 150 x 150 m area source and receptors extending out to 1575 m from the source. Model predictions were analyzed to characterize the range of concentrations predicted as a function of stability class and source height. Test cases were designed to identify changes in predicted concentrations associated with specific changes in the source-receptor configuration. These tests were analyzed to identify strengths and weaknesses in each area source algorithm, independent of each model's treatment of atmospheric dispersion.

3.5.1 Short-Term Models

Five short-term models (ISCST, FDM, PAL, RAM, SHORTZ) were analyzed in the greatest depth. In general, FDM predicted the lowest centerline concentrations. Within 200 m of the source, SHORTZ predicted the highest concentrations. Beyond 400 m, RAM predicted the highest values. (The low concentrations predicted by FDM result primarily from differences in dispersion rates, not from the area source algorithm.)

The tests of physical principles provide a basis for judging each area source algorithm's strengths and weaknesses based on "absolute" performance criteria, independent of any measured concentrations. The results are summarized in Table 3-1 and are briefly discussed below:

Stability Comparison. All of the models' predictions agreed with the expected changes in concentrations with stability class and downwind distance.

Source Height. All of the models predicted lower near-source concentrations when the source height was increased from zero to 10 m. For SHORTZ, however, predictions did not converge at a distance of 1575 m.

Far-Field Convergence. Predictions were obtained for three area sources with different dimensions but the same total emissions. For all of the models except RAM, predicted concentrations were independent of source size at a distance of 8000 m.

Center/Edge. Near the source, predicted concentrations downwind of the area source edge should be one-half of centerline concentrations. FDM, PAL, and SHORTZ correctly predicted this behavior. RAM and ISCST predicted no difference in concentration between centerline and edge receptors.

Subdivision. The base case area source was subdivided into four equal parts, representing (in total) the identical source. PAL, RAM and SHORTZ correctly predicted identical concentrations. FDM predictions were different by 10 to 20 percent. ISCST predictions for the subdivided source were higher by a factor of 2.

TABLE 3-1

SUMMARY OF SENSITIVITY TEST RESULTS FOR SHORT-TERM MODELS

Test	Stability Comparison	Source Height	Far-Field Convergence	Center/Edge	Subdivision	Source Orientation
ISCST	OK	OK	OK	NO (no difference)	NO (large difference)	NO (no difference)
FDM	OK	OK (little sensitiviaty)	OK	OK	Marginal (small difference)	OK
PAL	OK	OK (strong sensitivity)	OK	OK	OK	OK
SHORTZ	OK	MARGINAL	OK	OK	OK	NO (no difference)
RAM	OK	OK (strong sensitivity)	NO	NO (no difference)	OK	NO

Overall, the FDM, PAL, and SHORTZ algorithms gave physically reasonable results most often. The ISCST algorithm failed two tests sensitive to source geometry. The RAM algorithm showed numerous serious deficiencies.

Source Orientation. Centerline concentrations were compared for wind directions along a source side and along the diagonal. Near-source impacts should be higher for the diagonal direction, but differences should be negligible at greater distances. ISCST and PAL predicted this behavior correctly. FDM predicted near-source impacts correctly, but predicted differences at large distances. ISCST and SHORTZ predicted no differences near the source. RAM predicted substantial differences at large distances.

Overall, the FDM and PAL algorithms consistently gave physically reasonable results. SHORTZ gave reasonable results except for the source orientation test. The ISCST algorithm failed three tests sensitive to source geometry. The RAM algorithm showed numerous serious deficiencies.

3.5.2 Sector Average Models

Three sector average models were examined: ISCLT, CDM, and VALLEY. Results for all three models indicate that source integration methods are subject to inaccuracies of 10 or 20 percent. Aside from these inaccuracies, the ISCLT algorithm gave reasonable results based on the stability comparison, source height, and far-field convergence tests. ISCLT failed to account properly for source geometry, however, based on the subdivision test. CDM gave reasonable results for the subdivision, stability, and source height comparisons, but the far-field predictions at 8km were not reasonable. The VALLEY algorithm gave physically unreasonable results based upon the stability comparison, the subdivision test, and its lack of sensitivity to source height.

Figure 3-3

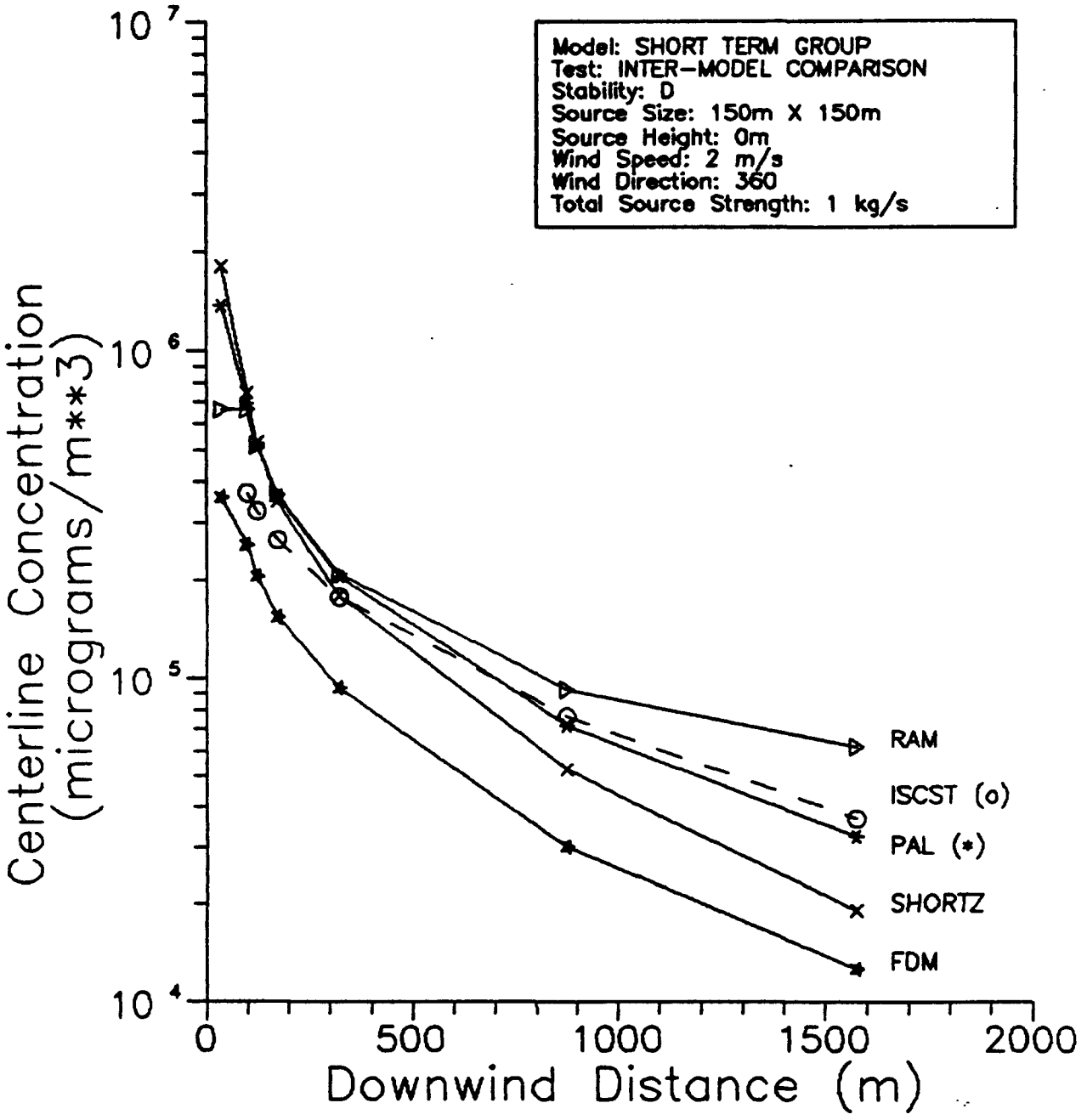
Model: SHORT TERM GROUP
Test: INTER-MODEL COMPARISON
Stability: D
Source Size: 150m X 150m
Source Height: 0m
Wind Speed: 2 m/s
Wind Direction: 360
Total Source Strength: 1 kg/s
Centerline Concentration (micrograms/m**3)
10 7
10 6
10 5
10 4
0
500
1000
1500
2000
Downwind Distance (m)
RAM
ISCST (o)
PAL (*)
SHORTZ
FDM

Figure 3-4

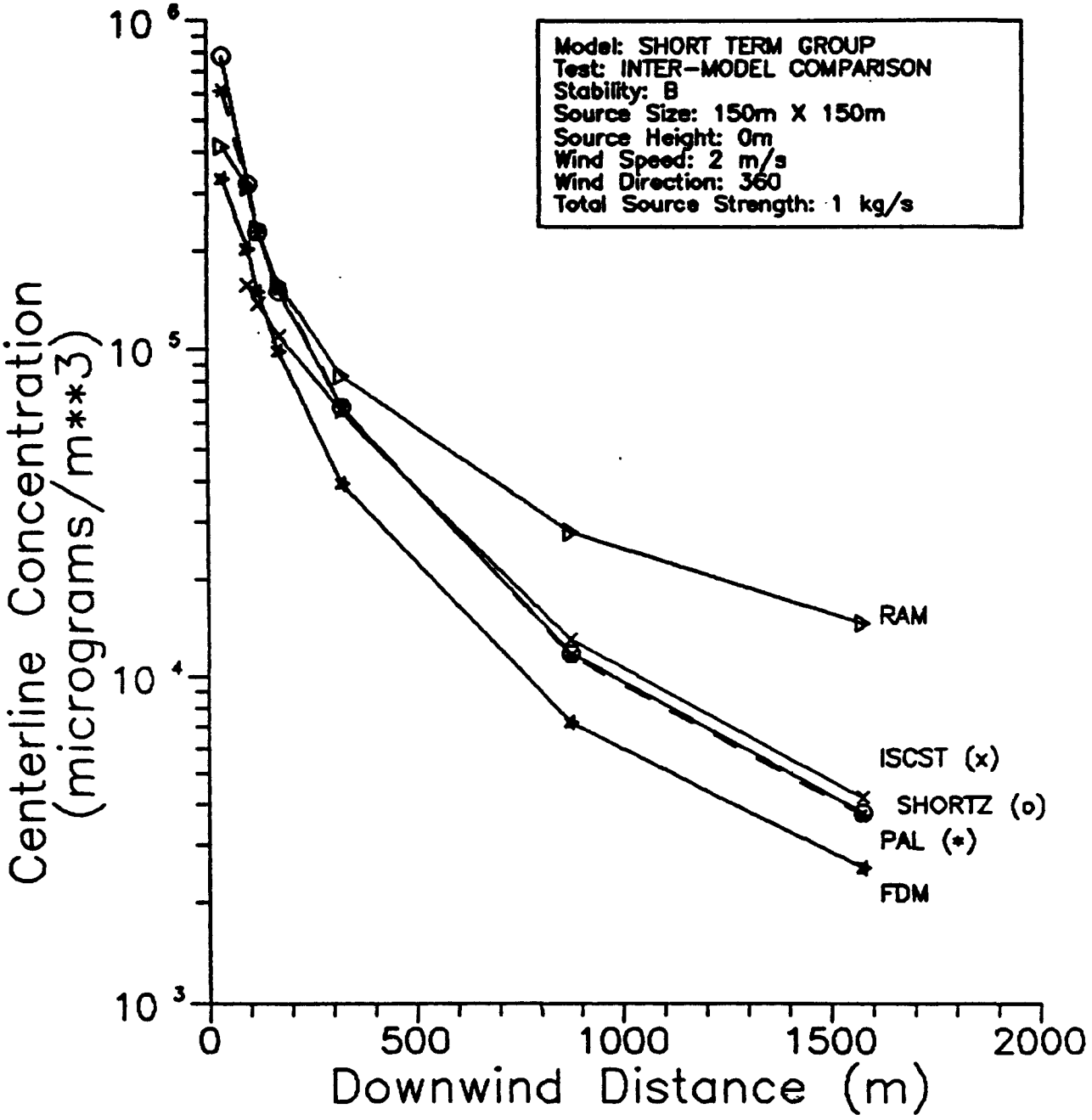
Model: SHORT TERM GROUP
Test: INTER-MODEL COMPARISON
Stability: B
Source Size: 150m X 150m
Source Height: 0m
Wind Speed: 2 m/s
Wind Direction: 360
Total Source Strength: 1 kg/s
Centerline Concentration (micrograms/m**3)
10 6
10 5
10 4
10 3
0
500
1000
1500
2000
Downwind Distance (m)
RAM
ISCST (x)
SHORTZ (o)
PAL (*)
FDM

Figure 3-5

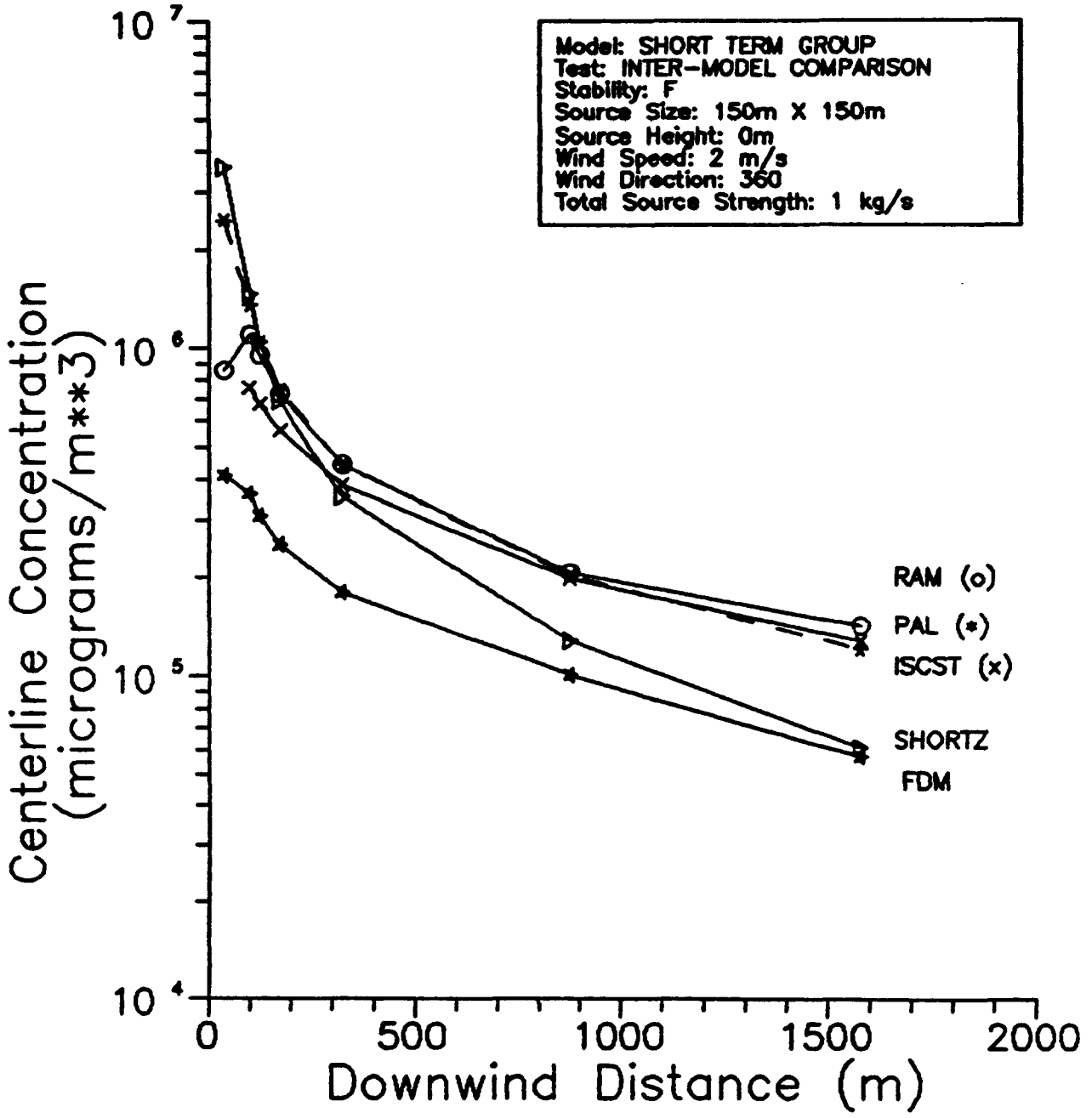
Model: SHORT TERM GROUP
Test: INTER-MODEL COMPARISON
Stability: F
Source Size: 150m X 150m
Source Height: 0m
Wind Speed: 2 m/s
Wind Direction: 360
Total Source Strength: 1 kg/s
Centerline Concentration (micrograms/m**3)
10 7
10 6
10 5
10 4
0
500
1000
1500
2000
Downwind Distance (m)
RAM (o)
PAL (*)
ISCST (x)
SHORTZ
FDM

Figure 3-6

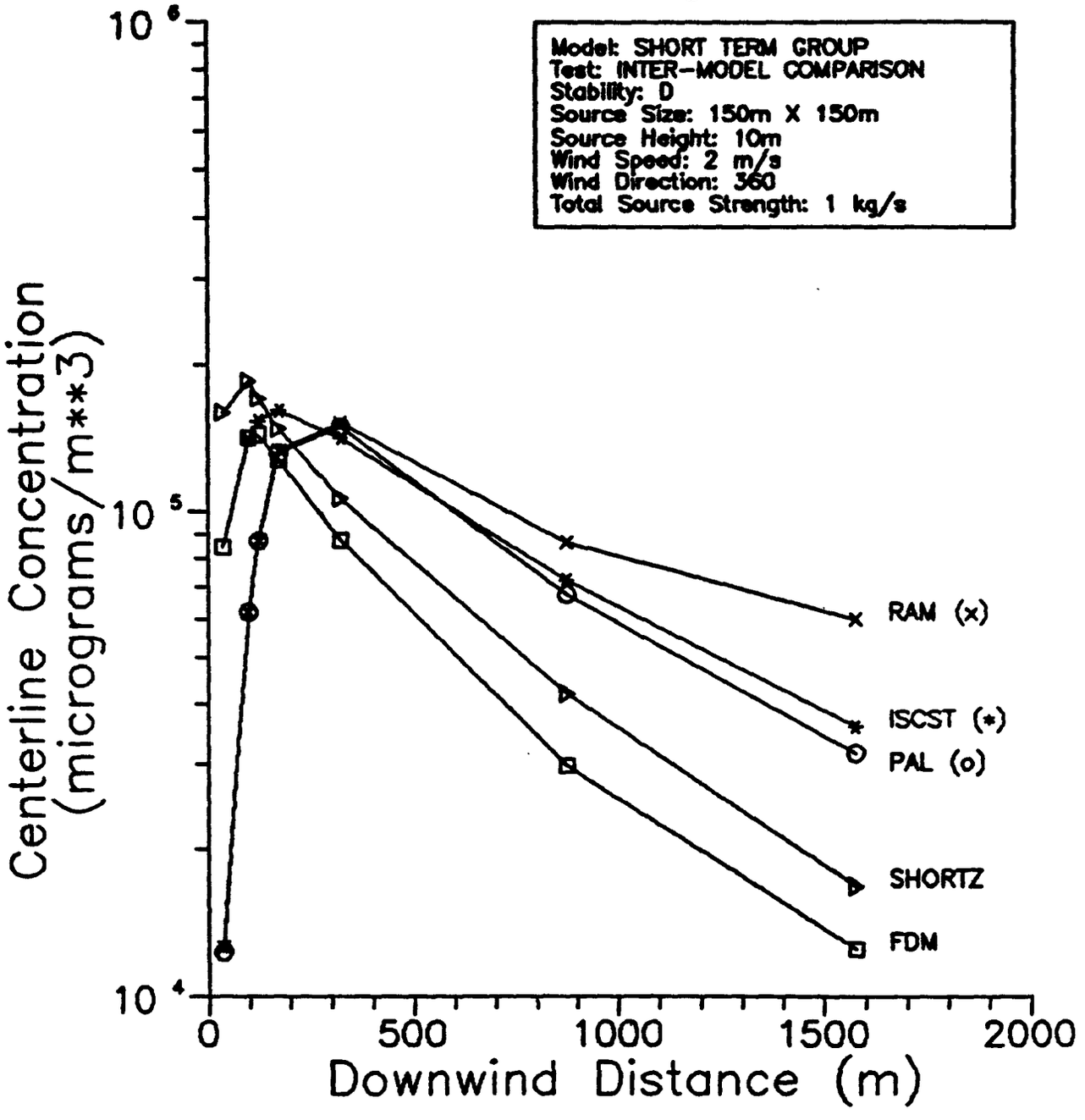
Model: SHORT TERM GROUP
Test: INTER-MODEL COMPARISON
Stability: D
Source Size: 150m X 150m
Source Height: 10m
Wind Speed: 2 m/s
Wind Direction: 360
Total Source Strength: 1 kg/s
Centerline Concentration (micrograms/m**3)
10 6
10 5
10 4
0
500
1000
1500
2000
Downwind Distance (m)
RAM (x)
ISCST (*)
PAL (o)
SHORTZ
FDM

Figure 3-7

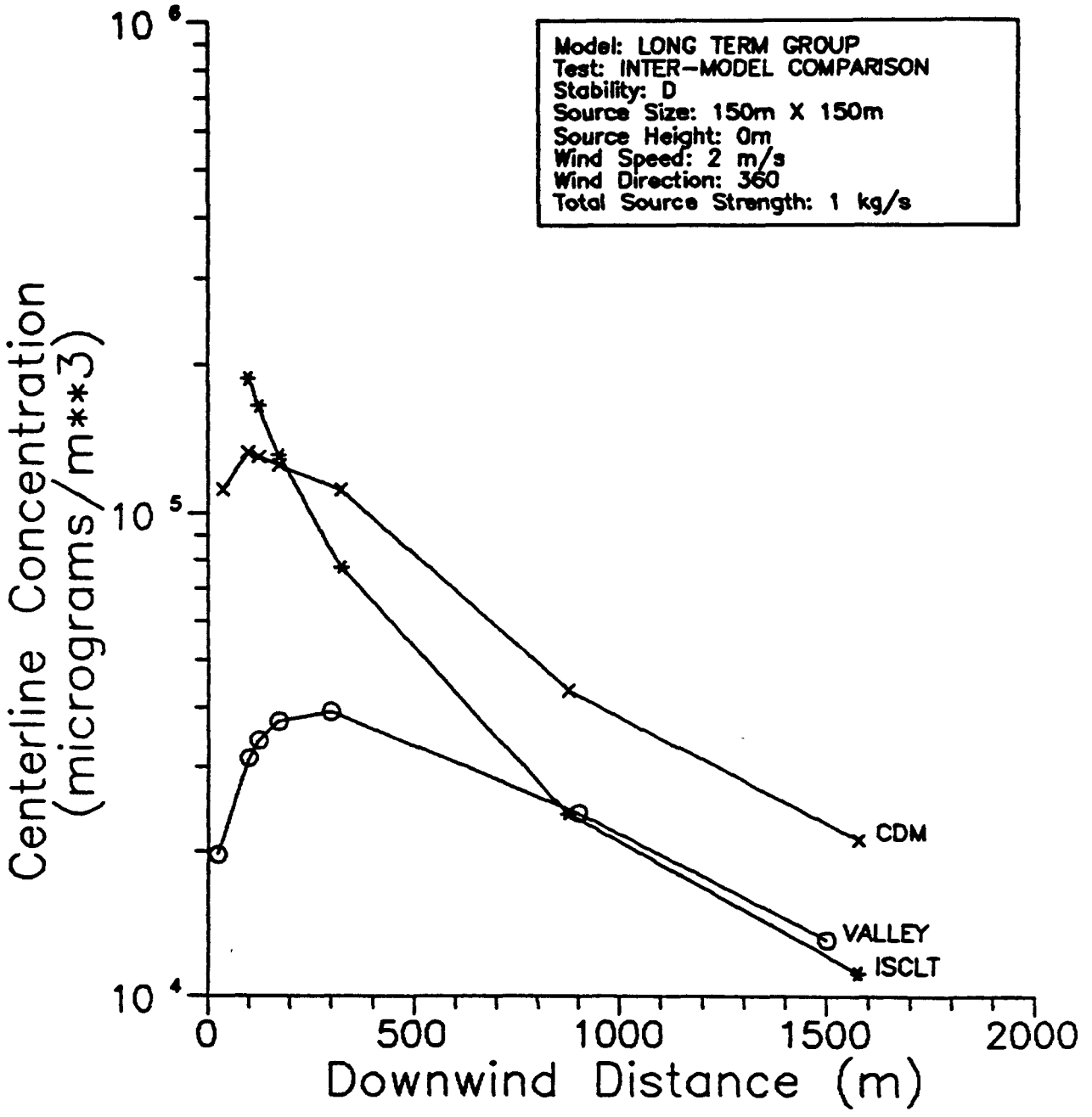
Model: LONG TERM GROUP
Test: INTER-MODEL COMPARISON
Stability: D
Source Size: 150m X 150m
Source Height: 0m
Wind Speed: 2 m/s
Wind Direction: 360
Total Source Strength: 1 kg/s
Centerline Concentration (micrograms/m**3)
10 6
10 5
10 4
0
500
1000
1500
2000
Downwind Distance (m)
CDM
VALLEY
ISCLT

Figure 3-8

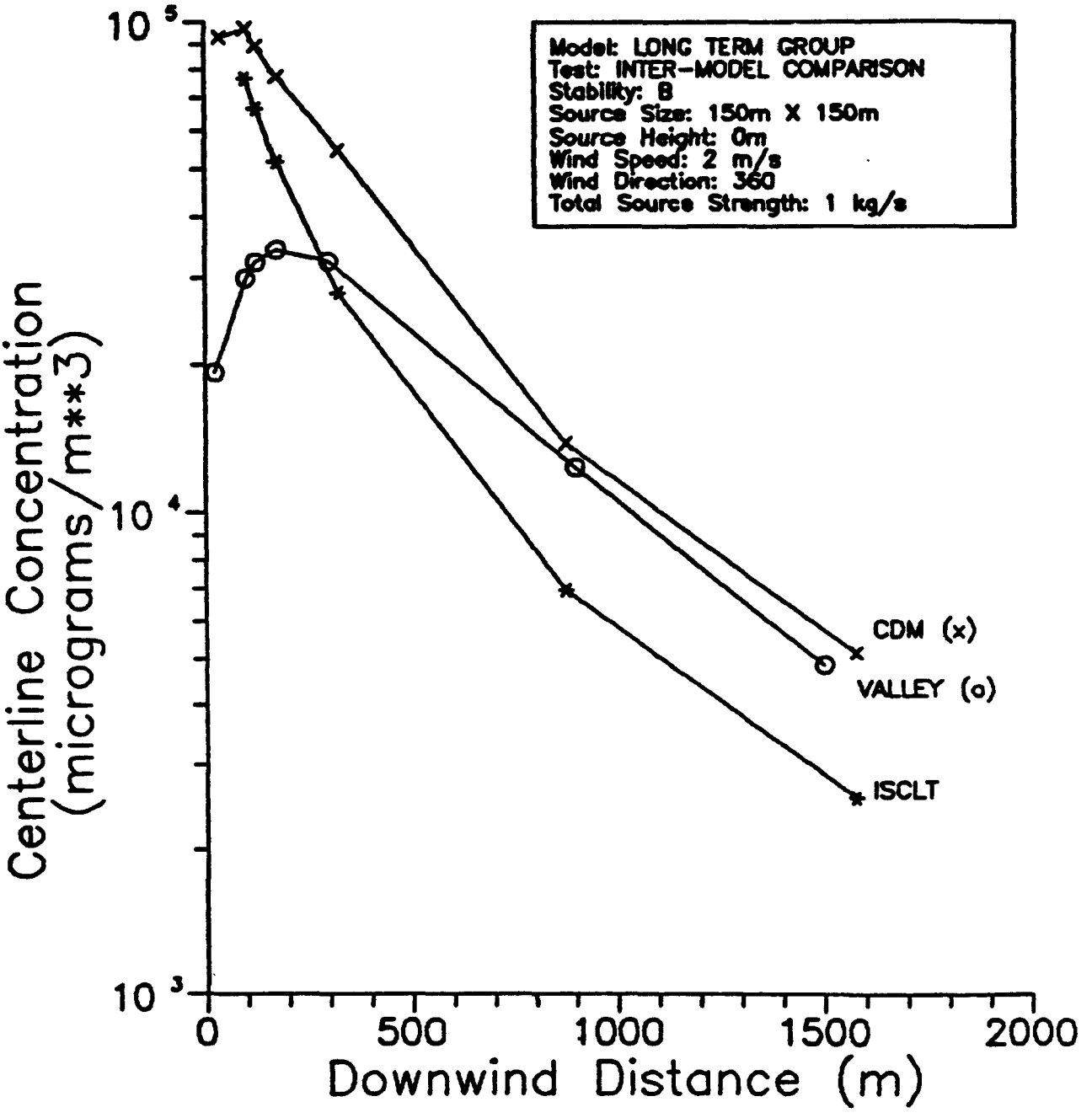
Model: LONG TERM GROUP
Test: INTER-MODEL COMPARISON
Stability: B
Source Size: 150m X 150m
Source Height: 0m
Wind Speed: 2 m/s
Wind Direction: 360
Total Source Strength: 1 kg/s
Centerline Concentration (micrograms/m**3)
10 5
10 4
10 3
0
500
1000
1500
2000
Downwind Distance (m)
CDM (x)
VALLEY (o)
ISCLT

Figure 3-9

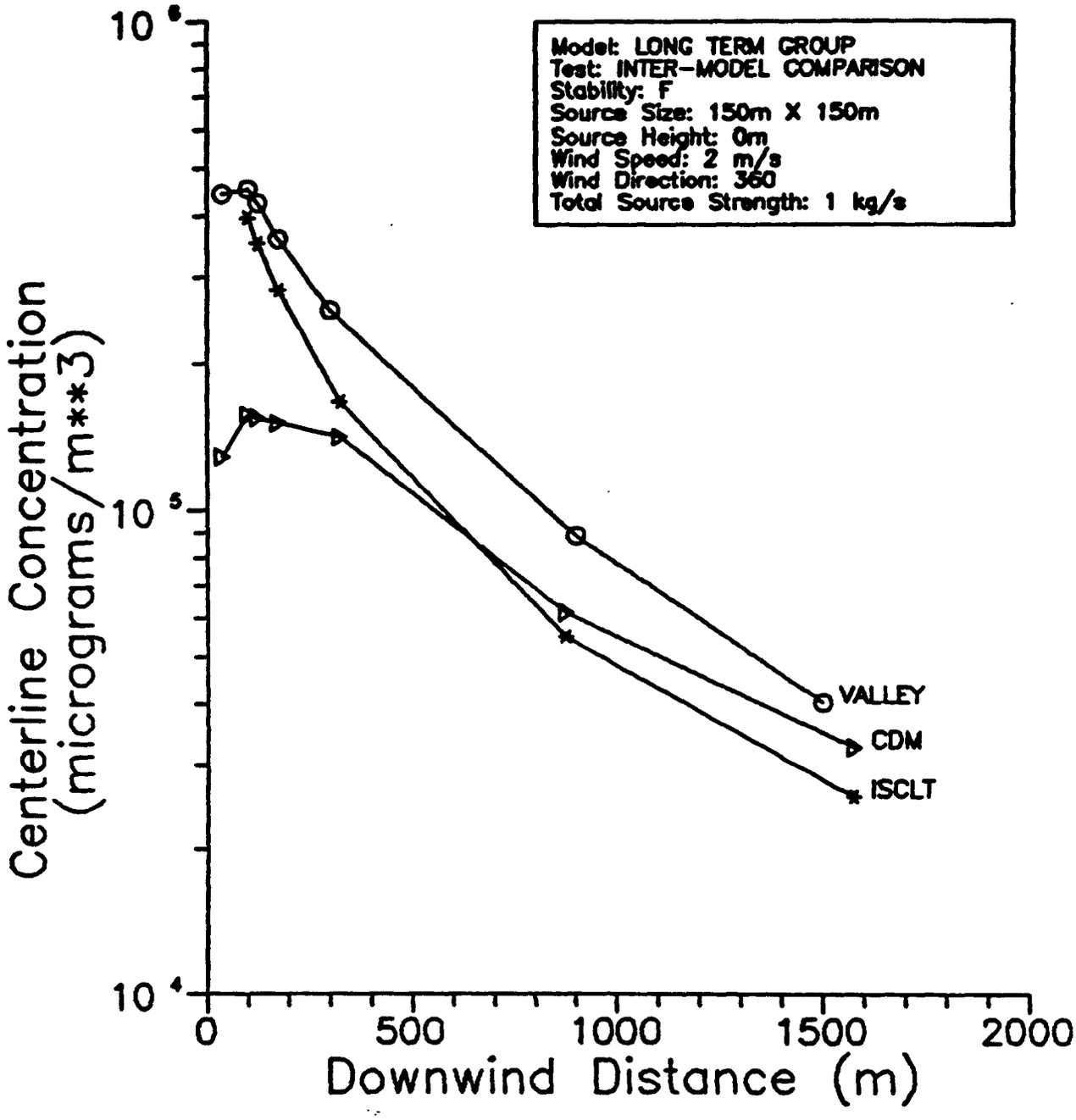
Model: LONG TERM GROUP
Test: INTER-MODEL COMPARISON
Stability: F
Source Size: 150m X 150m
Source Height: 0m
Wind Speed: 2 m/s
Wind Direction: 360
Total Source Strength: 1 kg/s
Centerline Concentration (micrograms/m**3)
10 6
10 5
10 4
0
500
1000
1500
2000
Downwind Distance (m)
VALLEY
CDM
ISCLT

Figure 3-10

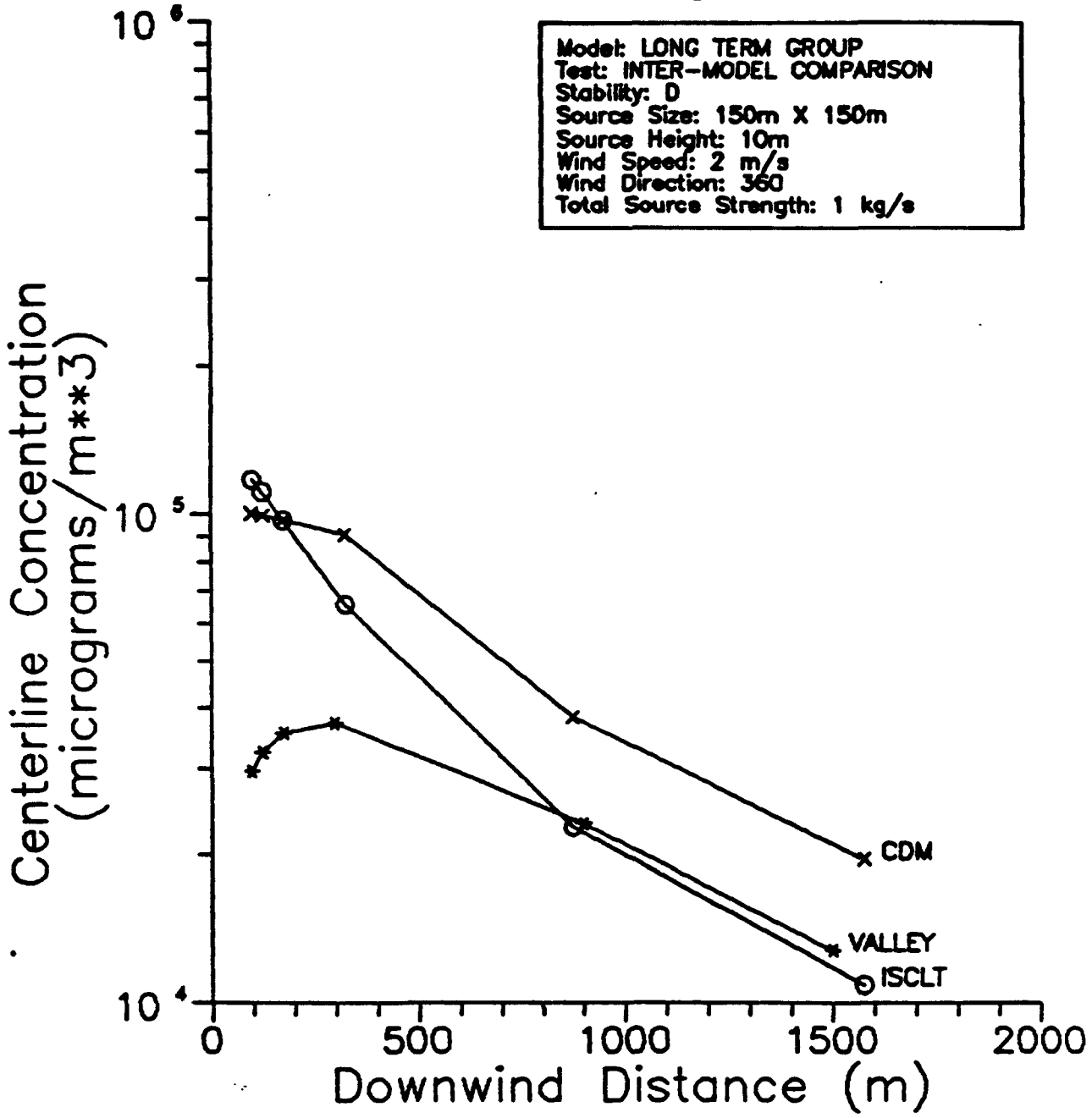
Model: LONG TERM GROUP
Test: INTER-MODEL COMPARISON
Stability: D
Source Size: 150m X 150m
Source Height: 10m
Wind Speed: 2 m/s
Wind Direction: 360
Total Source Strength: 1 kg/s
Centerline Concentration (micrograms/m**3)
10 6
10 5
10 4
0
500
1000
1500
2000
Downwind Distance (m)
CDM
VALLEY
ISCLT

Figure 3-11

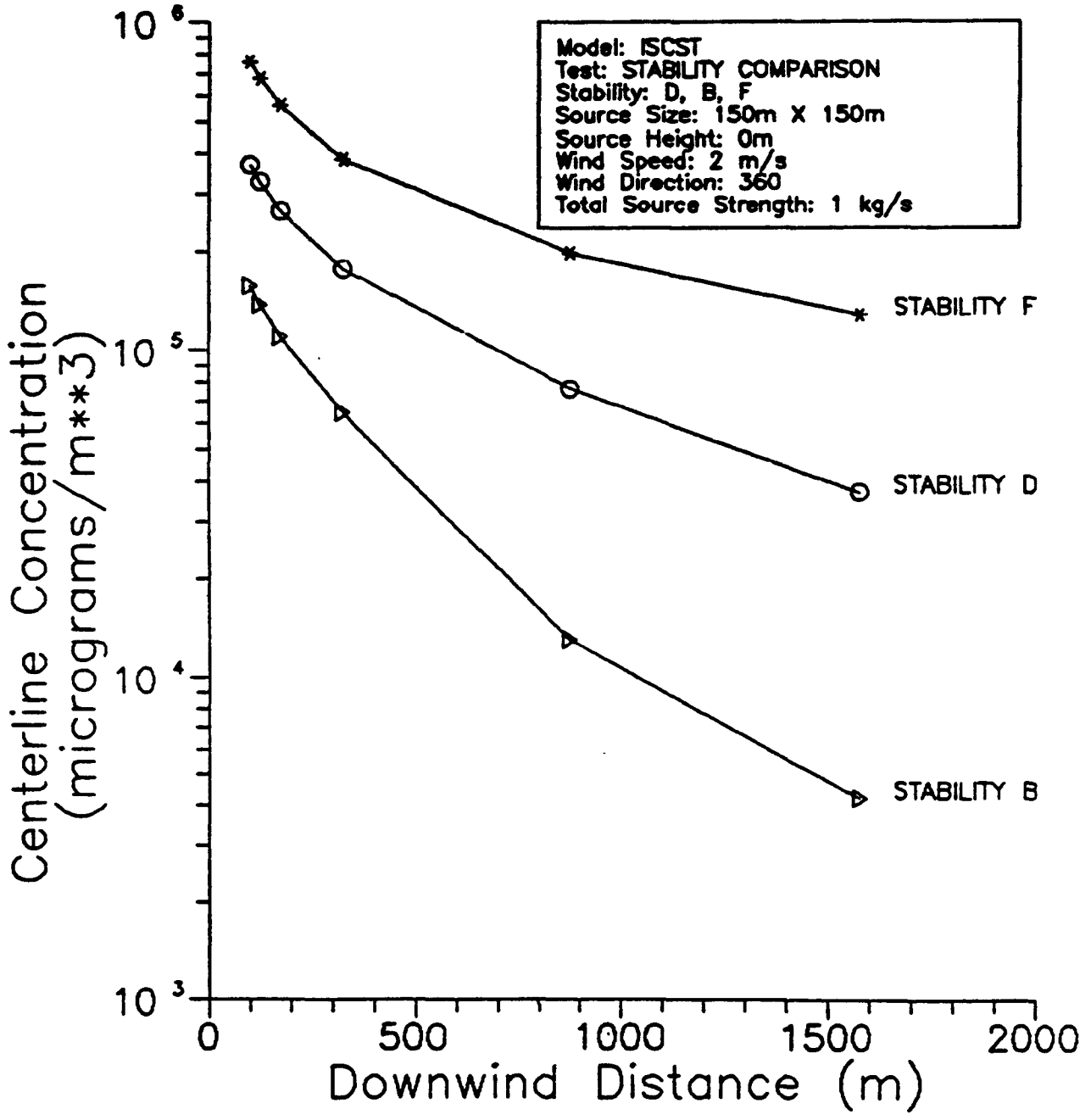
Model: ISCST
Test: STABILITY COMPARISON
Stability: D, B, F
Source Size: 150m X 150m
Source Height: 0m
Wind Speed: 2 m/s
Wind Direction: 360
Total Source Strength: 1 kg/s
STABILITY F
STABILITY D
STABILITY B
Centerline Concentration (micrograms/m**3)
10 6
10 5
10 4
10 3
0
500
1000
1500
2000
Downwind Distance (m)

Figure 3-12

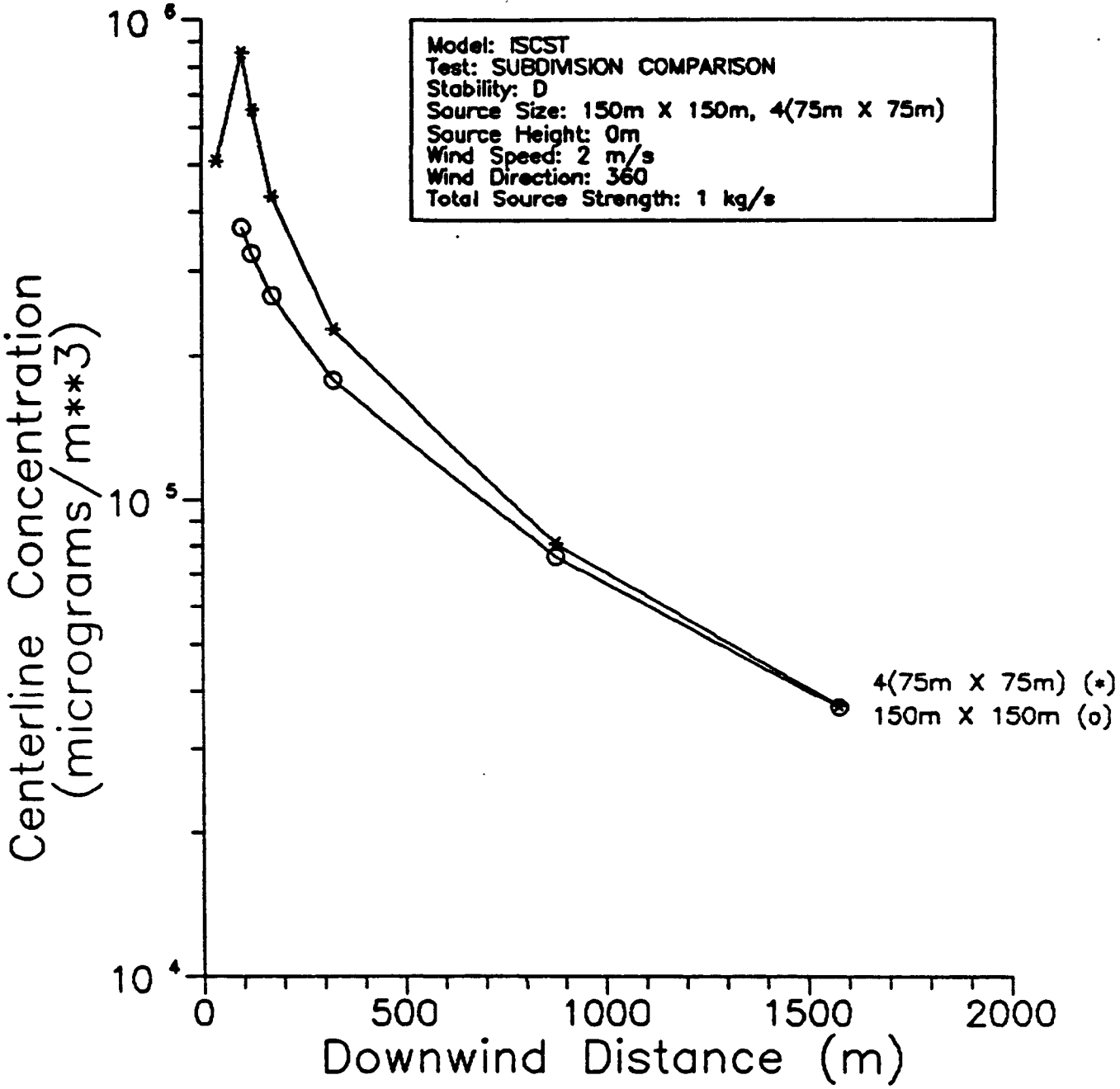
Model: ISCST
Test: SUBDIVISION COMPARISON
Stability: D
Source Size: 150m X 150m, 4(75m X 75m)
Source Height: 0m
Wind Speed: 2 m/s
Wind Direction: 360
Total Source Strength: 1 kg/s
Centerline Concentration (micrograms/m**3)
10 6
10 5
10 4
0
500
1000
1500
2000
Downwind Distance (m)
4(75m X 75m) (*)
150m X 150m (o)

Figure 3–13

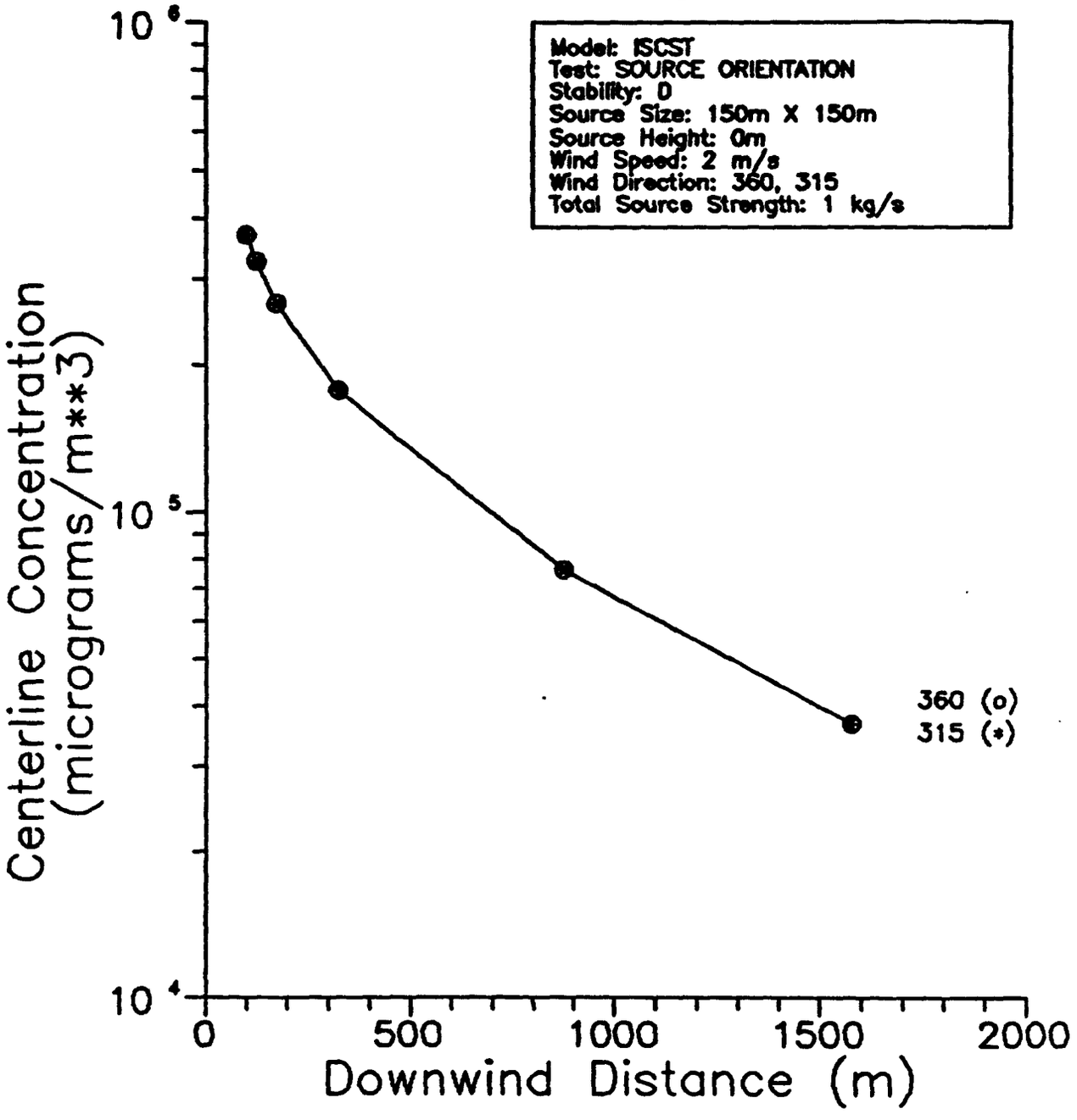
Model: ISCST
Test: SOURCE ORIENTATION
Stability: D
Source Size: 150m X 150m
Source Height: 0m
Wind Speed: 2 m/s
Wind Direction: 360, 315
Total Source Strength: 1 kg/s
Centerline Concentration (micrograms/m**3)
10 6
10 5
10 4
0
500
1000
1500
2000
Downwind Distance (m)
360 (o)
315 (*)

Figure 3–14

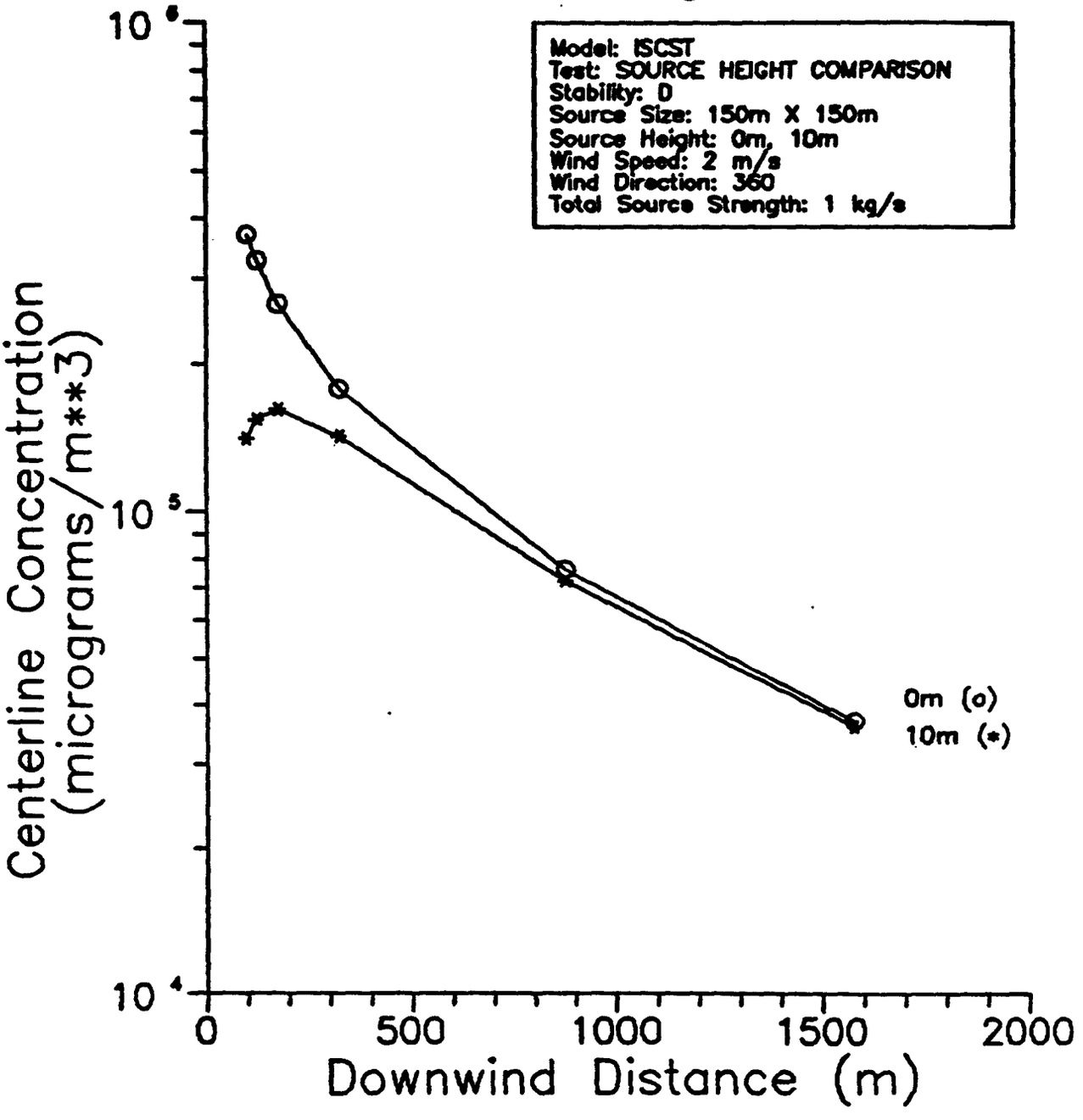
Model: ISCST
Test: SOURCE HEIGHT COMPARISON
Stability: D
Source Size: 150m X 150m
Source Height: 0m, 10m
Wind Speed: 2 m/s
Wind Direction: 360
Total Source Strength: 1 kg/s
Centerline Concentration (micrograms/m**3)
10 6
10 5
10 4
0
500
1000
1500
2000
Downwind Distance (m)
0m (o)
10m (*)

Figure 3-15

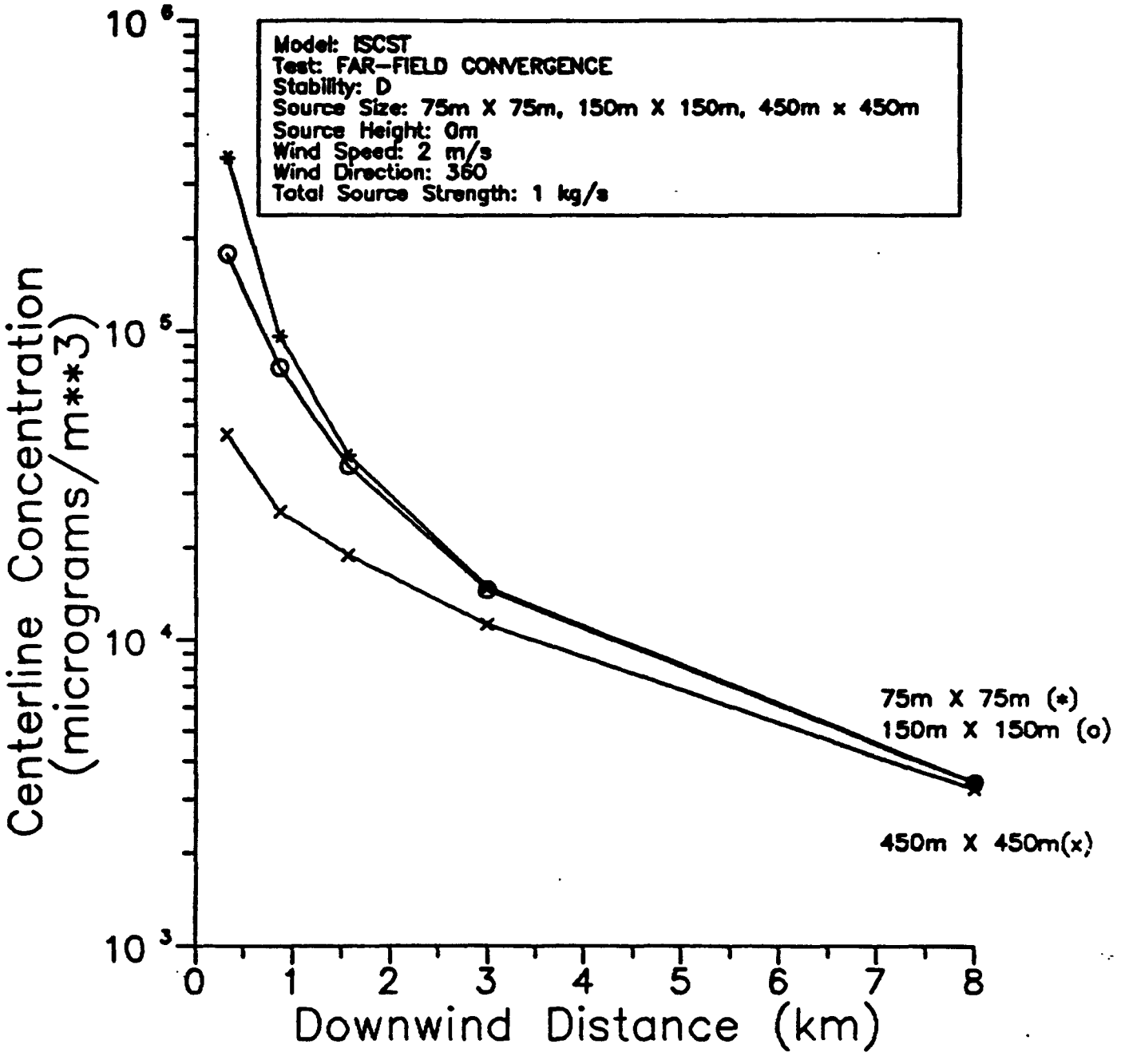
Model: ISCST
Test: FAR-FIELD CONVERGENCE
Stability: D
Source Size: 75m X 75m, 150m X 150m, 450m x 450m
Source Height: 0m
Wind Speed: 2 m/s
Wind Direction: 360
Total Source Strength: 1 kg/s
Centerline Concentration (micrograms/m**3)
10 6
10 5
10 4
10 3
0
1
2
3
4
5
6
7
8
Downwind Distance (km)
75m X 75m (*)
150m X 150m (o)
450m X 450m(x)

Figure 3–16

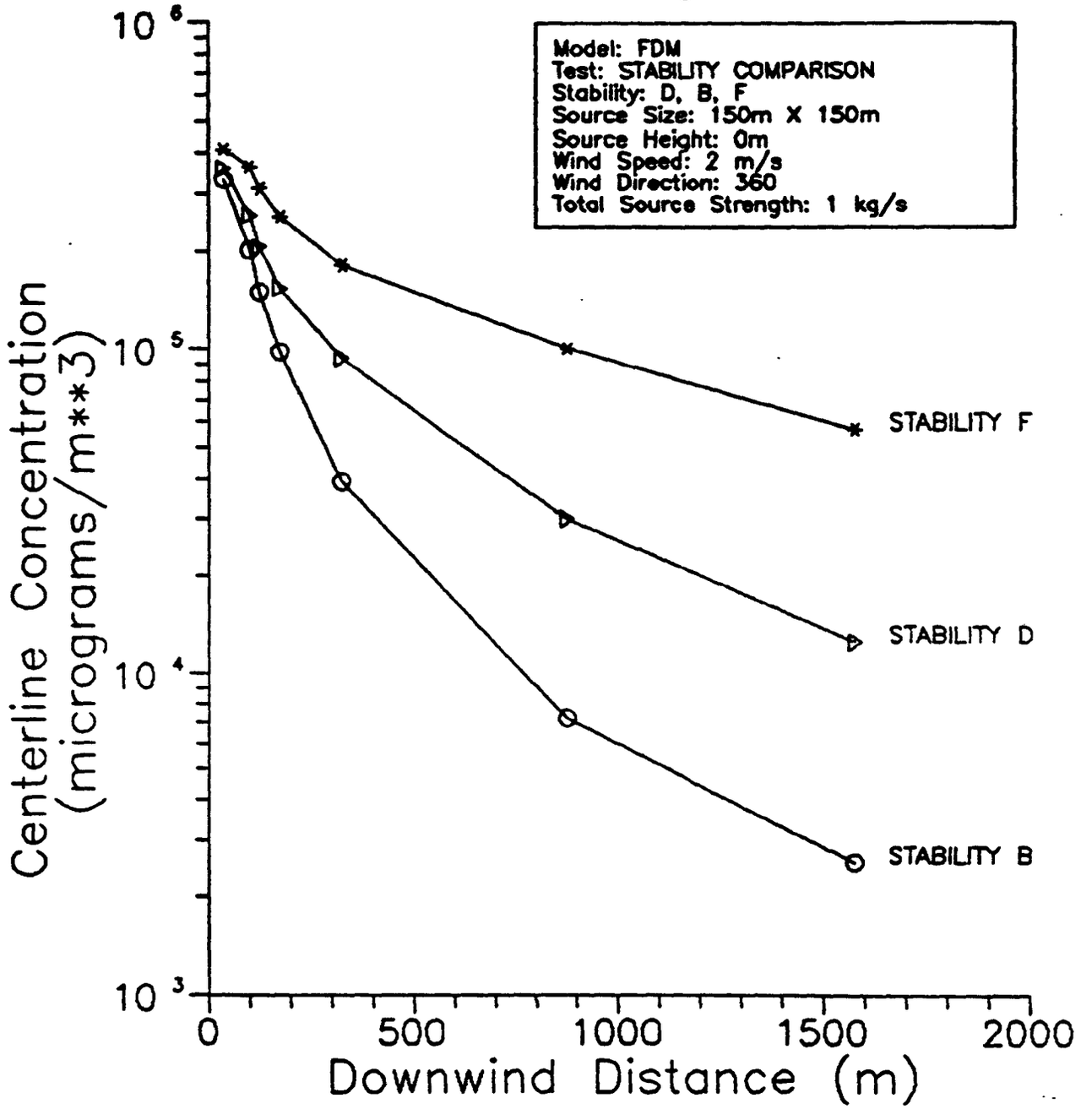
Model: FDM
Test: STABILITY COMPARISON
Stability: D, B, F
Source Size: 150m X 150m
Source Height: 0m
Wind Speed: 2 m/s
Wind Direction: 360
Total Source Strength: 1 kg/s
Centerline Concentration (micrograms/m**3)
10 6
10 5
10 4
10 3
STABILITY F
STABILITY D
STABILITY B
0
500
1000
1500
2000
Downwind Distance (m)

Figure 3–17

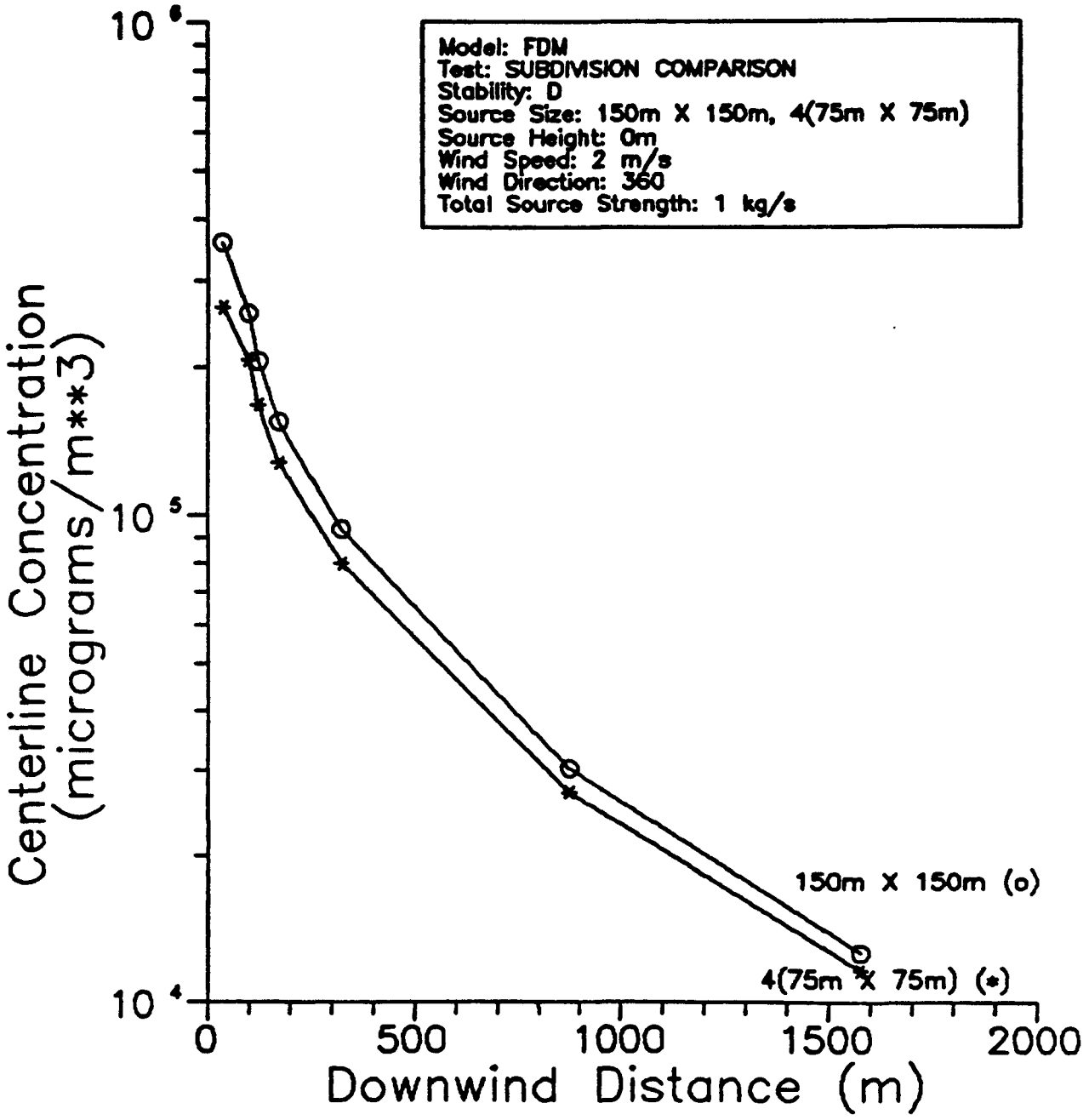
Model: FDM
Test: SUBDIVISION COMPARISON
Stability: D
Source Size: 150m X 150m, 4(75m X 75m)
Source Height: 0m
Wind Speed: 2 m/s
Wind Direction: 360
Total Source Strength: 1 kg/s
Centerline Concentration (micrograms/m**3)
10 6
10 5
10 4
150m X 150m (o)
4(75m X 75m) (*)
0
500
1000
1500
2000
Downwind Distance (m)

Figure 3–18

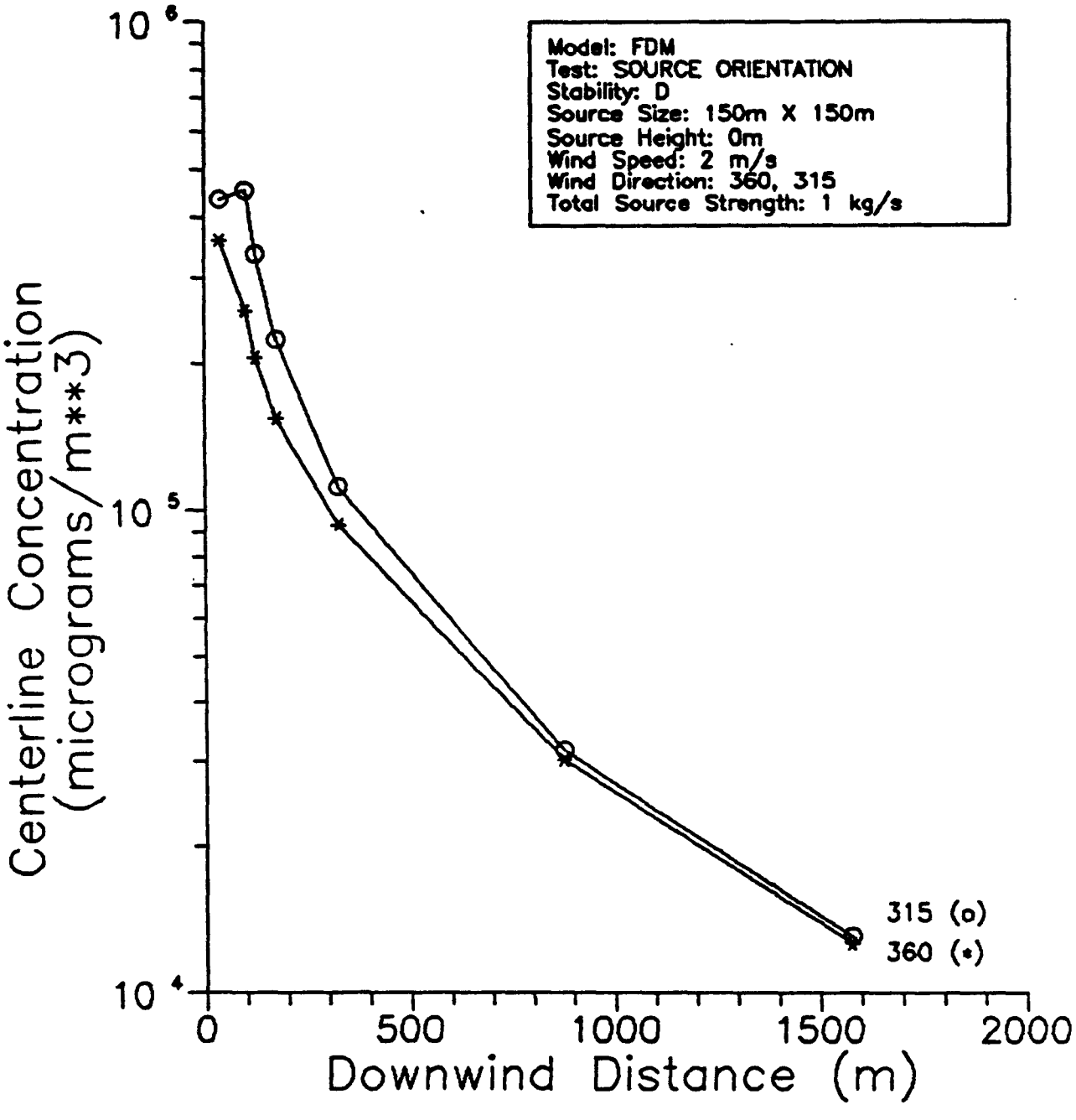
Model: FDM
Test: SOURCE ORIENTATION
Stability: D
Source Size: 150m X 150m
Source Height: 0m
Wind Speed: 2 m/s
Wind Direction: 360, 315
Total Source Strength: 1 kg/s
Centerline Concentration (micrograms/m**3)
10 6
10 5
10 4
0
500
1000
1500
2000
Downwind Distance (m)
315 (o)
360 (*)

Figure 3–19

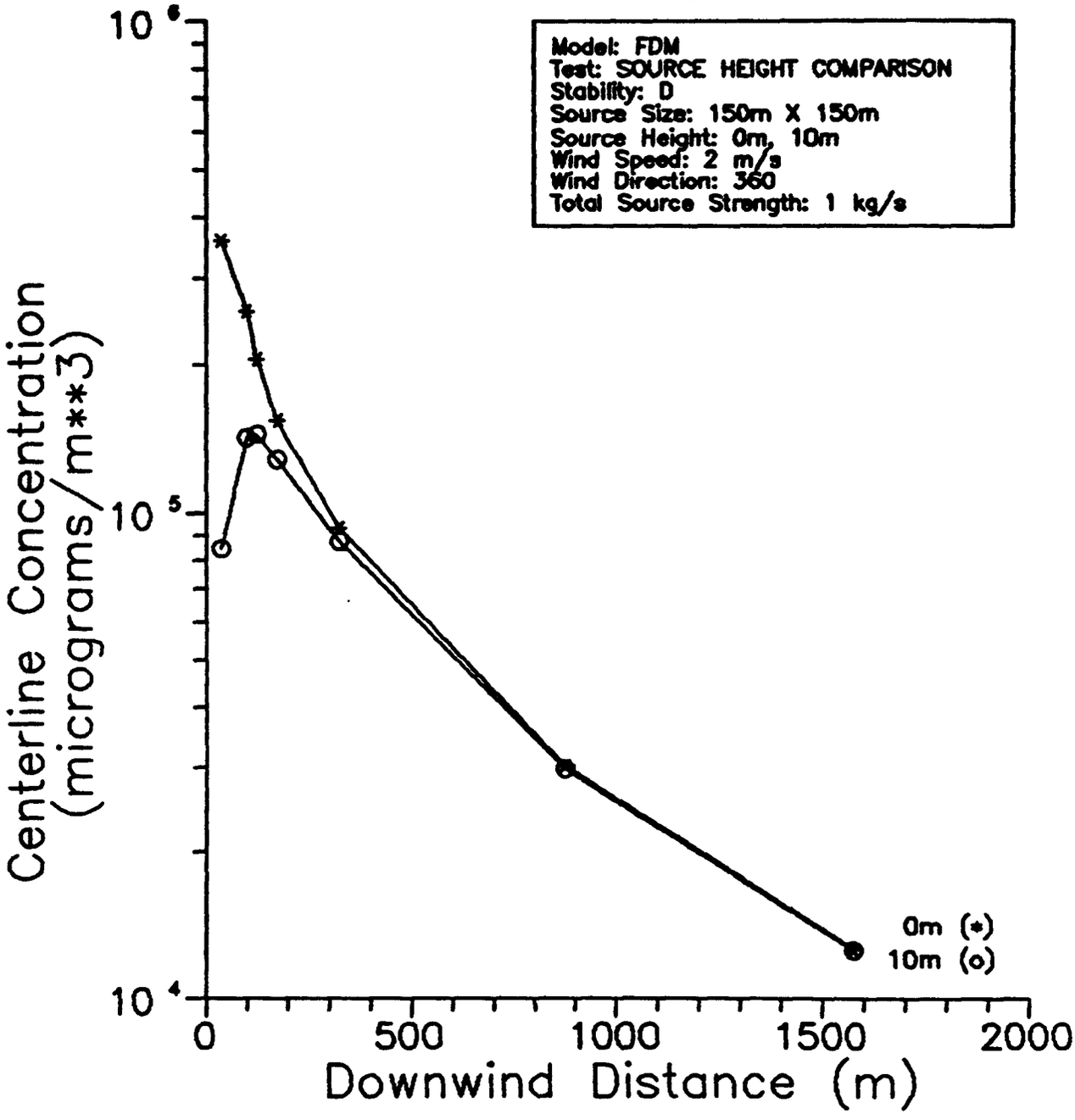
Model: FDM
Test: SOURCE HEIGHT COMPARISON
Stability: D
Source Size: 150m X 150m
Source Height: 0m, 10m
Wind Speed: 2 m/s
Wind Direction: 360
Total Source Strength: 1 kg/s
Centerline Concentration (micrograms/m**3)
10 6
10 5
10 4
0
500
1000
1500
2000
Downwind Distance (m)
0m (*)
10m (o)

Figure 3-20

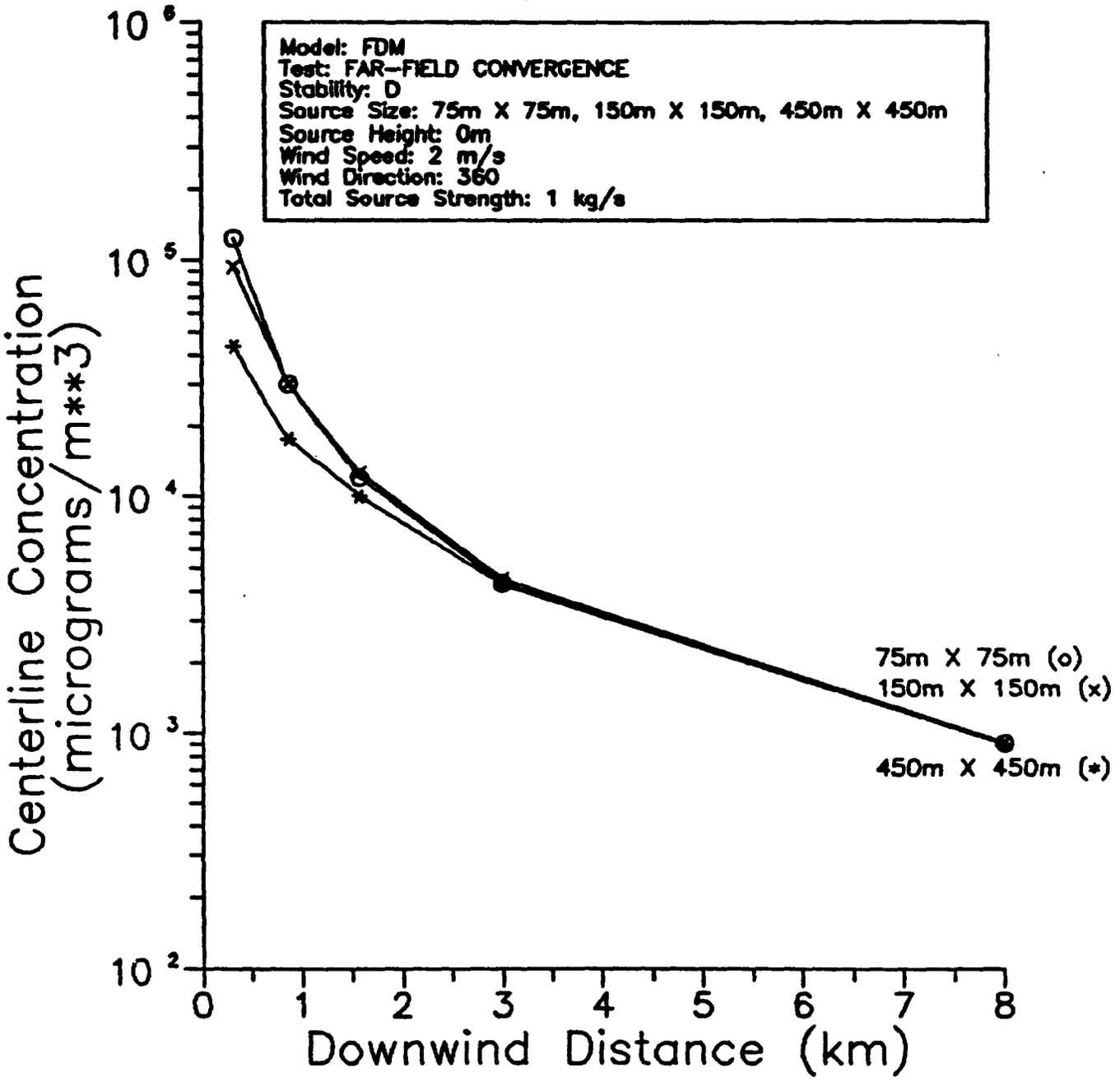
Model: FDM
Test: FAR-FIELD CONVERGENCE
Stability: D
Source Size: 75m X 75m, 150m X 150m, 450m X 450m
Source Height: 0m
Wind Speed: 2 m/s
Wind Direction: 360
Total Source Strength: 1 kg/s
Centerline Concentration (micrograms/m**3)
10 6
10 5
10 4
10 3
10 2
0 1 2 3 4 5 6 7 8
Downwind Distance (km)
75m X 75m (o)
150m X 150m (x)
450m X 450m (*)

Figure 3–21

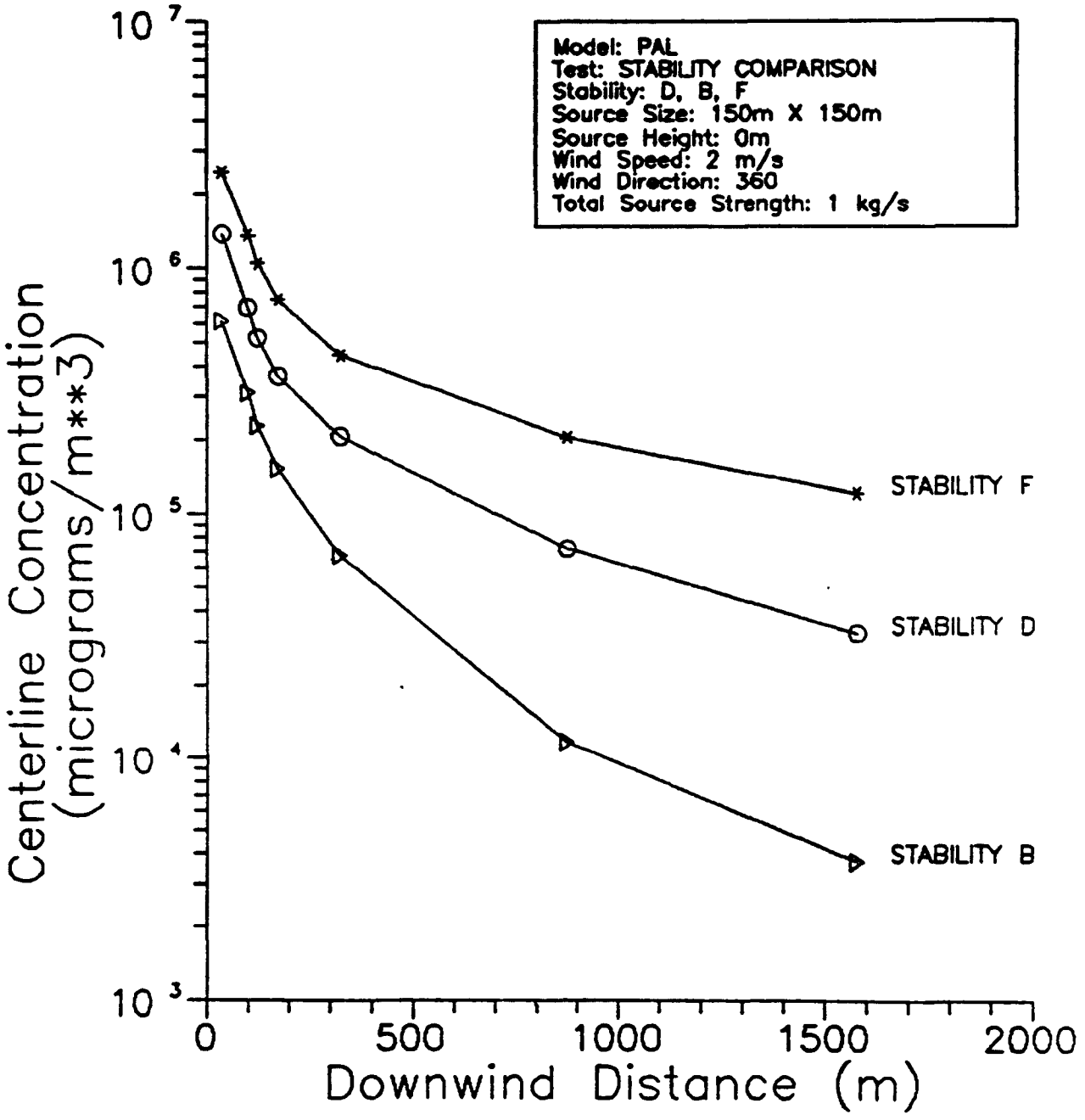
Model: PAL
Test: STABILITY COMPARISON
Stability: D, B, F
Source Size: 150m X 150m
Source Height: 0m
Wind Speed: 2 m/s
Wind Direction: 360
Total Source Strength: 1 kg/s
Centerline Concentration (micrograms/m**3)
10 7
10 6
10 5
10 4
10 3
0
500
1000
1500
2000
Downwind Distance (m)
STABILITY F
STABILITY D
STABILITY B

Figure 3–22

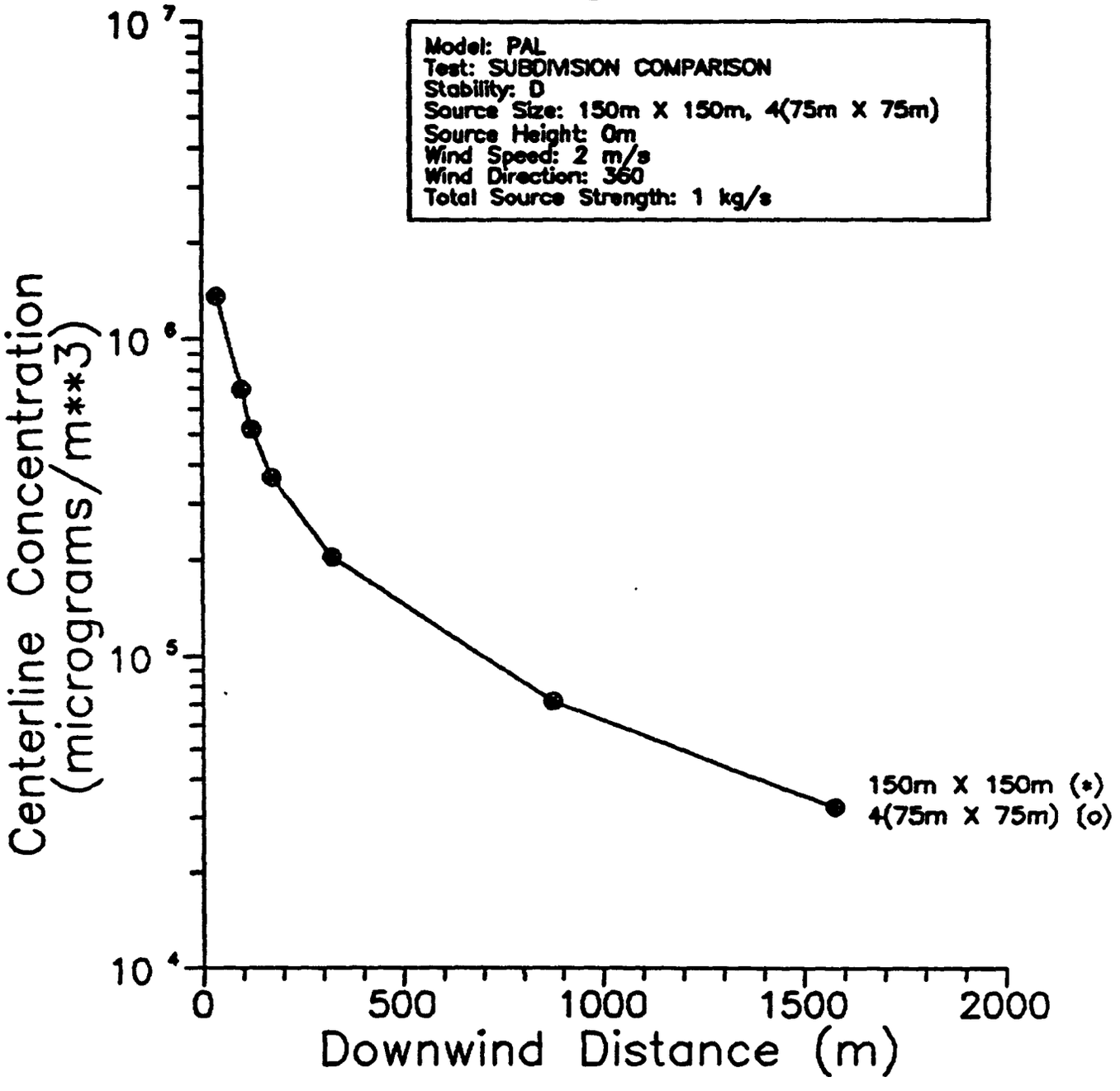
Model: PAL
Test: SUBDIVISION COMPARISON
Stability: D
Source Size: 150m X 150m, 4(75m X 75m)
Source Height: 0m
Wind Speed: 2 m/s
Wind Direction: 360
Total Source Strength: 1 kg/s
Centerline Concentration (micrograms/m**3)
10 7
10 6
10 5
10 4
0
500
1000
1500
2000
Downwind Distance (m)
150m X 150m (*)
4(75m X 75m) (o)

Figure 3-23

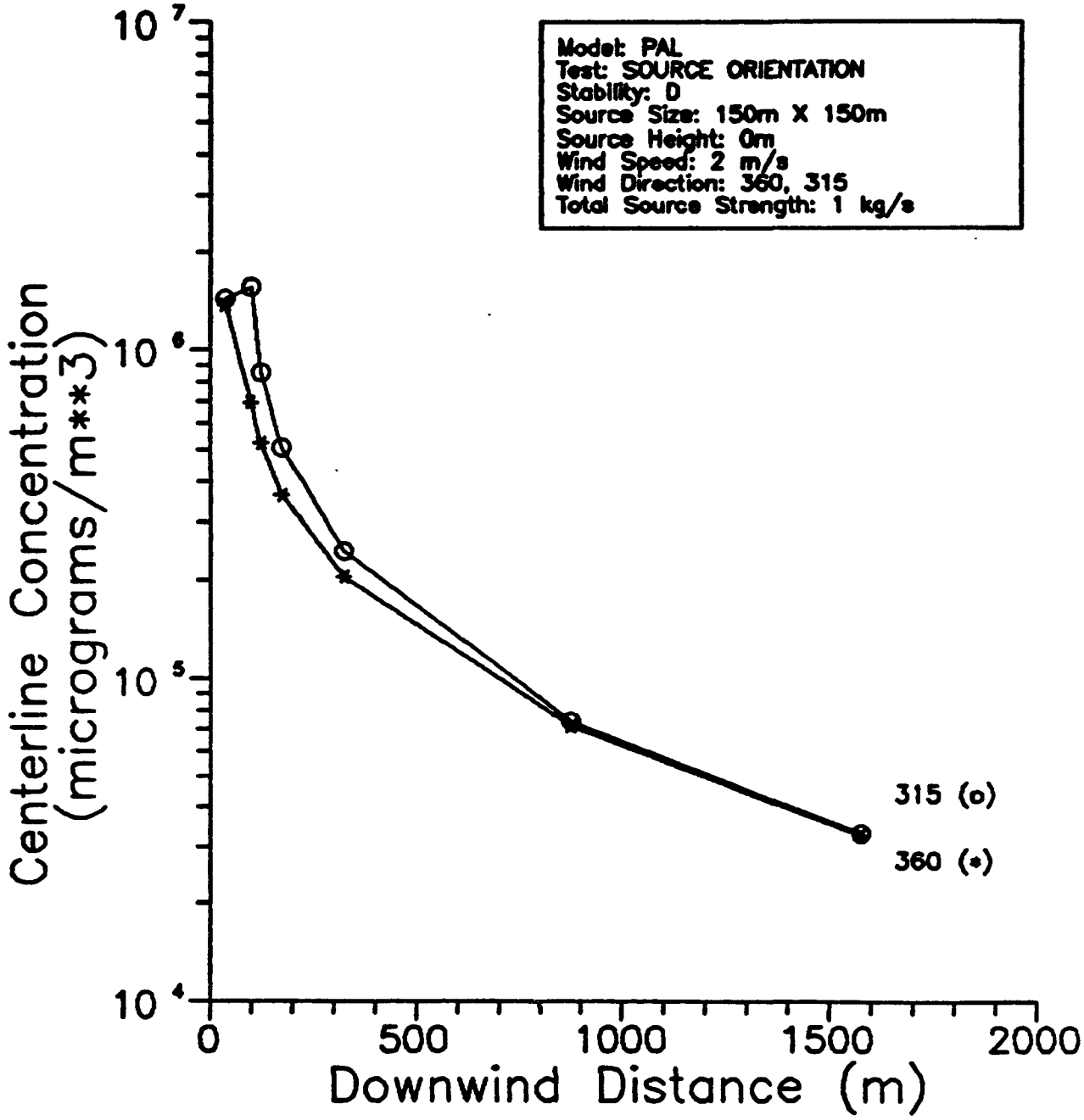
Model: PAL
Test: SOURCE ORIENTATION
Stability: D
Source Size: 150m X 150m
Source Height: 0m
Wind Speed: 2 m/s
Wind Direction: 360, 315
Total Source Strength: 1 kg/s
Centerline Concentration (micrograms/m**3)
10 7
10 6
10 5
10 4
0
500
1000
1500
2000
Downwind Distance (m)
315 (o)
360 (*)

Figure 3-24

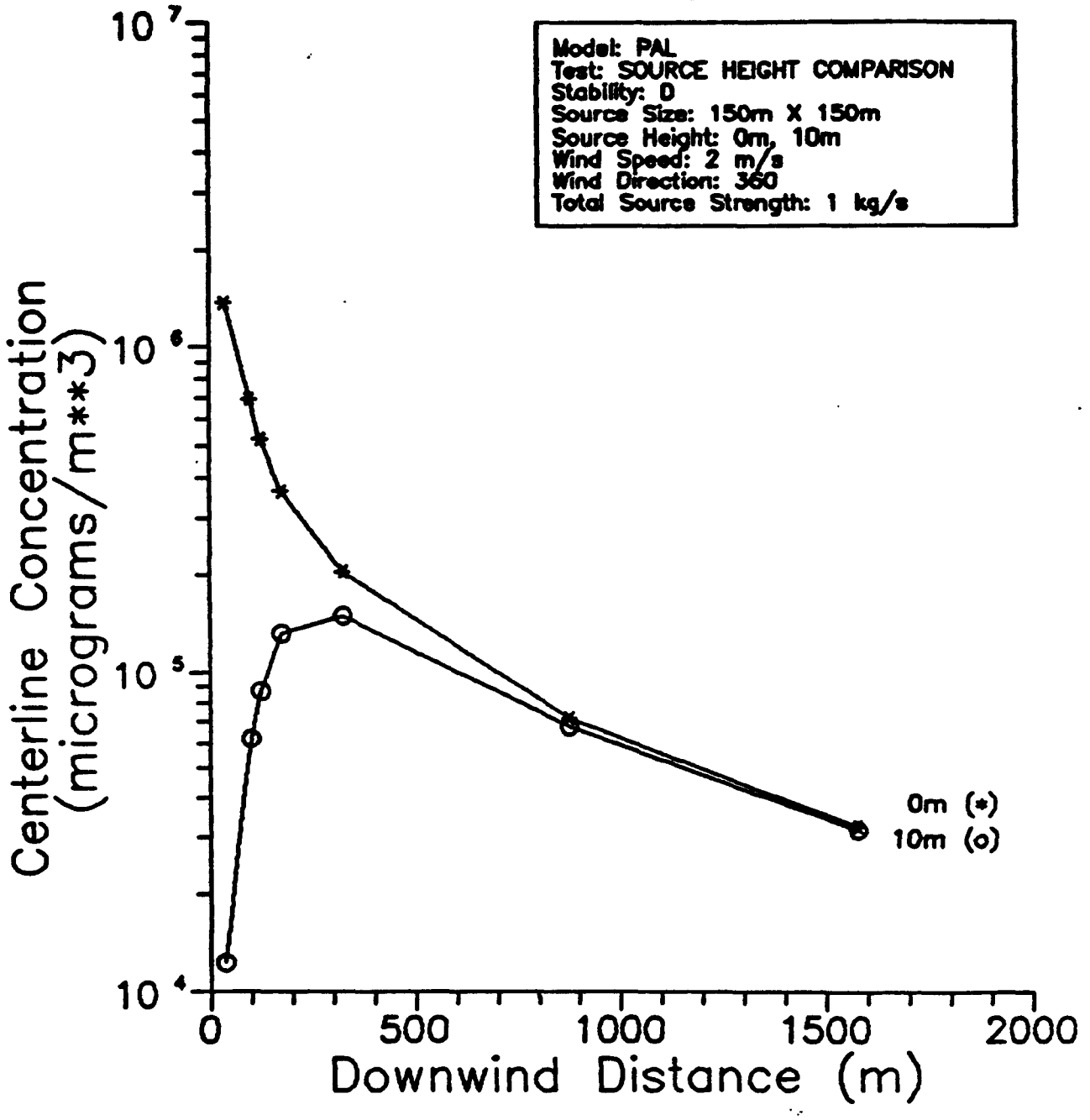
Model: PAL
Test: SOURCE HEIGHT COMPARISON
Stability: D
Source Size: 150m X 150m
Source Height: 0m, 10m
Wind Speed: 2 m/s
Wind Direction: 360
Total Source Strength: 1 kg/s
Centerline Concentration (micrograms/m**3)
10 7
10 6
10 5
10 4
0
500
1000
1500
2000
Downwind Distance (m)
0m (*)
10m (o)

Figure 3-25

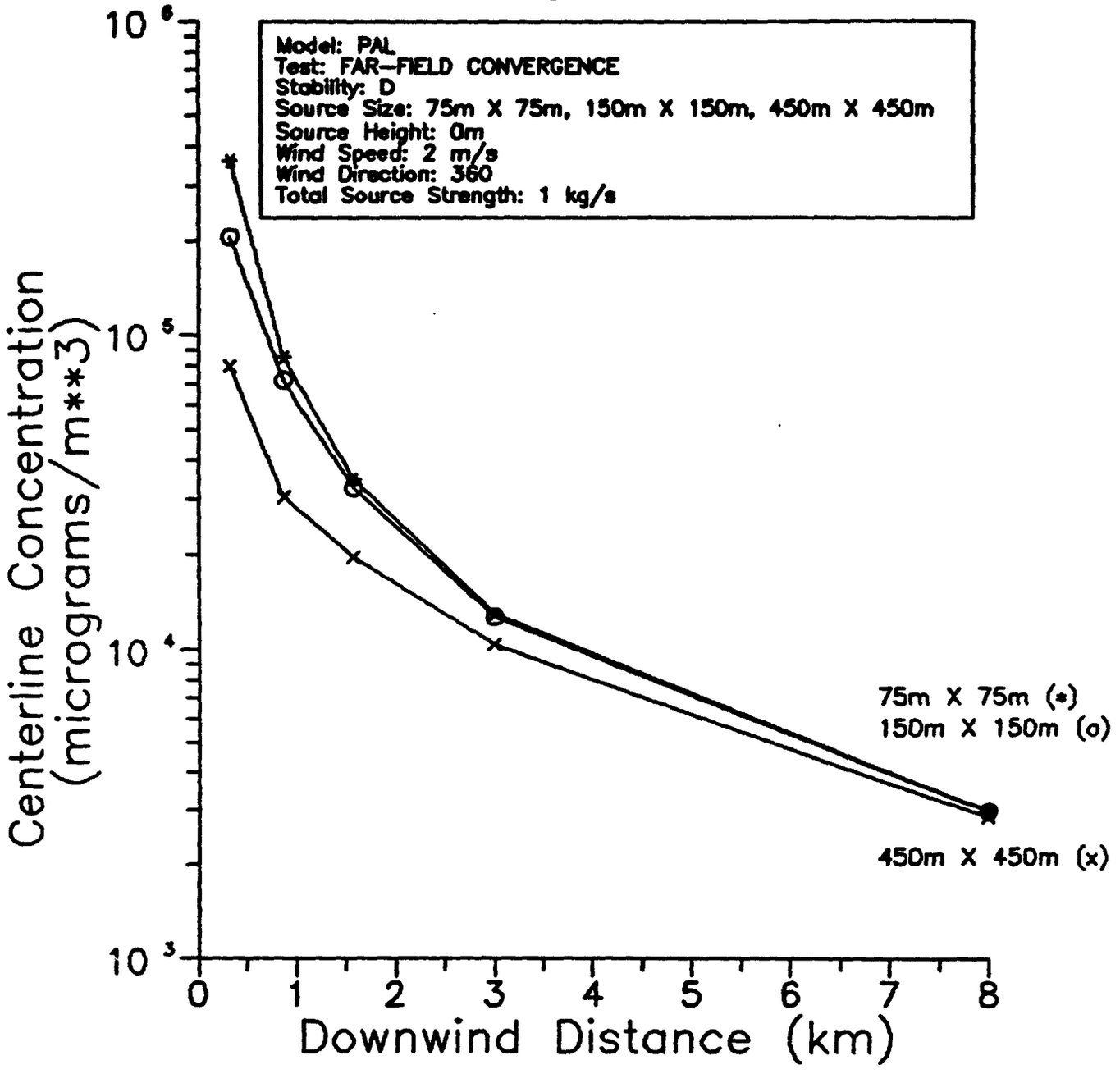
Model: PAL
Test: FAR-FIELD CONVERGENCE
Stability: D
Source Size: 75m X 75m, 150m X 150m, 450m X 450m
Source Height: 0m
Wind Speed: 2 m/s
Wind Direction: 360
Total Source Strength: 1 kg/s
Centerline Concentration (micrograms/m**3)
10 6
10 5
10 4
10 3
0
1
2
3
4
5
6
7
8
Downwind Distance (km)
75m X 75m (*)
150m X 150m (o)
450m X 450m (x)

Figure 3–26

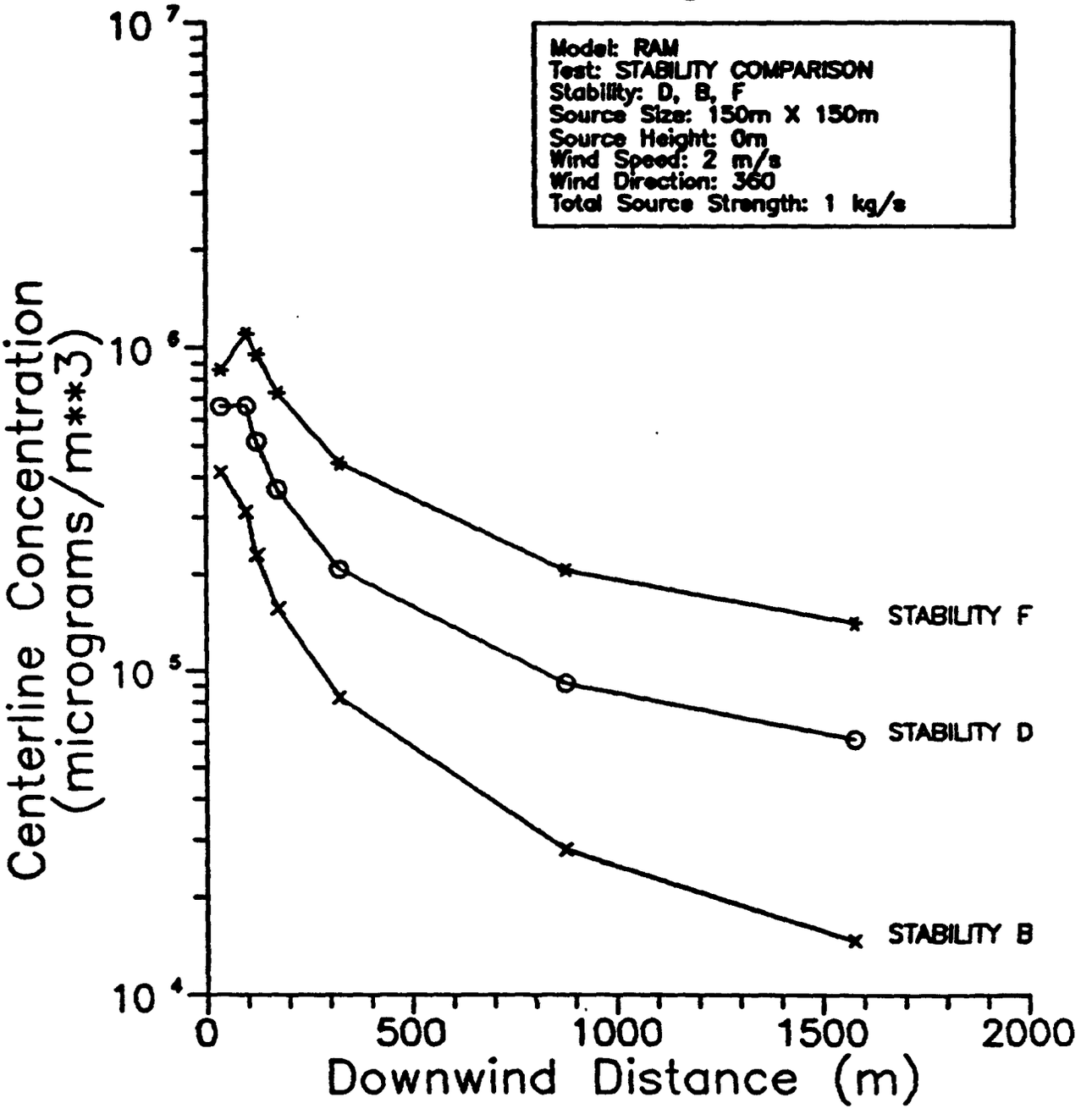
Model: RAM
Test: STABILITY COMPARISON
Stability: D, B, F
Source Size: 150m X 150m
Source Height: 0m
Wind Speed: 2 m/s
Wind Direction: 360
Total Source Strength: 1 kg/s
Centerline Concentration (micrograms/m**3)
10 7
10 6
10 5
10 4
0
500
1000
1500
2000
Downwind Distance (m)
STABILITY F
STABILITY D
STABILITY B

Figure 3-27

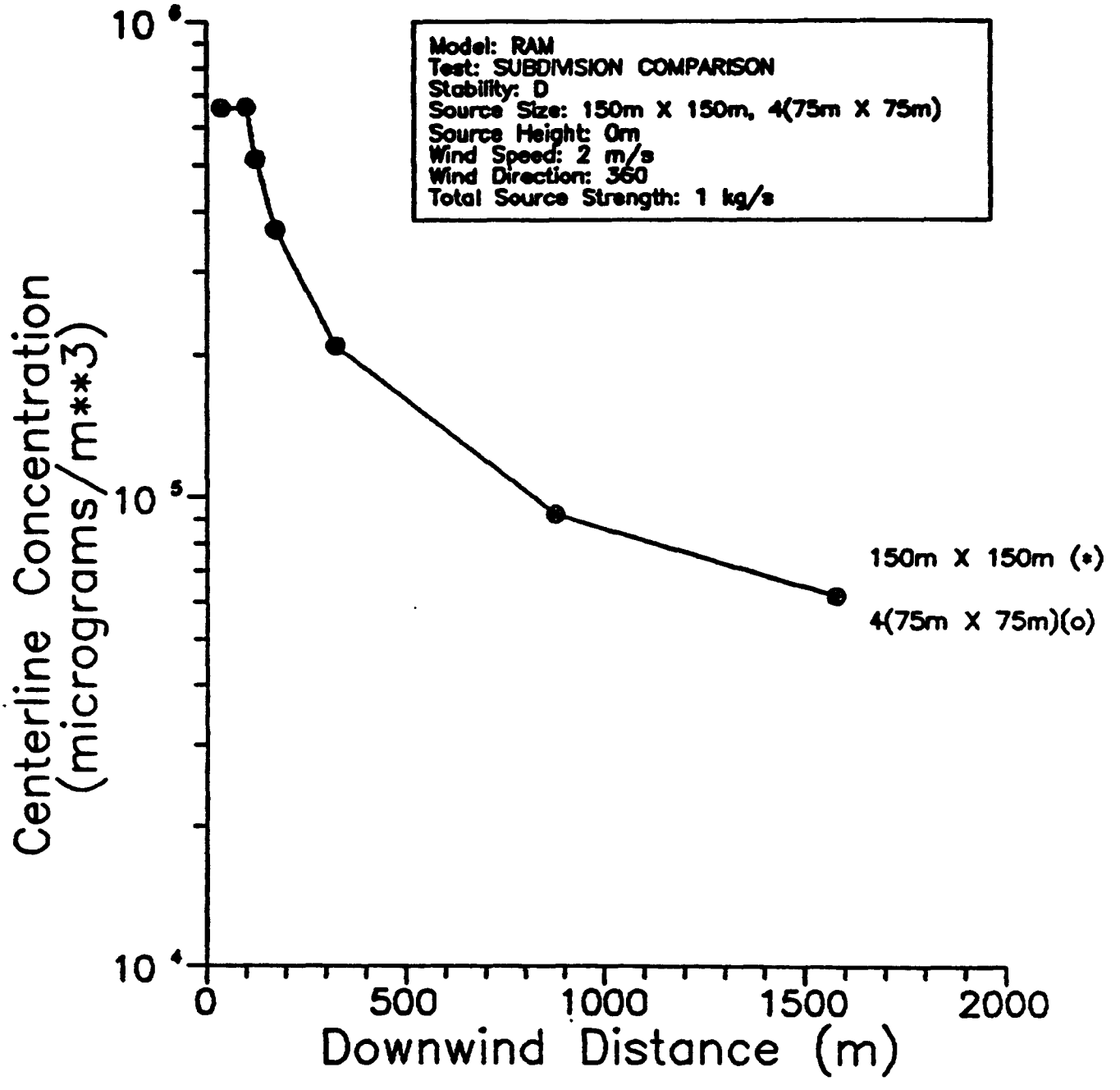
Model: RAM
Test: SUBDIVISION COMPARISON
Stability: D
Source Size: 150m X 150m, 4(75m X 75m)
Source Height: 0m
Wind Speed: 2 m/s
Wind Direction: 360
Total Source Strength: 1 kg/s
Centerline Concentration (micrograms/m**3)
10 6
10 5
10 4
0
500
1000
1500
2000
Downwind Distance (m)
150m X 150m (*)
4(75m X 75m)(o)

Figure 3–28

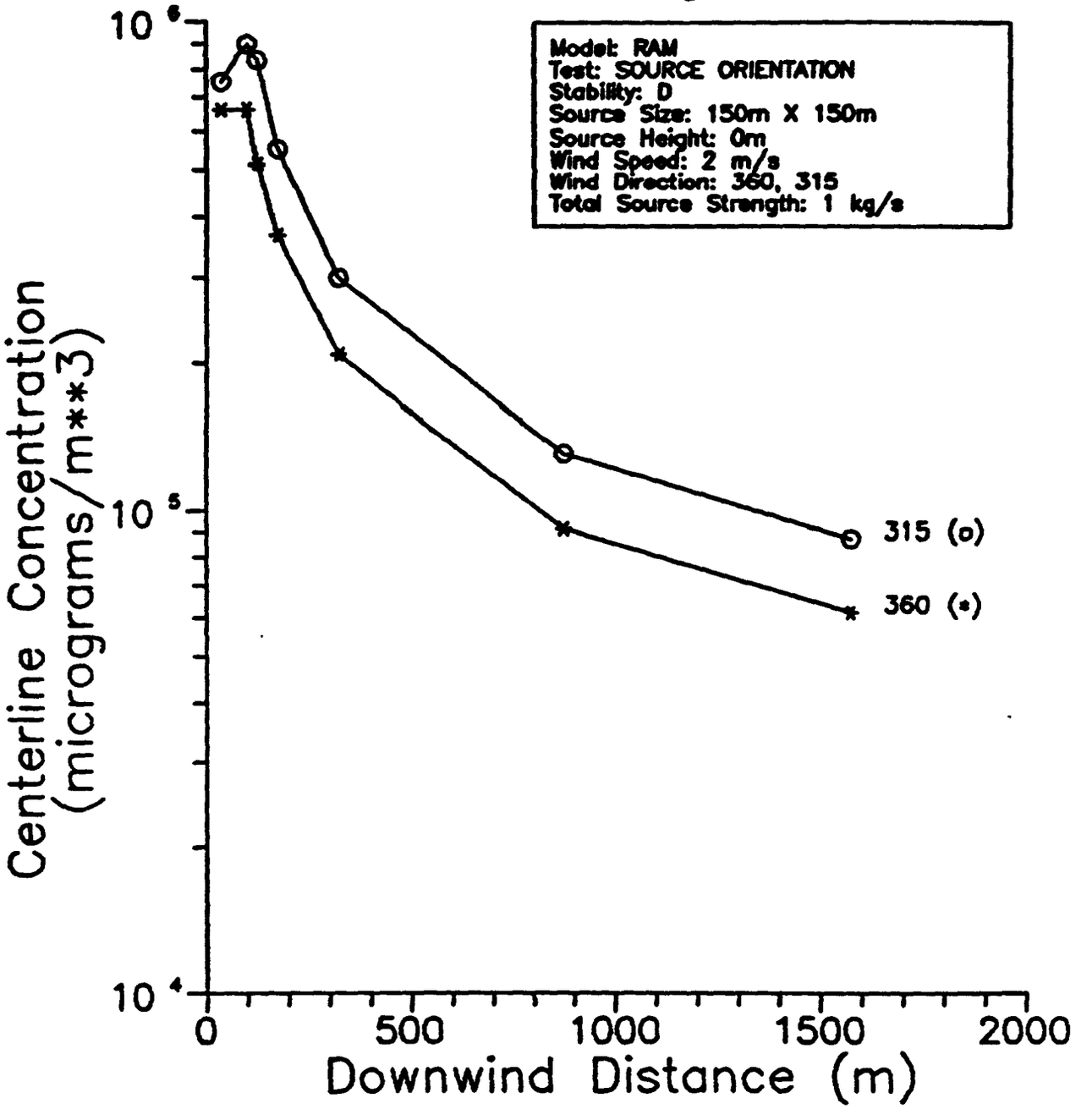
Model: RAM
Test: SOURCE ORIENTATION
Stability: D
Source Size: 150m X 150m
Source Height: 0m
Wind Speed: 2 m/s
Wind Direction: 360, 315
Total Source Strength: 1 kg/s
Centerline Concentration (micrograms/m**3)
10 6
10 5
10 4
0
500
1000
1500
2000
Downwind Distance (m)
315 (o)
360 (*)

Figure 3-29

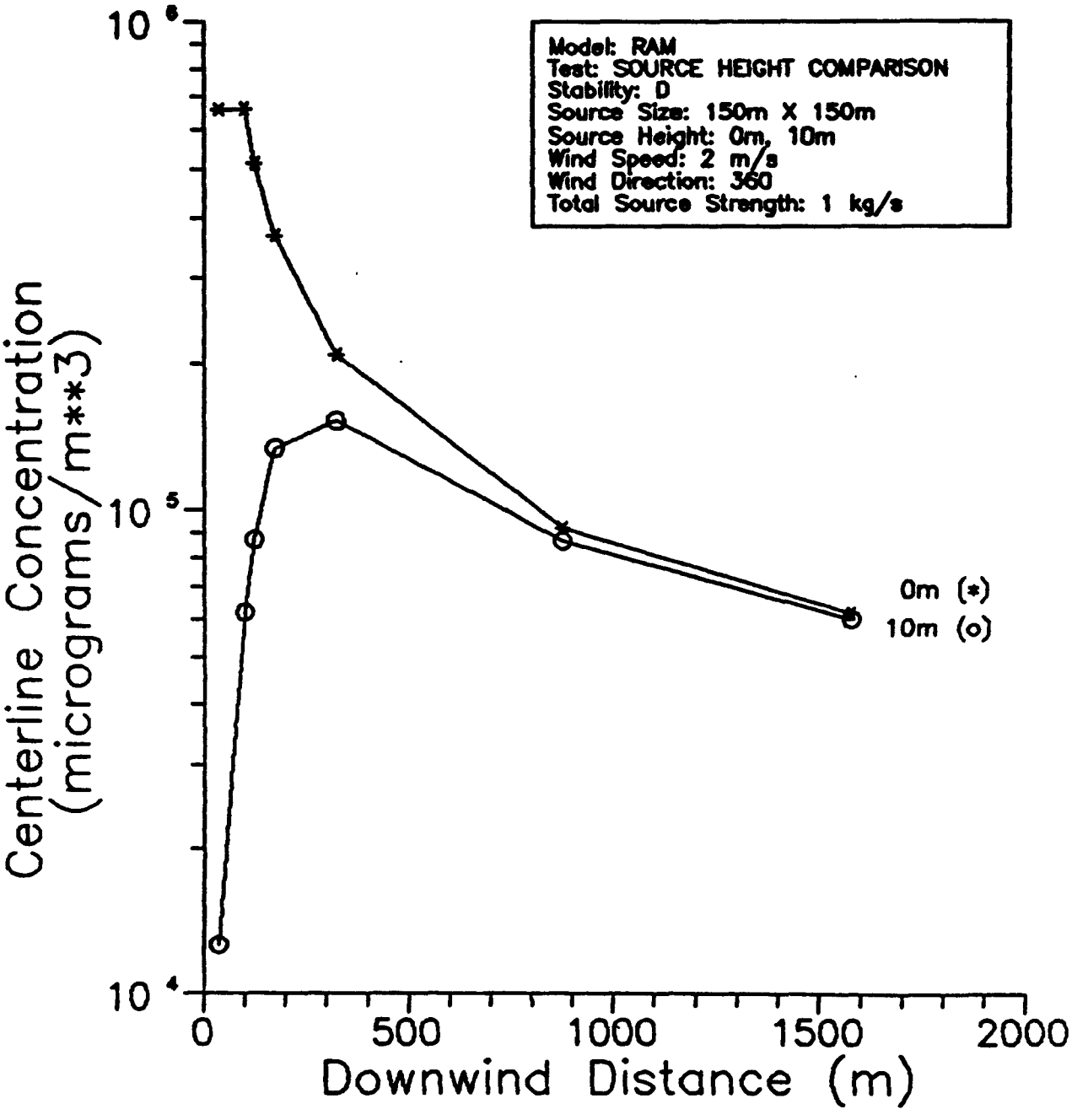
Model: RAM
Test: SOURCE HEIGHT COMPARISON
Stability: D
Source Size: 150m X 150m
Source Height: 0m, 10m
Wind Speed: 2 m/s
Wind Direction: 360
Total Source Strength: 1 kg/s
Centerline Concentration (micrograms/m**3)
10 6
10 5
10 4
0m (*)
10m (o)
0
500
1000
1500
2000
Downwind Distance (m)

Figure 3-30

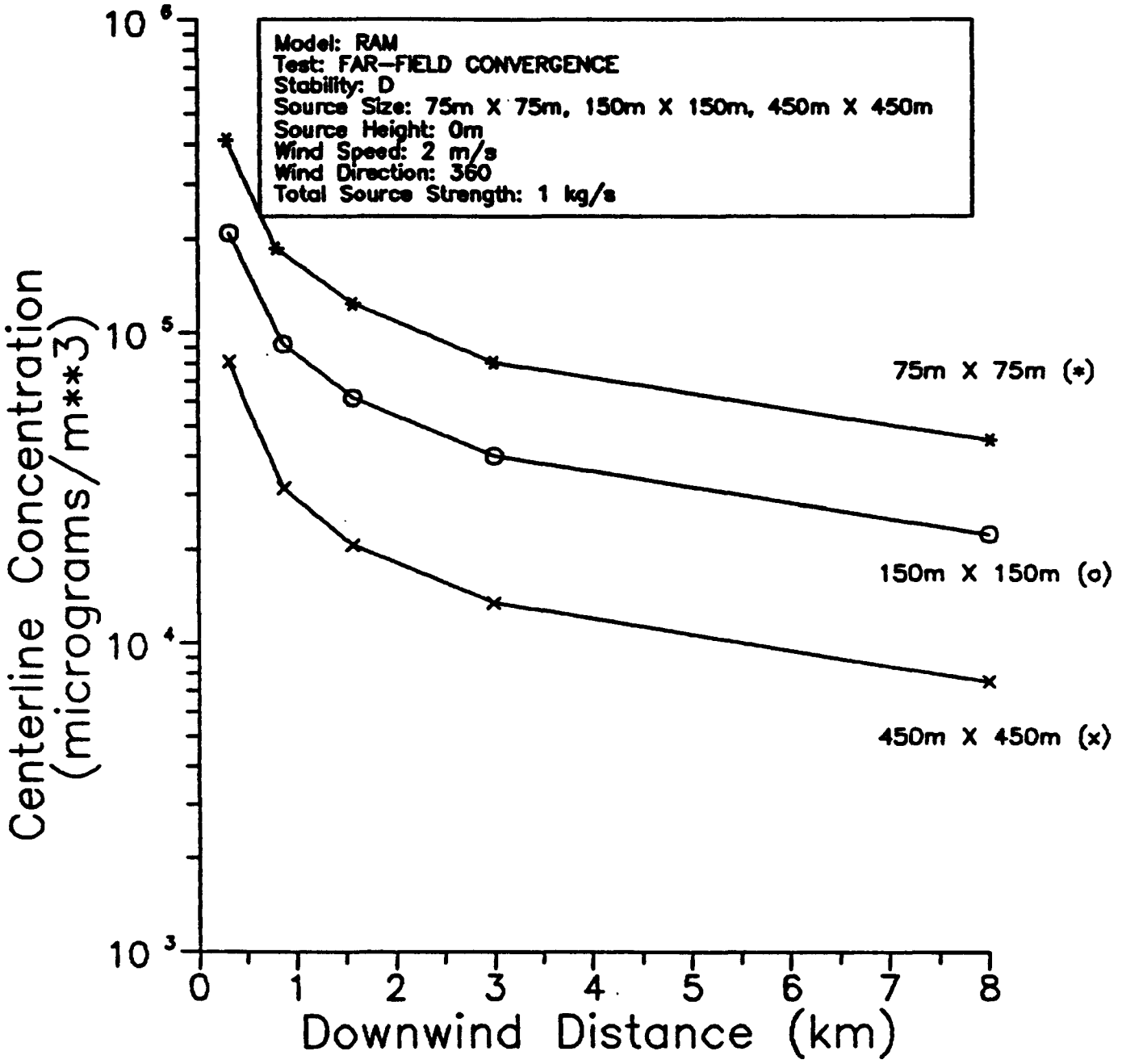
Model: RAM
Test: FAR-FIELD CONVERGENCE
Stability: D
Source Size: 75m X 75m, 150m X 150m, 450m X 450m
Source Height: 0m
Wind Speed: 2 m/s
Wind Direction: 360
Total Source Strength: 1 kg/s
Centerline Concentration (micrograms/m**3)
10 6
10 5
10 4
10 3
75m X 75m (*)
150m X 150m (o)
450m X 450m (x)
0
1
2
3
4
5
6
7
8
Downwind Distance (km)

Figure 3-31

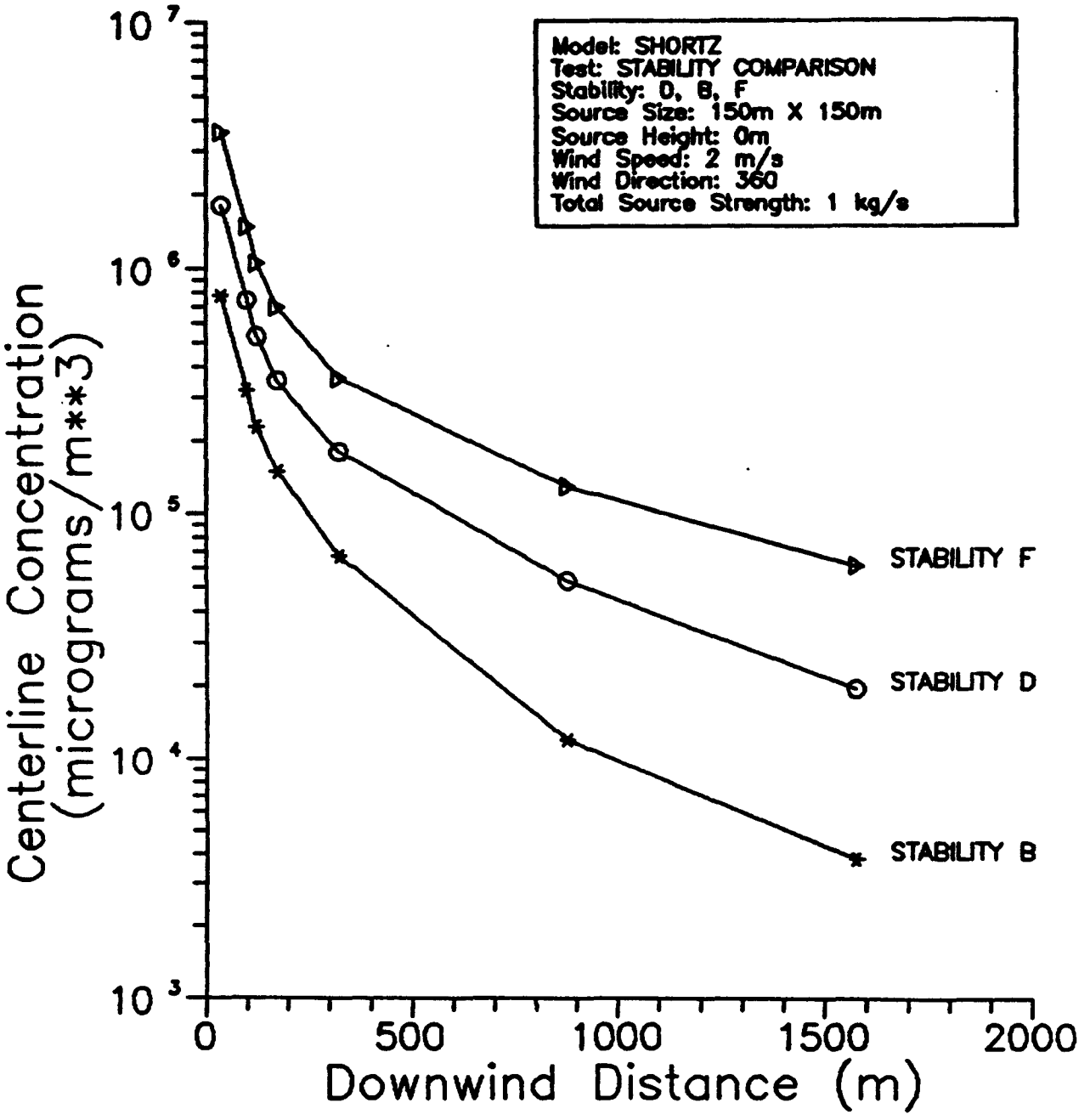
Model: SHORTZ
Test: STABILITY COMPARISON
Stability: D, B, F
Source Size: 150m X 150m
Source Height: 0m
Wind Speed: 2 m/s
Wind Direction: 360
Total Source Strength: 1 kg/s
Centerline Concentration (micrograms/m**3)
10 7
10 6
10 5
10 4
10 3
0
500
1000
1500
2000
Downwind Distance (m)
STABILITY F
STABILITY D
STABILITY B

Figure 3-32

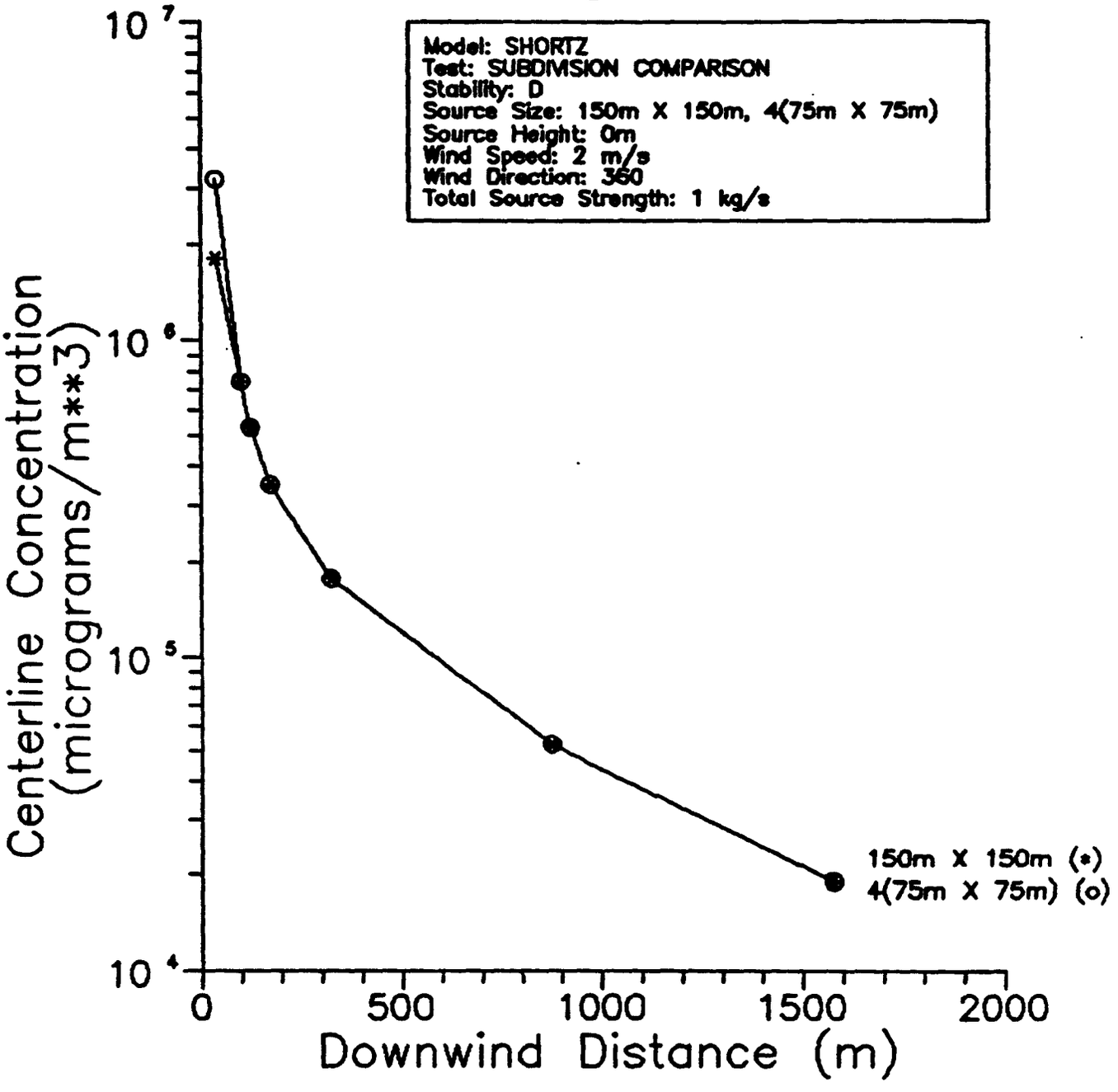
Model: SHORTZ
Test: SUBDIVISION COMPARISON
Stability: D
Source Size: 150m X 150m, 4(75m X 75m)
Source Height: 0m
Wind Speed: 2 m/s
Wind Direction: 360
Total Source Strength: 1 kg/s
Centerline Concentration (micrograms/m**3)
10 7
10 6
10 5
10 4
0
500
1000
1500
2000
Downwind Distance (m)
150m X 150m (*)
4(75m X 75m) (o)

Figure 3-33

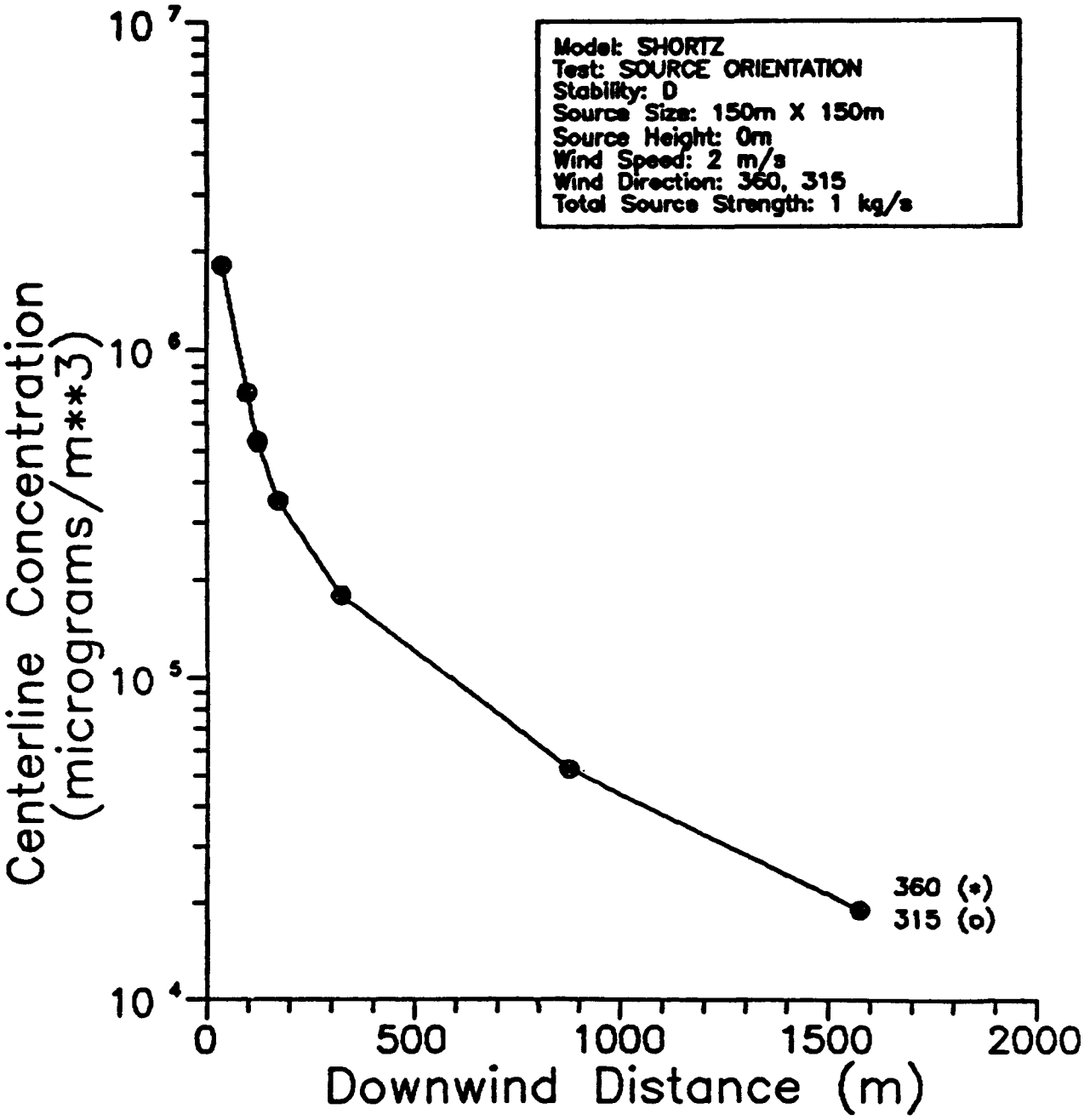
Model: SHORTZ
Test: SOURCE ORIENTATION
Stability: D
Source Size: 150m X 150m
Source Height: 0m
Wind Speed: 2 m/s
Wind Direction: 360, 315
Total Source Strength: 1 kg/s
Centerline Concentration (micrograms/m**3)
10 7
10 6
10 5
10 4
0
500
1000
1500
2000
Downwind Distance (m)
360 (*)
315 (o)

Figure 3-34

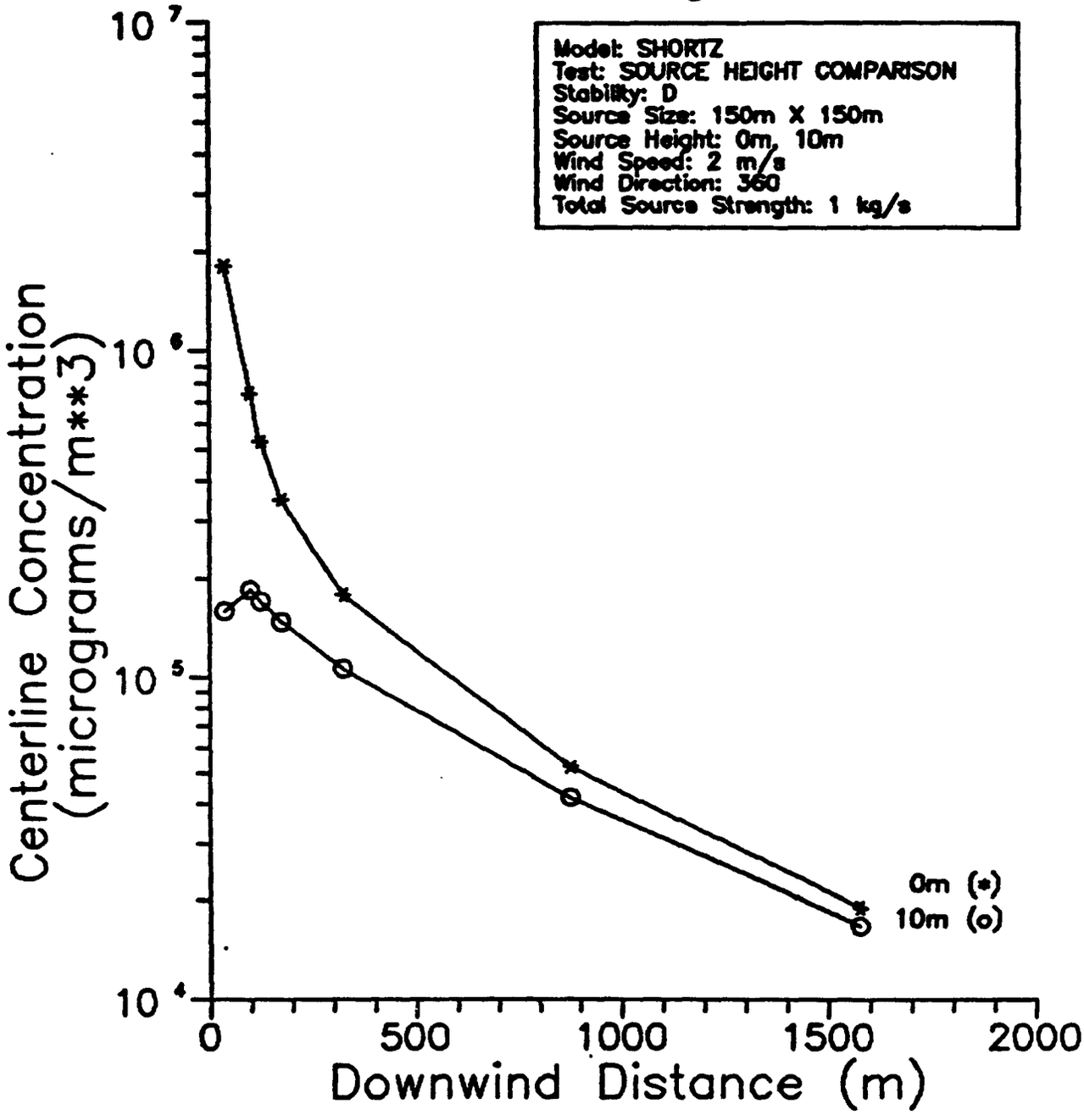
Model: SHORTZ
Test: SOURCE HEIGHT COMPARISON
Stability: D
Source Size: 150m X 150m
Source Height: 0m, 10m
Wind Speed: 2 m/s
Wind Direction: 360
Total Source Strength: 1 kg/s
Centerline Concentration (micrograms/m**3)
10 7
10 6
10 5
10 4
0
500
1000
1500
2000
Downwind Distance (m)
0m (*)
10m (o)

Figure 3–35

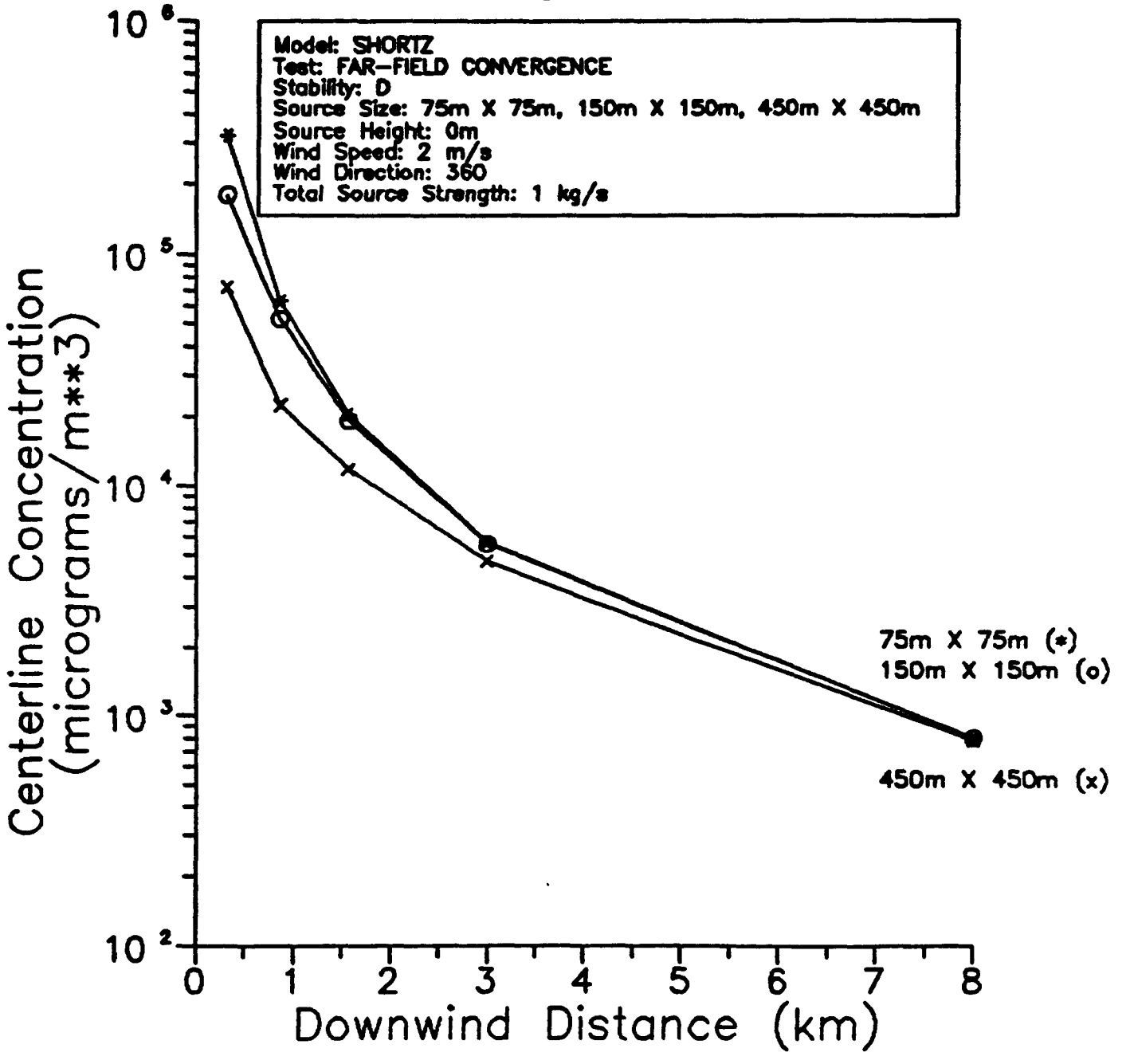
Model: SHORTZ
Test: FAR–FIELD CONVERGENCE
Stability: D
Source Size: 75m X 75m, 150m X 150m, 450m X 450m
Source Height: 0m
Wind Speed: 2 m/s
Wind Direction: 360
Total Source Strength: 1 kg/s
Centerline Concentration (micrograms/m**3)
10 6
10 5
10 4
10 3
10 2
0
1
2
3
4
5
6
7
8
Downwind Distance (km)
75m X 75m (*)
150m X 150m (o)
450m X 450m (x)

Figure 3–36

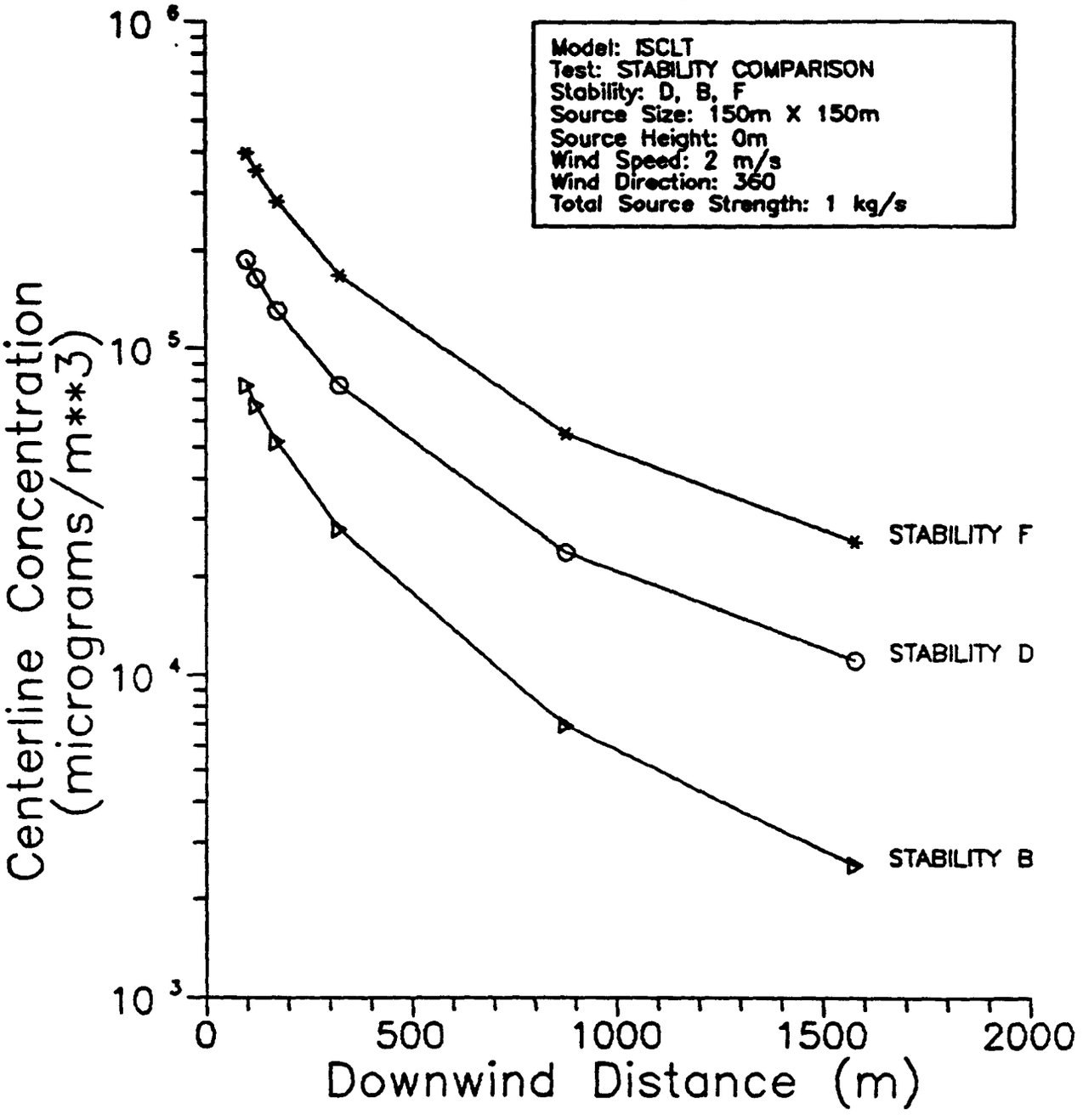
Model: ISCLT
Test: STABILITY COMPARISON
Stability: D, B, F
Source Size: 150m X 150m
Source Height: 0m
Wind Speed: 2 m/s
Wind Direction: 360
Total Source Strength: 1 kg/s
Centerline Concentration (micrograms/m**3)
10 6
10 5
10 4
10 3
STABILITY F
STABILITY D
STABILITY B
0
500
1000
1500
2000
Downwind Distance (m)

Figure 3-37

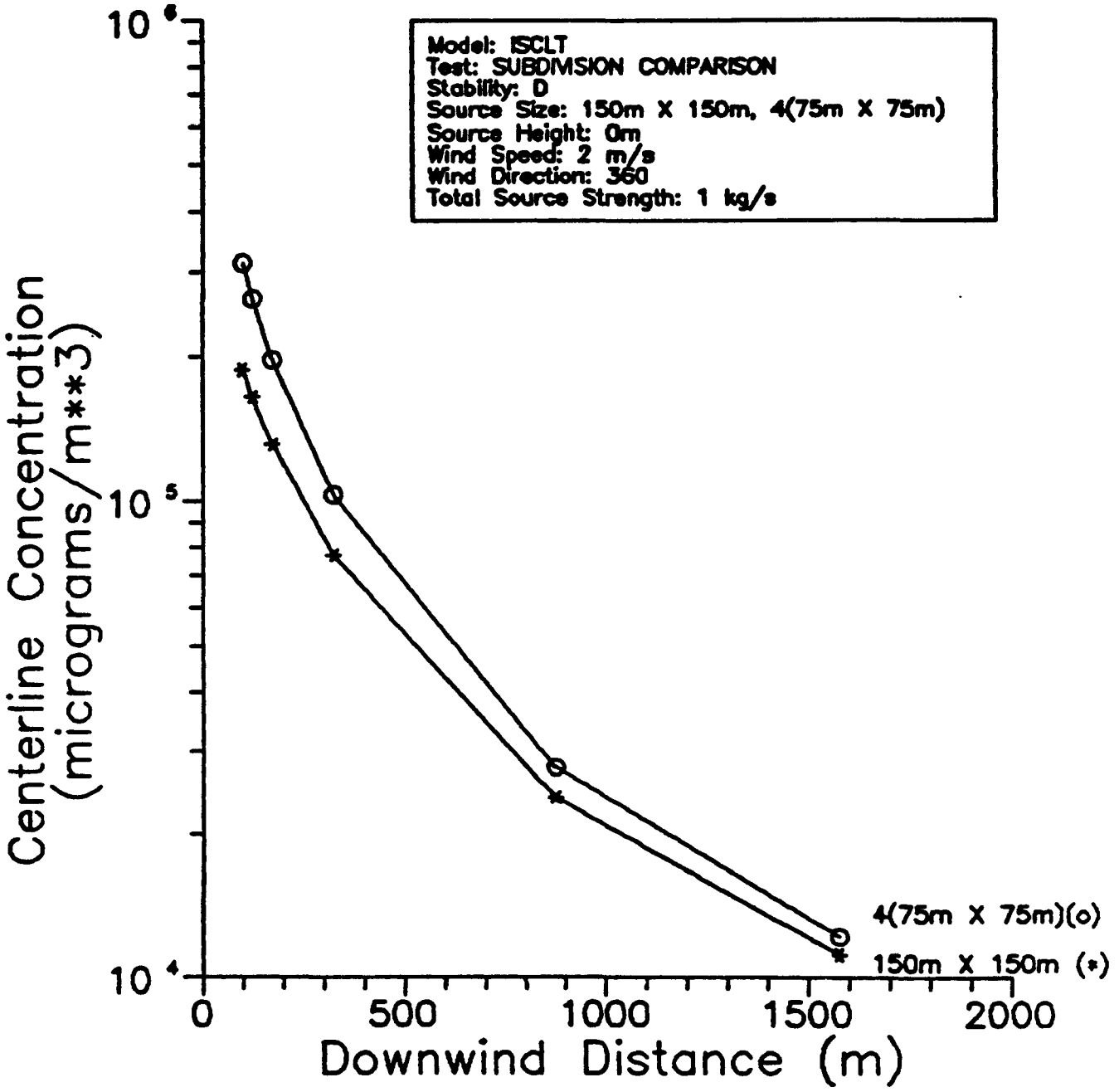
Model: ISCLT
Test: SUBDIVISION COMPARISON
Stability: D
Source Size: 150m X 150m, 4(75m X 75m)
Source Height: 0m
Wind Speed: 2 m/s
Wind Direction: 360
Total Source Strength: 1 kg/s
Centerline Concentration (micrograms/m**3)
10 6
10 5
10 4
0
500
1000
1500
2000
Downwind Distance (m)
4(75m X 75m)(o)
150m X 150m (*)

Figure 3-38

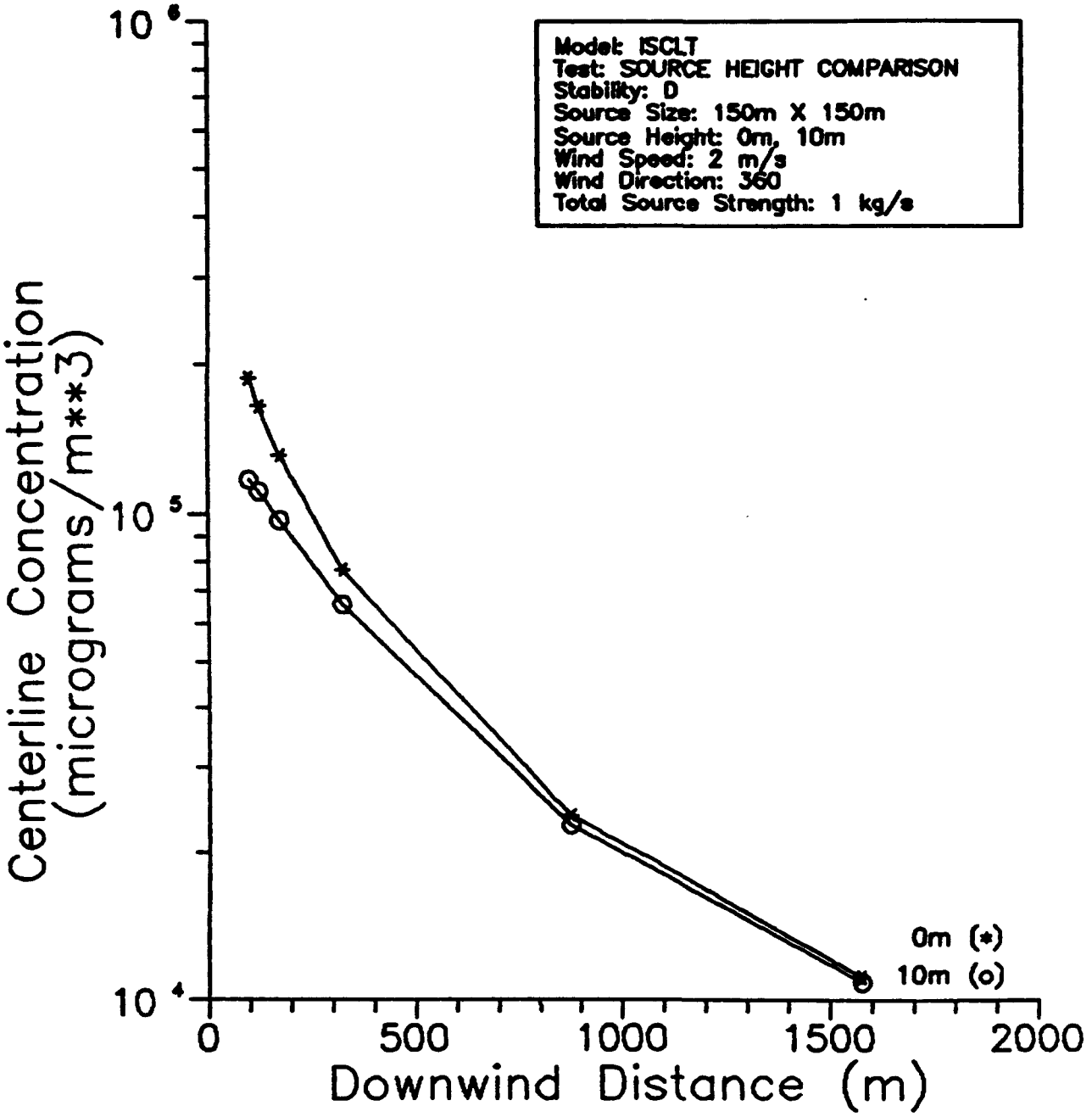
Model: ISCLT
Test: SOURCE HEIGHT COMPARISON
Stability: D
Source Size: 150m X 150m
Source Height: 0m, 10m
Wind Speed: 2 m/s
Wind Direction: 360
Total Source Strength: 1 kg/s
Centerline Concentration (micrograms/m**3)
10 6
10 5
10 4
0
500
1000
1500
2000
Downwind Distance (m)
0m (*)
10m (o)

Figure 3-39

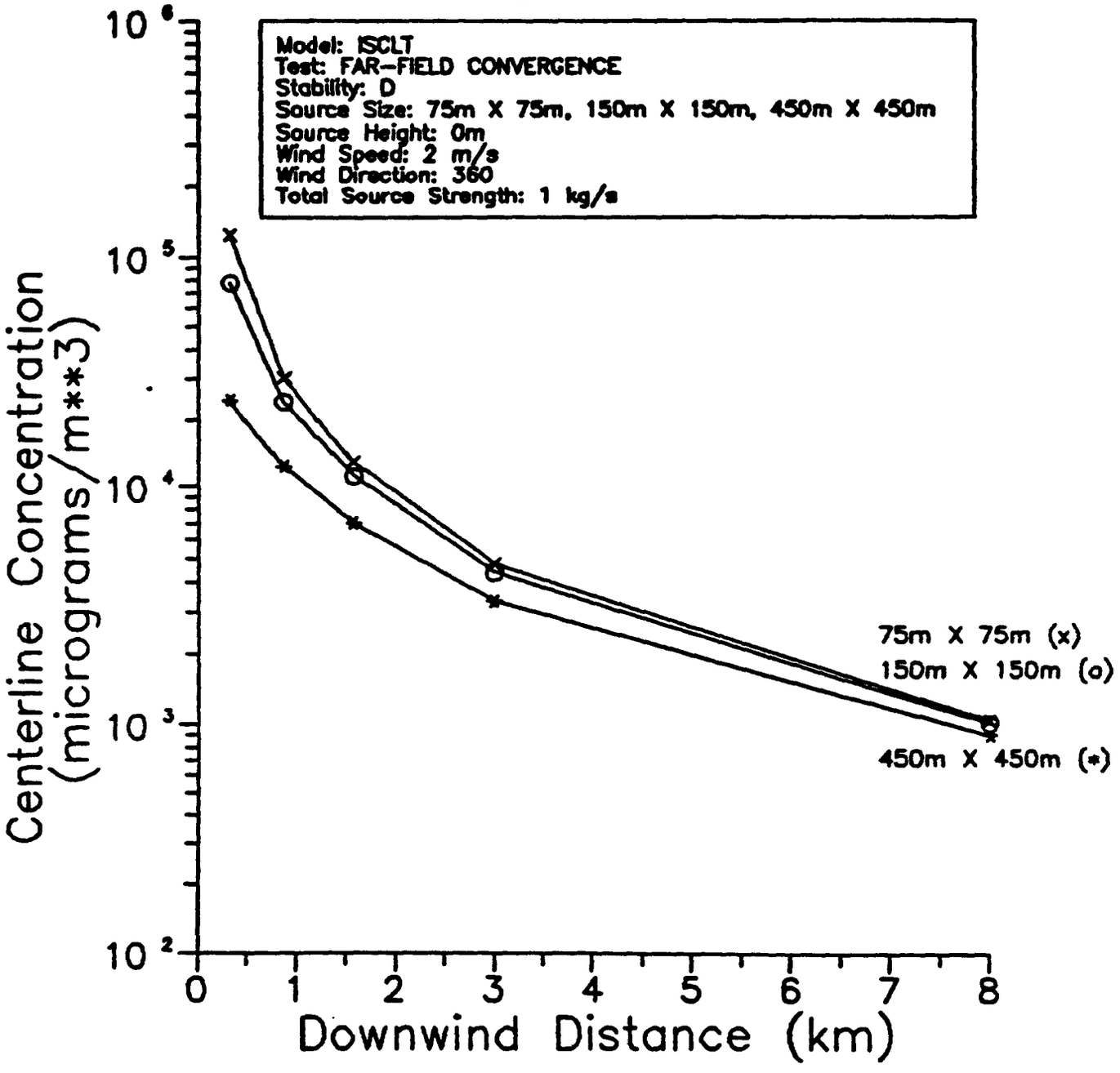
Model: ISCLT
Test: FAR-FIELD CONVERGENCE
Stability: D
Source Size: 75m X 75m, 150m X 150m, 450m X 450m
Source Height: 0m
Wind Speed: 2 m/s
Wind Direction: 360
Total Source Strength: 1 kg/s
Centerline Concentration (micrograms/m**3)
10 6
10 5
10 4
10 3
10 2
0
1
2
3
4
5
6
7
8
Downwind Distance (km)
75m X 75m (x)
150m X 150m (o)
450m X 450m (*)

Figure 3-40

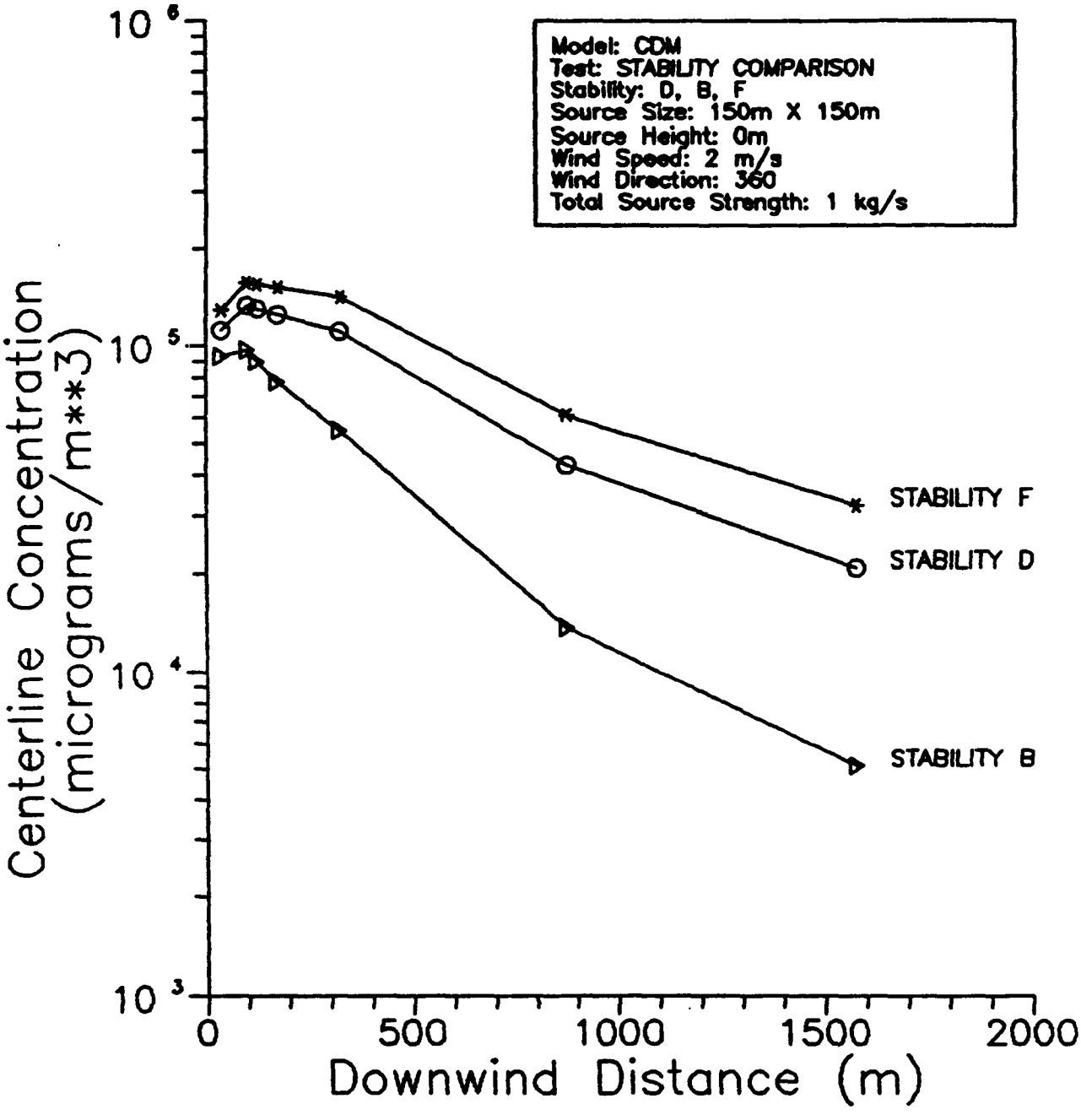
Model: CDM
Test: STABILITY COMPARISON
Stability: D, B, F
Source Size: 150m X 150m
Source Height: 0m
Wind Speed: 2 m/s
Wind Direction: 360
Total Source Strength: 1 kg/s
Centerline Concentration (micrograms/m**3)
10 6
10 5
10 4
10 3
0
500
1000
1500
2000
Downwind Distance (m)
STABILITY F
STABILITY D
STABILITY B

Figure 3-41

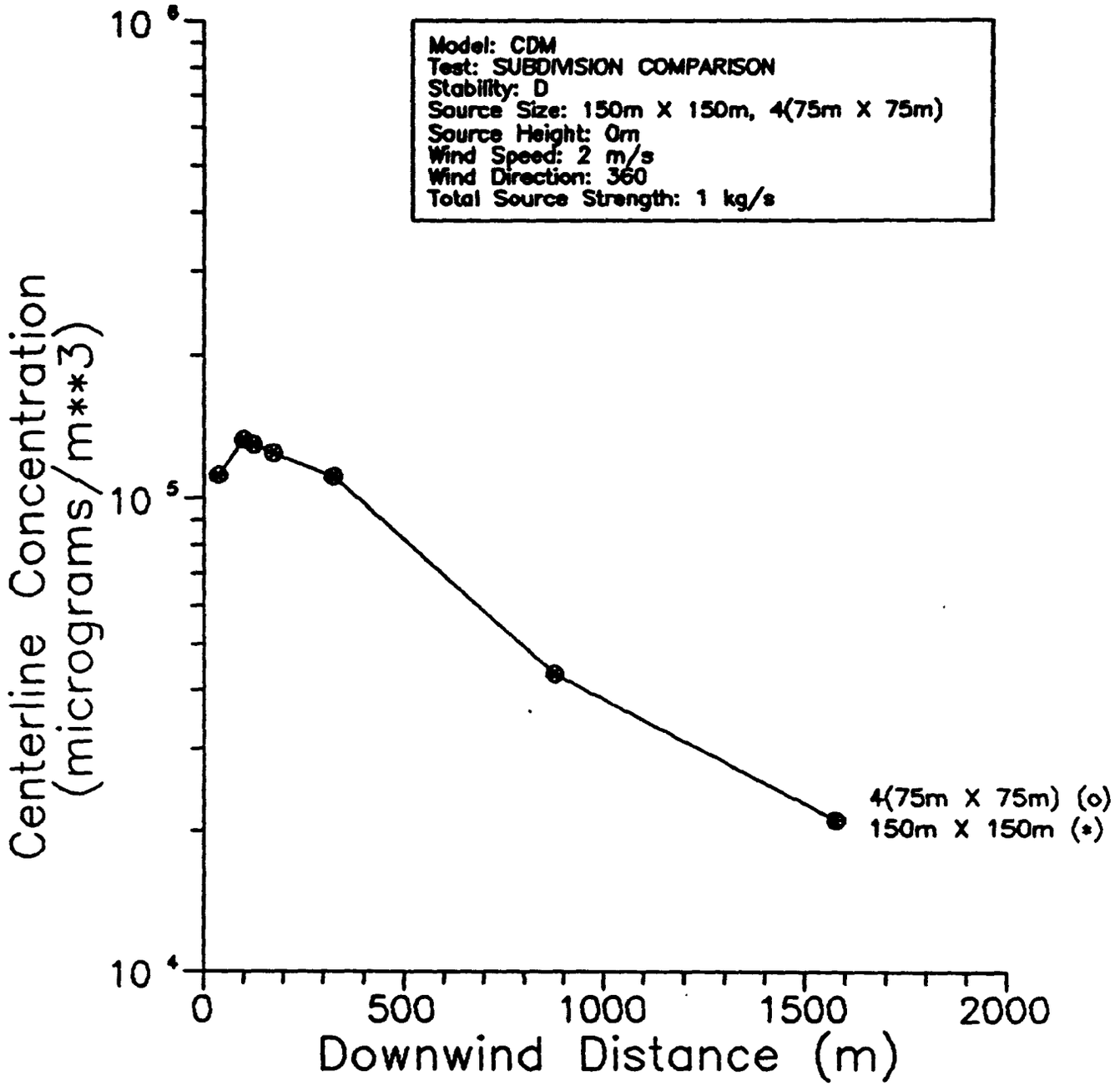
Model: CDM
Test: SUBDIVISION COMPARISON
Stability: D
Source Size: 150m X 150m, 4(75m X 75m)
Source Height: 0m
Wind Speed: 2 m/s
Wind Direction: 360
Total Source Strength: 1 kg/s
Centerline Concentration (micrograms/m**3)
10 6
10 5
10 4
0
500
1000
1500
2000
Downwind Distance (m)
4(75m X 75m) (o)
150m X 150m (*)

Figure 3-42

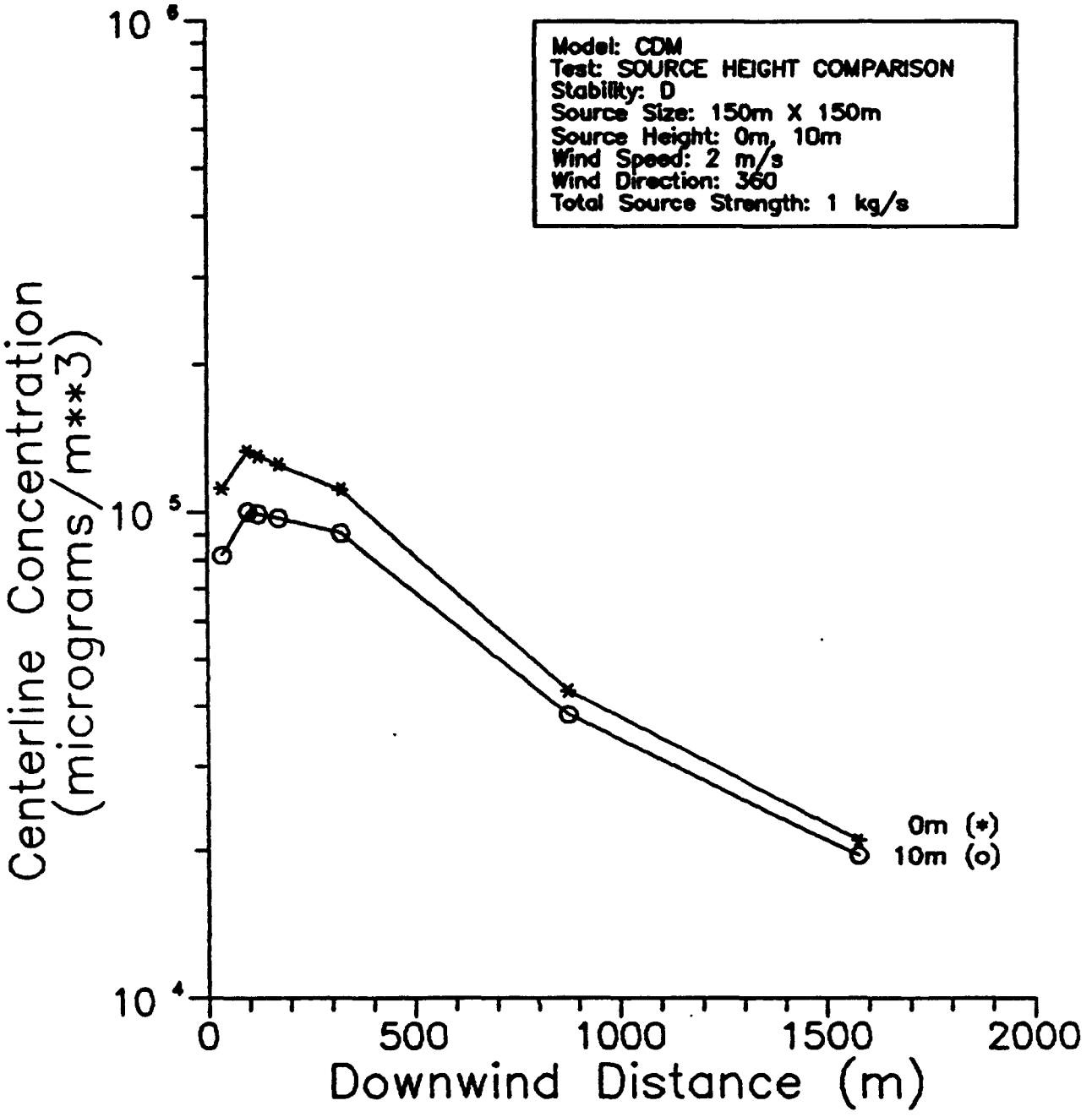
Model: CDM
Test: SOURCE HEIGHT COMPARISON
Stability: D
Source Size: 150m X 150m
Source Height: 0m, 10m
Wind Speed: 2 m/s
Wind Direction: 360
Total Source Strength: 1 kg/s
Centerline Concentration (micrograms/m**3)
10 6
10 5
10 4
0
500
1000
1500
2000
Downwind Distance (m)
0m (*)
10m (o)

Figure 3-43

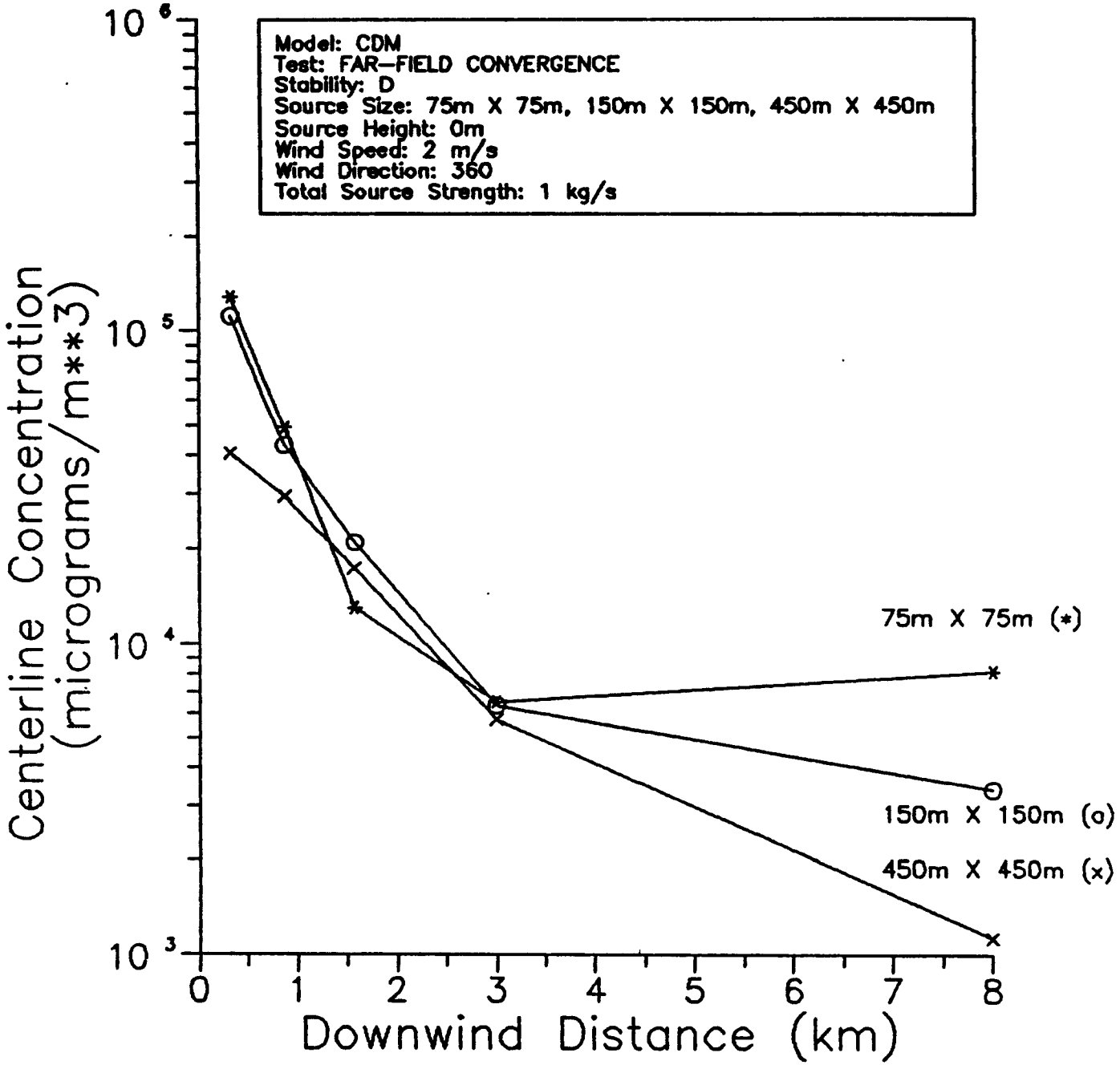
Model: CDM
Test: FAR-FIELD CONVERGENCE
Stability: D
Source Size: 75m X 75m, 150m X 150m, 450m X 450m
Source Height: 0m
Wind Speed: 2 m/s
Wind Direction: 360
Total Source Strength: 1 kg/s
Centerline Concentration (micrograms/m**3)
10 6
10 5
10 4
10 3
0
1
2
3
4
5
6
7
8
Downwind Distance (km)
75m X 75m (*)
150m X 150m (o)
450m X 450m (x)

Figure 3-44

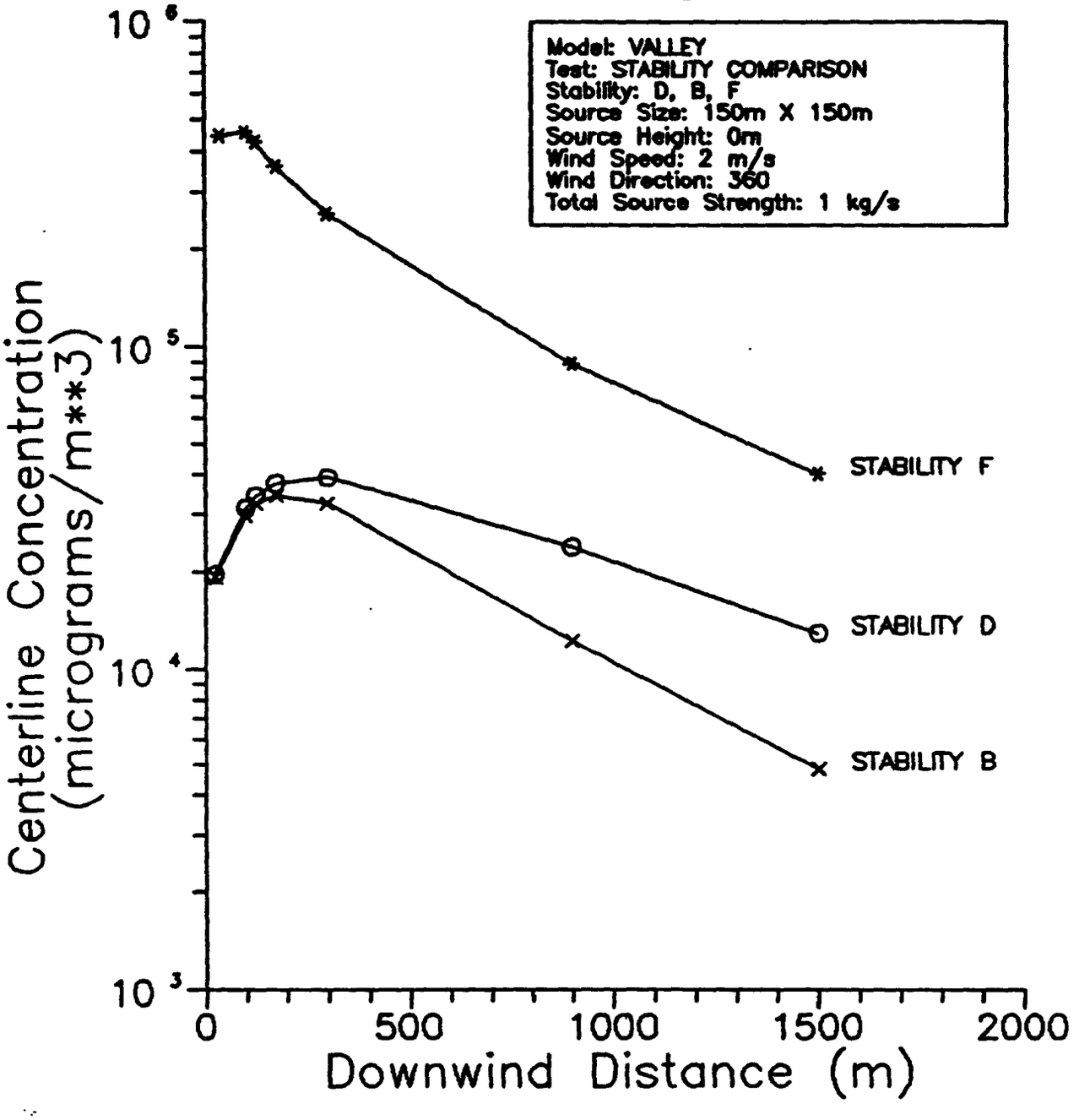
Model: VALLEY
Test: STABILITY COMPARISON
Stability: D, B, F
Source Size: 150m X 150m
Source Height: 0m
Wind Speed: 2 m/s
Wind Direction: 360
Total Source Strength: 1 kg/s
STABILITY F
STABILITY D
STABILITY B
Centerline Concentration (micrograms/m**3)
10 6
10 5
10 4
10 3
0
500
1000
1500
2000
Downwind Distance (m)

Figure 3-45

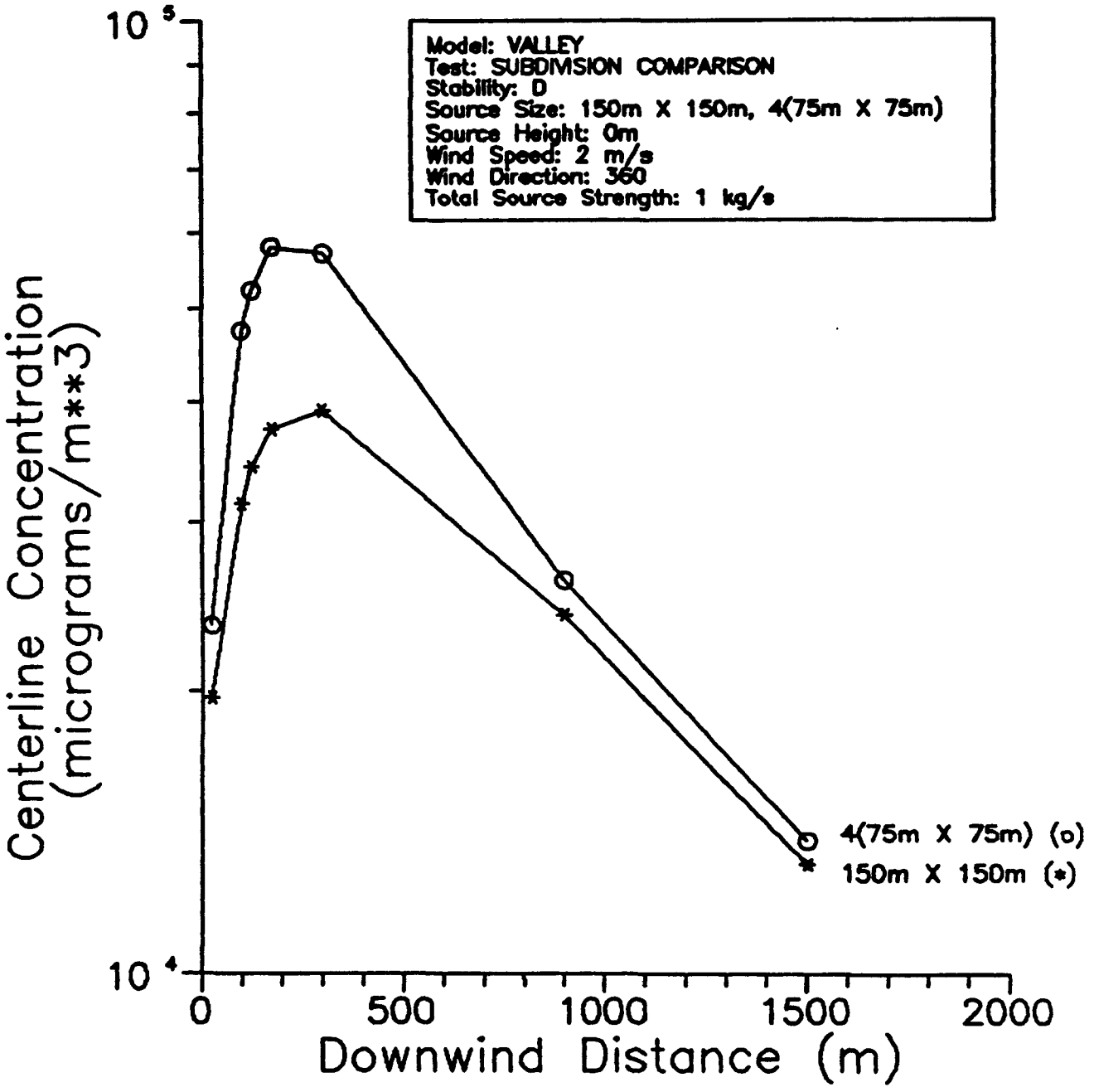
Model: VALLEY
Test: SUBDIVISION COMPARISON
Stability: D
Source Size: 150m X 150m, 4(75m X 75m)
Source Height: 0m
Wind Speed: 2 m/s
Wind Direction: 360
Total Source Strength: 1 kg/s
10 5
10 4
Centerline Concentration (micrograms/m**3)
0
500
1000
1500
2000
Downwind Distance (m)
4(75m X 75m) (o)
150m X 150m (*)

Figure 3-46

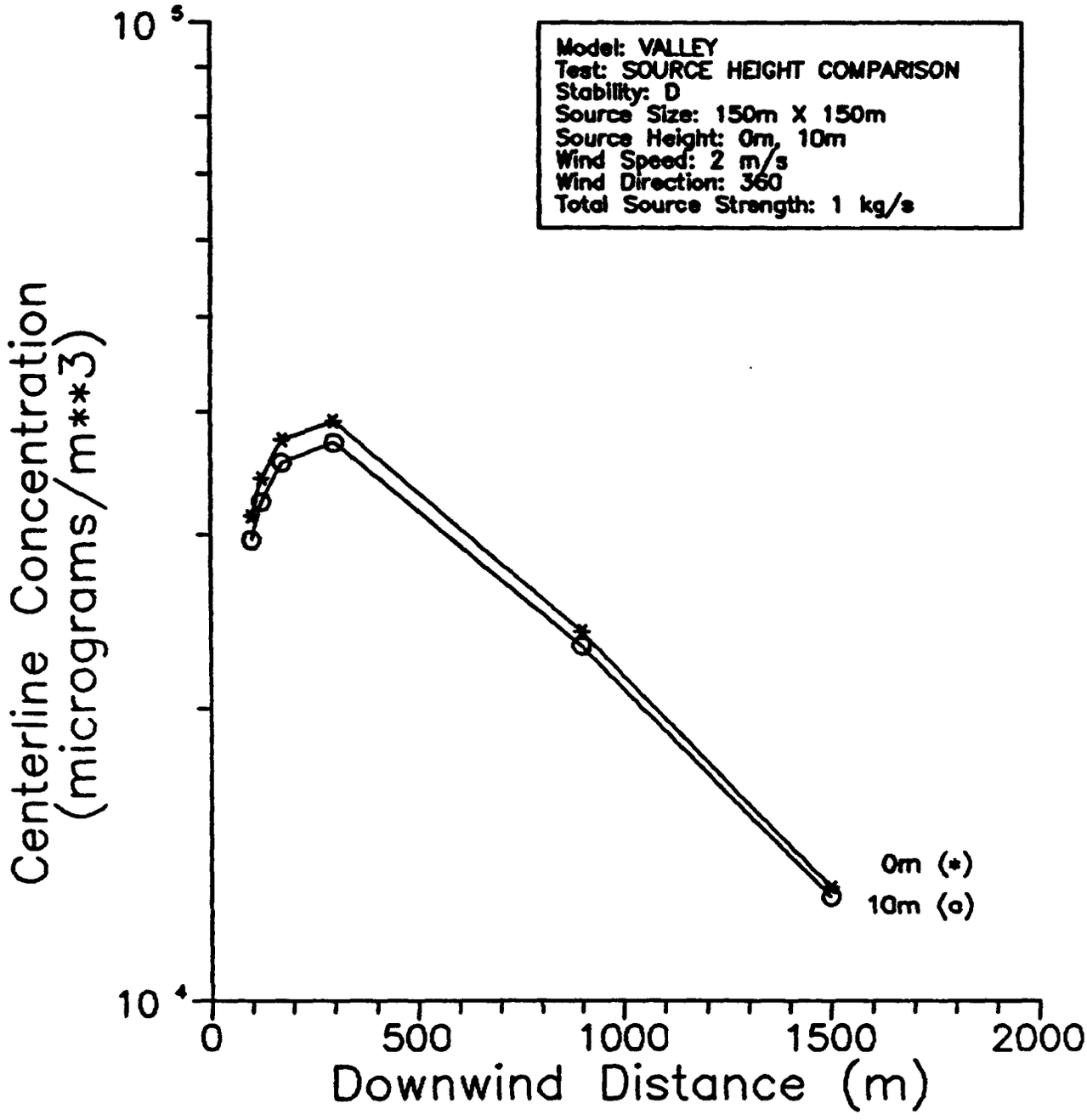
Model: VALLEY
Test: SOURCE HEIGHT COMPARISON
Stability: D
Source Size: 150m X 150m
Source Height: 0m, 10m
Wind Speed: 2 m/s
Wind Direction: 360
Total Source Strength: 1 kg/s
10 5
10 4
Centerline Concentration (micrograms/m**3)
0
500
1000
1500
2000
Downwind Distance (m)
0m (*)
10m (o)

Figure 3-47

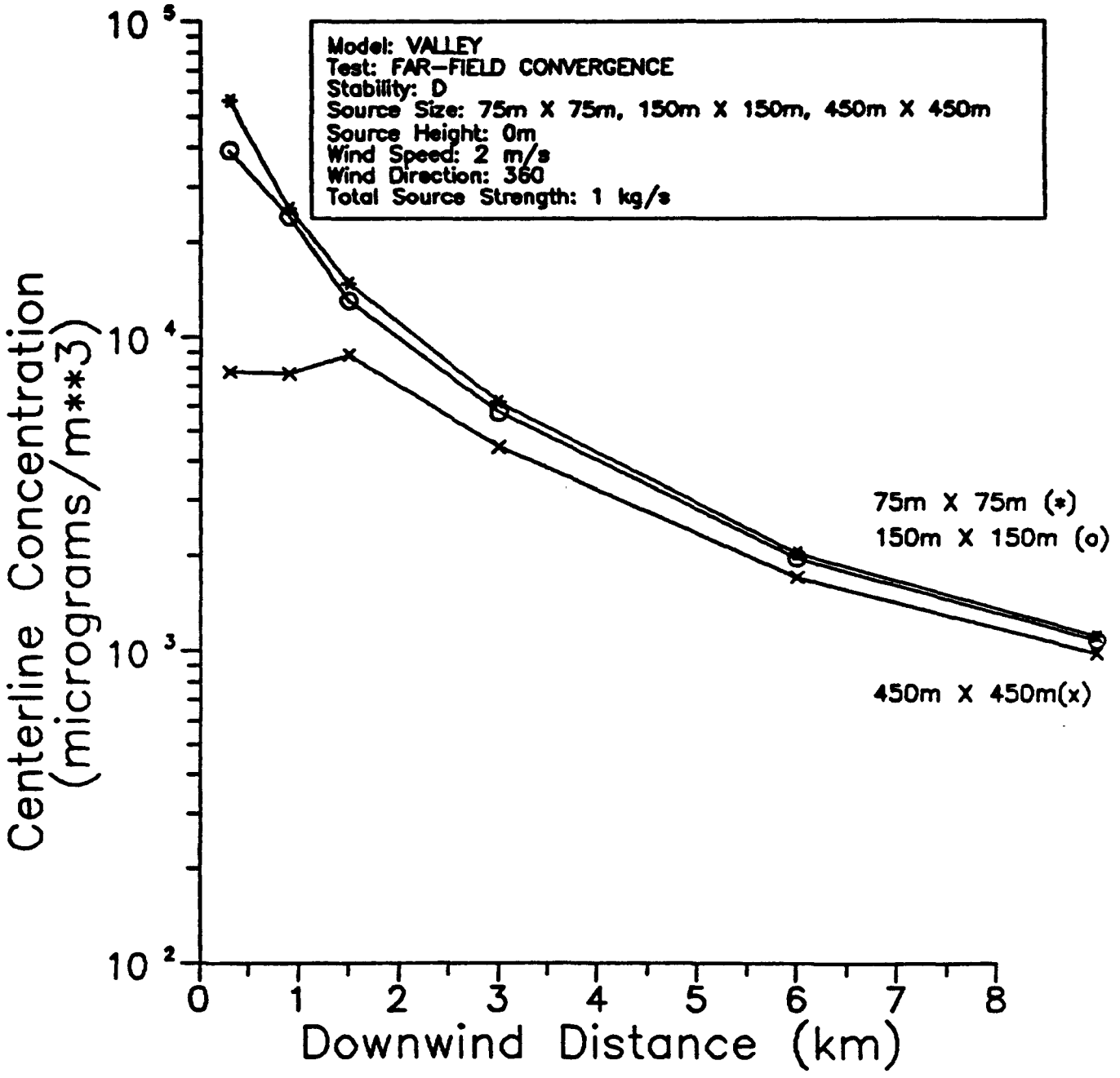
Model: VALLEY
Test: FAR-FIELD CONVERGENCE
Stability: D
Source Size: 75m X 75m, 150m X 150m, 450m X 450m
Source Height: 0m
Wind Speed: 2 m/s
Wind Direction: 360
Total Source Strength: 1 kg/s
75m X 75m (*)
150m X 150m (o)
450m X 450m(x)
Centerline Concentration (micrograms/m**3)
10 5
10 4
10 3
10 2
0 1 2 3 4 5 6 7 8
Downwind Distance (km)

4.0 COMPARISON OF MODEL PREDICTIONS WITH EXPERIMENTAL DATA

Predictions for the short-term area source models have been compared to measured concentrations for an experimental data set involving releases of an inert gaseous tracer within an isolated stand of trees, surrounded by open grassland. These experiments produced a distributed emission source which can be simulated as an area source. Comparisons of observed and predicted concentrations for this small set of experiments provide an informative test of model performance.

4.1 Database Description

A review of available information from field measurement programs characterizing observed concentrations in the vicinity of area source releases was recently carried out as part of a larger effort to identify and acquire databases for the evaluation of air toxics models (Zapert, et al., 1989). The criteria which were used to select databases for model evaluation included the following:

- Reliable emissions data
- Site-specific meteorological measurements
- Adequate spatial resolution of ambient concentrations

No suitable databases representing actual sources of toxic pollutant emissions were identified. In general, measurement programs for actual sources are characterized by uncertain emissions estimates and poor spatial resolution (concentration measurements at only two or three locations).

The five databases chosen for air toxics model evaluation all represent measurement programs with controlled, artificial releases designed to simulate actual pollutant releases. Four of these databases involve dense gas (heavier-than-air) releases and are not suitable for the present study.

The database selected for testing area source models represents a series of tracer experiments conducted in south-central Washington in 1982-83 (Allwine, et al., 1985). The inert gaseous tracer sulfur hexafluoride (SF_6) was released from an array of points within an isolated stand of oak trees. The stand covered an area of 1.5 hectares (15,000 m^2) to an average height of 8 m. The experiments were designed primarily to estimate isoprene emissions from the forest canopy. By measuring SF_6 and isoprene concentrations simultaneously, the isoprene emission rate could be inferred, assuming that SF_6 and isoprene were both emitted uniformly from the canopy. Integrated one-hour concentrations were measured at sampling points approximately 100 m downwind of the release area. Samplers were deployed at different locations depending upon the wind direction. The tracer release was initiated 10 minutes before ambient sampling began, and continued until sampling was completed. Wind speed, wind direction and temperature measurements were also collected during the experiments. A schematic diagram of the experimental configuration is provided in Figure 4-1.

Thirteen tracer experiments from this program were chosen for model evaluation. Three tests were excluded because the wind direction shifted during these experiments and the peak measured concentrations occurred at the end of a line of samplers. Emission characteristics and meteorological conditions for the thirteen selected tests are summarized in Table 4-1. All of the experiments were conducted during the daytime, when isoprene emissions were expected to be highest. Consequently, the tests only represent unstable and neutral conditions. This is a serious limitation for the present application, since worst-case short-term impacts from near-ground emission sources are expected during stable conditions.

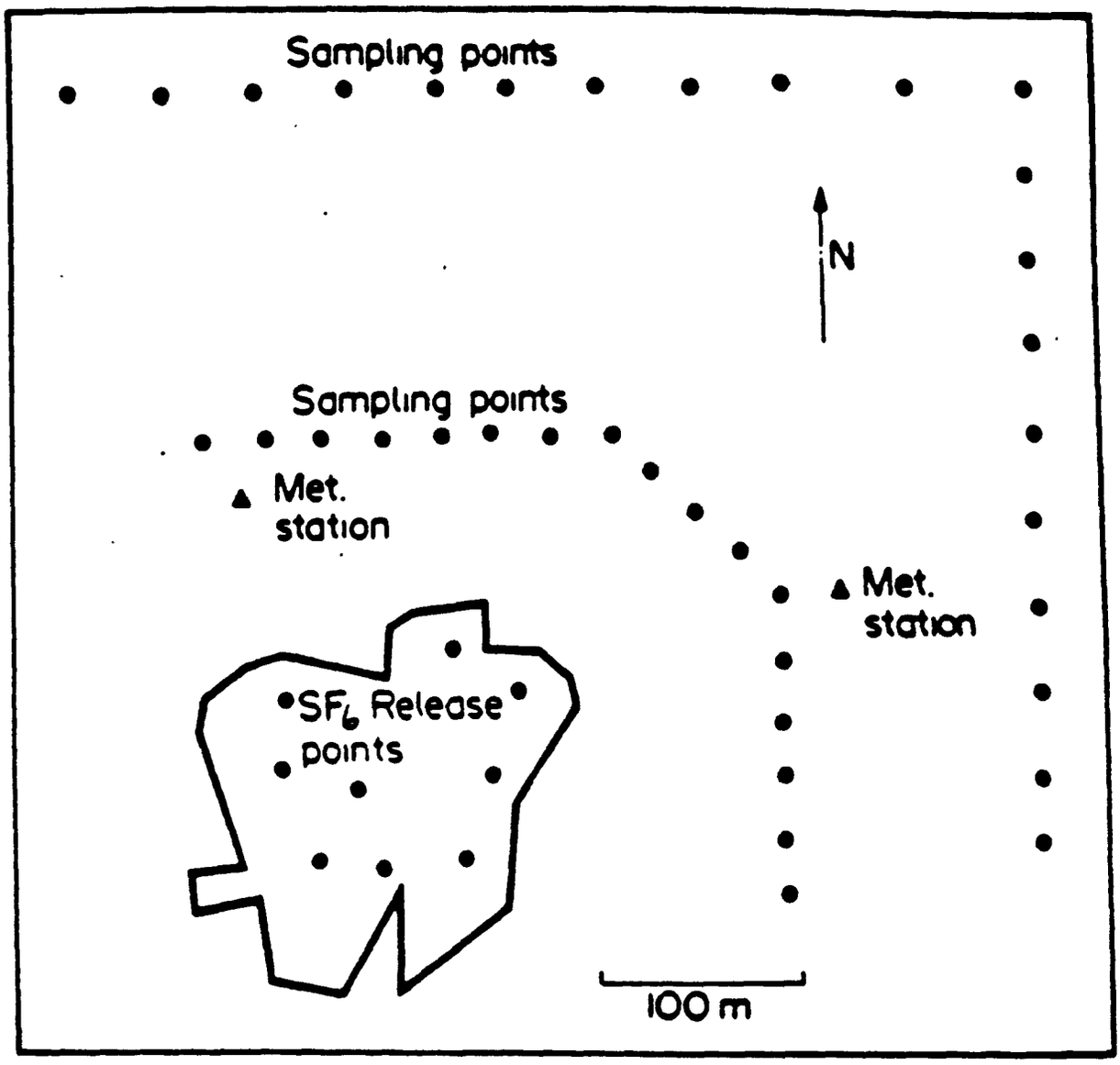

FIGURE 4 - 1
ISOPRENE FLUX EXPERIMENT SAMPLING GRID, RELEASE POINTS AND WOODLOT

TABLE 4-1

METEOROLOGICAL AND EMISSION CHARACTERISTICS FOR
TRACER RELEASE EXPERIMENTS IN A FOREST CANOPY

Test Number	Tracer Emission Rate (g/s)	Wind Speed (m/s)	Atmospheric Stability Class
1	.102	1.0	D
2	.074	3.6	D
3	.104	5.8	D
4	.084	6.2	D
5	.081	2.2	B
6	.089	8.5	D
7	.094	1.5	D
8	.097	1.1	C
9	.095	1.3	C
10	.093	1.6	C
11	.092	1.8	C
12	.113	2.2	D
13	.112	3.2	D

While these forest-canopy experiments represent a useful database for testing area source models, the experimental configuration introduces a number of complicating factors. The simple modeling scenario assumes that tracer emissions will become thoroughly mixed within the canopy and evolve out of the top of the source region. The following items contribute to the uncertainties involved in modeling these experiments:

- Dispersion within the canopy is probably incomplete, and emissions will not occur uniformly across the source region.
- Thermal stratification may "trap" some of the tracer within the canopy. Emissions to ambient air may persist for several hours after the tracer source is shut off.
- In the trunk space below the canopy, winds may transport some of the tracer material out of the source region.
- Enhanced turbulence is likely in the lee of the source region. The forest grove may produce the equivalent of a "building wake" as ambient air moves over and around this obstacle.

The effects of these complicating factors are difficult to quantify. Some will tend to increase observed tracer concentrations, others to lower concentrations. The modeling approach does not account for any of these factors. The source is modeled as four adjacent area source squares, each 61 x 61 m, comprising a total area of 1.5 hectares. The source emission height was chosen as 8 m, the average canopy height.

4.2 Results

Predicted and observed tracer concentrations were compared for each tracer experiment. Statistics were computed both for event-by-event comparisons (paired in time) and for measures based on unpaired comparisons. Observed and predicted concentrations were divided by the tracer emission rate before computing statistics.

4.2.1 Unpaired Comparisons

The maximum observed and predicted normalized concentration values are illustrated in Figure 4-2. Each vertical bar spans the range of the thirteen maximum values. All five of the short-term models overpredict the observed range of maximum values. The highest observed maximum value (over all tests) is 1.5 x 10^{-4} s/m^3, while maximum predicted values range from 2.4 x 10^{-4} s/m^3 by FDM up to 7.3 x 10^{-4} s/m^3 by RAM.

The range of maximum values predicted by FDM and SHORTZ overlaps considerably with the range of observed values. The lowest 8 or 9 maximum values predicted by these models fall in the same range as the top 10 observed maxima. By contrast, most of the maximum values predicted by ISC, PAL and RAM exceed the highest observed value. Overall, the maximum values predicted by FDM are higher than the maximum observed values by roughly a factor of 1.6, SHORTZ overpredicts by a factor of 2, and the remaining models by a factor of 4 to 5.

4.2.2 Paired Comparisons

The maximum observed and predicted normalized concentration values for each experiment are summarized in Table 4-2. The bias toward overprediction illustrated in Figure 4-2 is again evident in Table 4-2. Lack of correlation is also apparent, as events with peak predicted values do not coincide with high observed values. For example, Test 1 has the highest predicted value for all five models, but has the second-lowest observed maximum value. Correlation coefficients for observed and predicted maximum values are negative for all five models. (By contrast, the correlation between maximum values predicted by any two models exceeds 0.95. Inter-model correlation results from the use of the same meteorological inputs for all of the models.) The relative differences between maximum observed and predicted

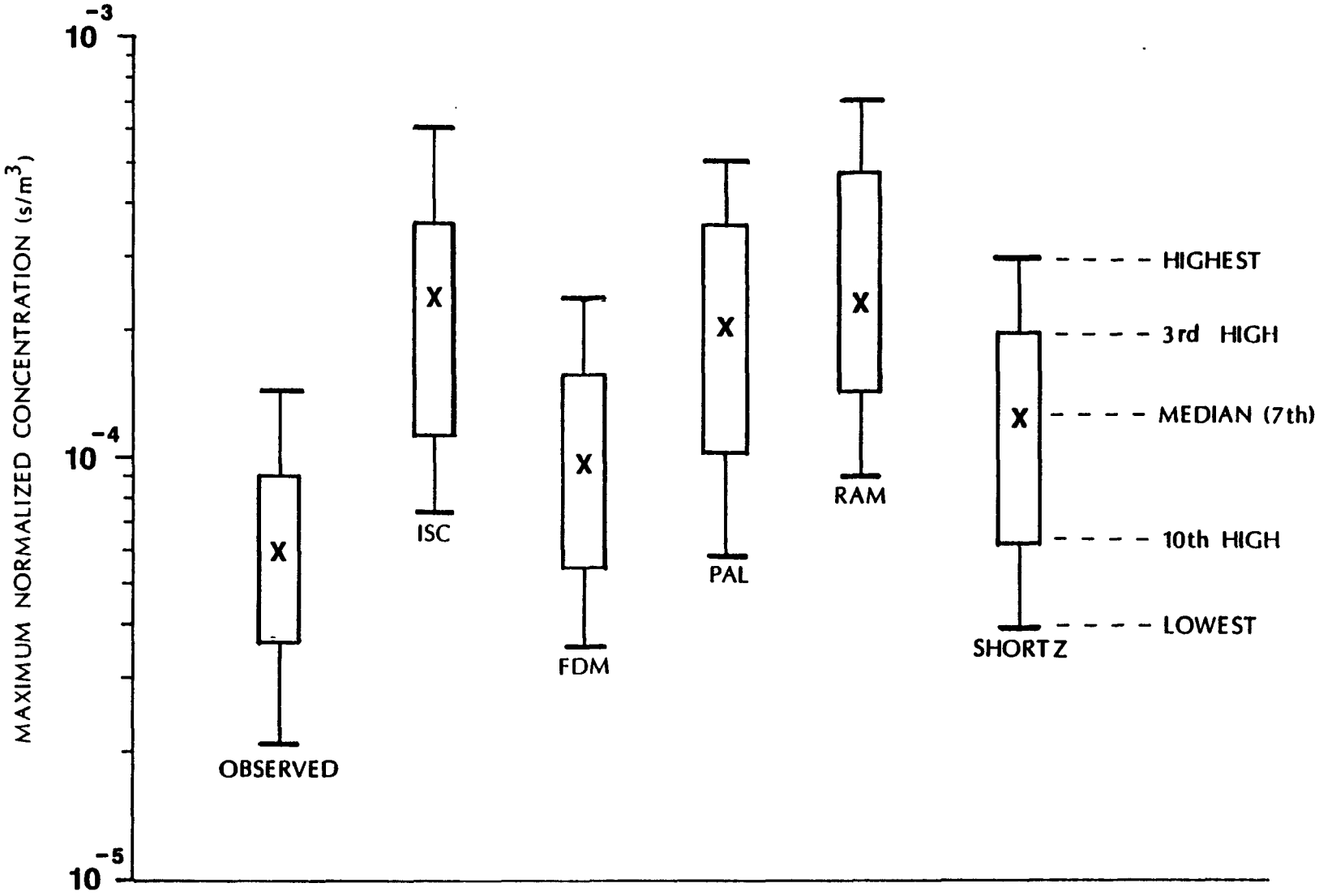

FIGURE 4-2. RANGE OF MAXIMUM PREDICTED AND OBSERVED CONCENTRATIONS FOR TRACER RELEASE EXPERIMENTS

TABLE 4-2

MAXIMUM OBSERVED AND PREDICTED NORMALIZED
TRACER CONCENTRATION FOR EXPERIMENT

Test Number	Observed Concentration (10^{-6} s/m^3)	ISC	FDM	PAL	RAM	SHORTZ
1	24.5	602.**	242.**	500.**	726.**	314.**
2	87.8	174.	88.	149.	232.	101.
3	33.7	101.	55.	89.	139.	64.
4	74.6	101.	53.	88.	135.	60.
5	88.5	109.	50.	102.	120.	38.
6	58.5	71.	36.	57.	91.	42.
7	67.1	394.	168.	343.	472.	213.
8	21.7	361.	153.	343.	432.	194.
9	37.0	302.	133.	287.	360.	158.
10	99.8	249.	113.	234.	258.	142.
11	151.9*	331.	101.	208.	228.	126.
12	45.9	246.	109.	220.	299.	140.
13	42.8	181.	81.	157.	209.	102.

* Maximum observed value
** Maximum predicted value

values for each event are summarized in Table 4-3. For FDM, predicted maximum values agreed within a factor of 2 with maximum observed values for eight of the 13 experiments. All five models overpredicted by more than a factor of 1.25 for the majority of events.

While maximum predicted values are closely tied to meteorological conditions, observed maximum values do not show a similar pattern. The highest observed values occurred for tests 10 and 11 (C stability, low wind speed), but tests 8 and 9 with similar meteorology have low observed maximum values. Three experiments with D stability and low wind speeds (tests 1, 7 and 12) have high predicted concentrations but relatively low observed values. The Turner stability method (based on wind speed and cloud cover) does not provide an effective method of classifying the observed dispersion behavior for these experiments.

Summary - Comparisons of observed and predicted maximum concentrations for the 13 one-hour experiments demonstrate systematic overprediction by all five short-term models. FDM showed the least bias, overpredicting by roughly a factor of 1.6. Maximum values predicted by FDM were within a factor of 2 of the observed maximum for 8 of 13 events. The range of maximum predicted by SHORTZ was about a factor of 2 higher than observed; predicted and observed maxima agreed within a factor of 2 for 6 events for SHORTZ. ISC, PAL and RAM all overpredicted the range of maximum values by more than a factor of 4. For these three models, predicted and observed values agreed within a factor of 2 for 4 or 5 events. RAM overpredicted by more than a factor of 1.25 for all 13 events. Paired comparisons showed negative correlation between observed and predicted maximum values for all models.

TABLE 4-3

SUMMARY OF RELATIVE DIFFERENCES BETWEEN
OBSERVED AND PREDICTED MAXIMUM VALUES

Ratio (R) of Predicted to Observed Maximum Concentration	ISC	FDM	PAL	RAM	SHORTZ
$R > 2$	9	5	8	9	6
$2 \geq R > 1.25$	2	2	2	4	2
$1.25 \geq R > 0.8$	2	2	3	-	3
$0.8 \geq R > 0.5$	-	4	-	-	1
$0.5 \geq R$	-	-	-	-	1

5.0 CONCLUSIONS AND RECOMMENDATIONS

5.1 Conclusions

A number of existing dispersion models are available for estimating ambient concentrations due to area source emissions from landfills, waste disposal areas and contaminated sites. Three basic methods of calculating concentrations due to area sources are employed by existing models: virtual point source, line source, and upwind (numerical) integration. A group of five short-term models (FDM, ISCST, PAL, RAM, SHORTZ) and three long-term (sector average) models (ISCLT, CDM, VALLEY) incorporating these methods were selected for evaluation in the present study.

None of these dispersion models incorporates a source algorithm capable of estimating evaporative emission rates from a landfill or waste disposal area. For many applications, the variation of emissions as a function of environmental factors (ambient or ground surface temperature, wind speed, moisture) is a major source of uncertainty for determining ambient concentrations.

Example Applications. Each of the eight models was applied to predict ambient concentrations for a base case hypothetical scenario and for several variations designed to examine whether model predictions are consistent with mathematical and physical principles.

The base case represented a single 150 x 150 m ground level area source, with receptors located downwind at distances ranging from 100 m to 1,575 m from the source center. Among the short-term models, FDM generally predicted the lowest concentrations. The other four models' predictions varied in rank, depending upon distance and stability class. At large distances, RAM consistently predicted the highest concentrations.

All of the models except RAM showed reasonable far-field behavior. PAL predictions were physically reasonable and consistent with source-receptor

geometry for all of the configurations analyzed. FDM produced small inconsistencies (generally 10 percent or less) for two tests sensitive to source geometry. Predictions by SHORTZ and ISCST in the near-field did not accurately reflect source-receptor geometry for one or more comparisons. RAM did not give physically reasonable results for either near-field or far-field predictions.

None of the three long-term average models consistently gave reasonable results. Comparisons of predictions for different scenarios indicated inaccuracies of 10 percent or more in calculated concentrations. Serious deficiencies in VALLEY were indicated by several tests. ISCLT and CDM gave reasonable results for most comparisons. ISCLT, however, predicted large differences for the subdivision comparison, while CDM gave erratic results for the far-field convergence test.

Comparison with Observed Concentrations. Observed and predicted concentrations were compared for a data base of thirteen one-hour experiments involving tracer releases within an isolated grove of trees. The release was modeled as a 1.5 ha area source. All five of the short-term models predicted higher maximum tracer concentrations than were measured roughly 100 m downwind of the source region. FDM and SHORTZ overpredicted by a factor of 2 or less, while ISCST, PAL and RAM overpredicted by roughly a factor of 4. All of the models showed poor correlation between observed and predicted maximum values, paired by event.

Recommendations. Overall, the short-term models which employ algorithms based on the line-source method (FDM, PAL) appear to provide an adequate treatment of near-source geometry and reasonable far-field behavior. Subject to further performance testing, either FDM or PAL is recommended for use with near-ground area sources. (The area source algorithm in FDM is not a separate modular component of the model. This algorithm is coupled to line source and

dispersion algorithms taken from CALINE, which uses a modified form of the Pasquill-Gifford rural dispersion coefficients.) It may also prove feasible to modify either SHORTZ or ISCST to provide more reasonable near-field predictions. The RAM model is not recommended for application to an isolated area source.

In light of the widespread use of ISCST for regulatory applications, the feasibility of modifying or replacing the ISC area source algorithm deserves serious consideration. The inaccuracy of near-field area source predictions by ISCST is sufficiently large that the users guide recommends subdividing the source if receptors are placed near that source. In the present study, results have clearly demonstrated that ISCST does not account properly for source-receptor geometry at near-field receptors.

The long-term average results indicated that ISCLT and CDM generally provide adequate treatment of area source dispersion, but each model has specific shortcomings. Subject to further testing, either ISCLT or CDM is recommended. The FDM, LONGZ and AQDM models contain area source algorithms similar to ISCLT and are expected to produce similar predictions. Potential modifications to correct specific model shortcomings should be investigated. The VALLEY model is not recommended for application to area sources.

REFERENCES

Allwine, G., Lamb, B. and Westberg, H., Application of Atmospheric Tracer Techniques for Determining Biogenic Hydrocarbon Fluxes from an Oak Forest, The Forest - Atmosphere Interaction, Ed. Hutchison, B.A. and Hicks, B.B., D. Reidel Publishing Company, Boston, 1985.

Benson, P.E., CALINE3 - A Versatile Dispersion Model for Predicting Air Pollutant Levels Near Highways and Arterial Streets, PB80-220841, November 1979.

Bjorklund, J.R. and Bowers, J.F., User's Instructions for the SHORTZ and LONGZ Computer Programs, Volumes I and II, EPA-903/9-82-004a and 004b, March 1982.

Burt, E.W., Valley Model User's Guide, EPA-450/2-77-018, September 1977.

Gschwandtner, G., Eldridge, K. and Zerbonia, R., "Sensitivity Analysis of Dispersion Models for Point and Area Sources," JAPCA, Vol. 32, #10, October 1982.

Guideline on Air Quality Models (Revised), EPA-450/2-78-027R, July 1986.

Hodanbosi, R.F. and Peters, L.K., "Evaluation of RAM Model for Cleveland, Ohio," JAPCA, Vol. 31, #3, March 1981.

Hwang, S.T., "Methods for Estimating On-Site Ambient Air Concentrations at Disposal Sites," Nuclear and Chemical Waste Management, Vol. 7, 1987.

Irwin, J.S. and Brown, T.M., "A Sensitivity Analysis of the Treatment of Area Sources by the Climatological Dispersion Model," JAPCA, Vol. 35, #4, April 1985.

Irwin, J.S., Chico, T. and Catalano, J., CDM 2.0 -- Climatological Dispersion Model, EPA/600/8-85/029, PB86-136546, November 1985.

Rao, K.S., User's Guide for PEM-2: Pollution Episodic Model (Version 2), EPA/600/8-86/040, PB 87-132 098, December 1986.

Schere, K.L. and Demerjian, K.L., User's Guide for the Photochemical Box Model (PBM), PB85-137164, November 1984.

Schulze, R., Practical Guide to Atmospheric Dispersion Modeling, Trinity Consultants, Inc., Dallas, 1989.

Schulze, R.H., Ed., "All Area Source Models Are Not Created Equal," Atmospheric Diffusion Notes, Trinity Consultants, Inc., Issue #7, July 1982.

Scire, J.S., Lurmann, F.W., Bass, A. and Hanna, S.R., User's Guide to the Mesopuff II Model and Related Processor Programs, EPA-600/8-84-013, April 1984.

Simmon, P.B., Patterson, R.M., Ludwig, F.L. and Jones, L.B., User's Manual for the APRAC-3/Mobilel Emissions and Diffusion Modeling Package, EPA/909-9-81-002, July 1981.

Turner, D.B., Workbook of Atmospheric Dispersion Estimates, EPA Office of Air Programs, Pub. # AP-26, 1970.

Turner, D.B. and Novak, J.H., User's Guide for RAM, Vol. 1, Algorithm Description and Use, EPA-600/8-78-016A, November 1978.

Wackter, D.J. and Foster, J.A., Industrial Source Complex (ISC) Dispersion Model User's Guide - Second Edition (Revised), Vol. 1, EPA-450/4-88-002a, December 1987.

TECHNICAL REPORT DATA *(Please read Instructions on the reverse before completing)*		
1. REPORT NO. EPA-450/4-89-020	2.	3. RECIPIENT'S ACCESSION NO.
4. TITLE AND SUBTITLE Review and Evaluation of Area Source Dispersion Algorithms for Emission Sources at Superfund Sites		5. REPORT DATE November 1989 6. PERFORMING ORGANIZATION CODE
7. AUTHOR(S)		8. PERFORMING ORGANIZATION REPORT NO.
9. PERFORMING ORGANIZATION NAME AND ADDRESS TRC Environmental Consultants, Inc. 800 Connecticut Boulevard East Hartford, CT 06108		10. PROGRAM ELEMENT NO. 11. CONTRACT/GRANT NO. 68-02-4399
12. SPONSORING AGENCY NAME AND ADDRESS U.S. Environmental Protection Agency Office of Air Quality Planning and Standards Research Triangle Park, N. C. 27711		13. TYPE OF REPORT AND PERIOD COVERED Final Report 14. SPONSORING AGENCY CODE
15. SUPPLEMENTARY NOTES EPA Project Officer: Jawad S. Touma		

16. ABSTRACT

This report examines air quality dispersion modeling algorithms and related technical issues associated with estimating ambient concentrations from area sources at Superfund sites. The report describes the area source emission characteristics associated with Superfund sites and provides a review of existing, available techniques for modeling area sources. It also describes the results of applying five short-term and three long-term area source models to a number of example applications and one field data base in order to compare the magnitude of concentration predictions and test whether concentration estimates are consistent with mathematical and physical principles. The report provides conclusions and recommendations from this study.

17. KEY WORDS AND DOCUMENT ANALYSIS

a. DESCRIPTORS	b. IDENTIFIERS/OPEN ENDED TERMS	c. COSATI Field/Group
Air Pollution Hazardous Waste Assessment Toxic Air Pollutants Air Quality Dispersion Models	Dispersion Modeling Meteorology Air Pollution Control	13 B

18. DISTRIBUTION STATEMENT	19. SECURITY CLASS *(This Report)*	21. NO OF PAGES
Release Unlimited	Unclassified	120
	20. SECURITY CLASS *(This page)*	22. PRICE
	Unclassified	

July 1991

ERRATA FOR

REVIEW AND EVALUATION OF AREA SOURCE DISPERSION ALGORITHMS

FOR EMISSION SOURCES AT SUPERFUND SITES

Office of Air Quality Planning and Standards
Technical Support Division
Research Triangle Park, NC 27711

LIST OF ERRATA

REVIEW AND EVALUATION OF AREA SOURCE DISPERSION ALGORITHMS FOR EMISSION SOURCES AT SUPERFUND SITES
EPA-450/4-89-020
NOVEMBER, 1989

NTIS ACCESSION NO. PB90-142753

The following pages are replaced:

1. Page ix
2. Page 2-22
3. Page 4-1
4. Page 4-4
5. Pages 4-6 through 4-10
6. Page 5-2
7. Page R-1

LIST OF TABLES

TABLE		PAGE
1-1	AREA SOURCE CHARACTERISTICS	1-4
2-1	CHARACTERIZATION OF AREA SOURCE ALGORITHMS IN EXISTING MODELS	2-8
3-1	SUMMARY OF SENSITIVITY TEST RESULTS FOR SHORT-TERM MODELS	3-21
4-1	METEOROLOGICAL AND EMISSION CHARACTERISTICS FOR TRACER RELEASE EXPERIMENTS IN A FOREST CANOPY	4-4
4-2	MAXIMUM OBSERVED AND PREDICTED NORMALIZED TRACER CONCENTRATION FOR EXPERIMENT	4-8
4-3	SUMMARY OF RELATIVE DIFFERENCES BETWEEN OBSERVED AND PREDICTED MAXIMUM VALUES	4-9

sources. Two published articles were identified which discussed alternative approaches to modeling area sources. Neither approach represents a computer algorithm suitable for evaluation in the present study.

The models suggested by Hwang (1987) and Chitgopekar et al. (1990) attempt to resolve some of the known shortcomings of the currently utilized area source dispersion algorithms. The discussion by Hwang is theoretical but examines both a Gaussian approach and one based on transport equations in the atmospheric boundary layer. Chitgopekar et al. (1990) attempts to resolve problems of near-field prediction through the use of a "top-hat" formulation.

Chitgopekar et al. (1990) presents an area source model developed in response to problems with virtual point models in the near-field for area sources. These authors state that "the most rigorous" treatment of Gaussian dispersion from area sources would be to model them as a dense matrix of multiple point sources. This idea can be conceptualized as increasing matrix density until, in the limit, inter-point spacing goes to zero and every point in the area is emitting. This approach is computationally intensive and is rarely used in the standard models. (The finite line segment approach in FDM or PAL is mathematically equivalent but far more efficient, if Gaussian dispersion is assumed.) Virtual point source methods do not require extensive computations and can be simplified to allow manual calculation. However, the virtual point source method should not be used if the source width is greater than 40% of the distance between the source centerpoint and the receptor (Hwang, 1986 as cited in Chitgopekar et al., 1990). This is a serious limitation due to the fact that the region of interest in many area source pollutant dispersion and exposure situations is in the near-field.

The treatment by Chitgopekar et al. is to divide the dispersion of the plume into high frequency and low frequency components. A low pass filter is used so plume meander is included but small turbulent scales are not. The

4.0 COMPARISON OF MODEL PREDICTIONS WITH EXPERIMENTAL DATA

Predictions for the short-term area source models have been compared to measured concentrations for an experimental data set involving releases of an inert gaseous tracer within an isolated stand of trees, surrounded by open grassland. These experiments produced a distributed emission source which can be simulated as an area source. Comparisons of observed and predicted concentrations for this small set of experiments provide an informative test of model performance.

4.1 Database Description

A review of available information from field measurement programs characterizing observed concentrations in the vicinity of area source releases was recently carried out as part of a larger effort to identify and acquire databases for the evaluation of air toxics models. The criteria which were used to select databases for model evaluation included the following:

- Reliable emissions data
- Site-specific meteorological measurements
- Adequate spatial resolution of ambient concentrations

No suitable databases representing actual sources of toxic pollutant emissions were identified. In general, measurement programs for actual sources are characterized by uncertain emissions estimates and poor spatial resolution (concentration measurements at only two or three locations).

The five databases chosen for air toxics model evaluation all represent measurement programs with controlled, artificial releases designed to simulate actual pollutant releases. Four of these databases involve dense gas (heavier-than-air) releases and are not suitable for the present study.

TABLE 4-1

METEOROLOGICAL AND EMISSION CHARACTERISTICS FOR
TRACER RELEASE EXPERIMENTS IN A FOREST CANOPY

Test Number	Tracer Emission Rate (g/s)	Wind Speed (m/s)	Atmospheric Stability Class
1	.102	1.0	B
2	.074	3.6	D
3	.104	5.8	D
4	.084	6.2	D
5	.081	2.2	B
6	.089	8.5	D
7	.094	1.5	B
8	.097	1.1	B
9	.095	1.3	B
10	.093	1.6	B
11	.092	1.8	B
12	.113	2.2	C
13	.112	3.2	D

4.2.1 Unpaired Comparisons

The maximum observed and predicted normalized concentration values are illustrated in Figure 4-2. Each vertical bar spans the range of the thirteen maximum values. Four of the five models overpredict the maximum observed value and all five models overpredict the minimum observed value. The highest observed maximum value (over all tests) is 1.5 x 10^{-4} s/m^3, while maximum predicted values range from 1.2 x 10^{-4} s/m^3 by FDM up to 3.2 x 10^{-4} s/m^3 by RAM.

The range of maximum values predicted by FDM is within the range of observed values. The lowest 12 maximum values predicted by SHORTZ fall in the same range as the top 10 observed maxima. By contrast, most of the maximum values predicted by ISC, PAL and RAM exceed the highest observed value. The median value predicted by FDM is higher than the maximum observed median by roughly a factor of 1.3, SHORTZ overpredicts by a factor of 1.7, and the remaining models by factors of between 2.7 and 3.2.

4.2.2 Paired Comparisons

The maximum observed and predicted normalized concentration values for each experiment are summarized in Table 4-2. The bias toward overprediction illustrated in Figure 4-2 is again evident in Table 4-2. Lack of correlation is also apparent, as events with peak predicted values do not coincide with high observed values. For example, Test 1 has the highest predicted value for all five models, but has the second-lowest observed maximum value. Correlation coefficients for observed and predicted maximum values are negative for all five models. The relative differences between maximum observed and predicted values for each event are summarized in Table 4-3. For FDM, predicted maximum values agreed within a factor of 2 with maximum

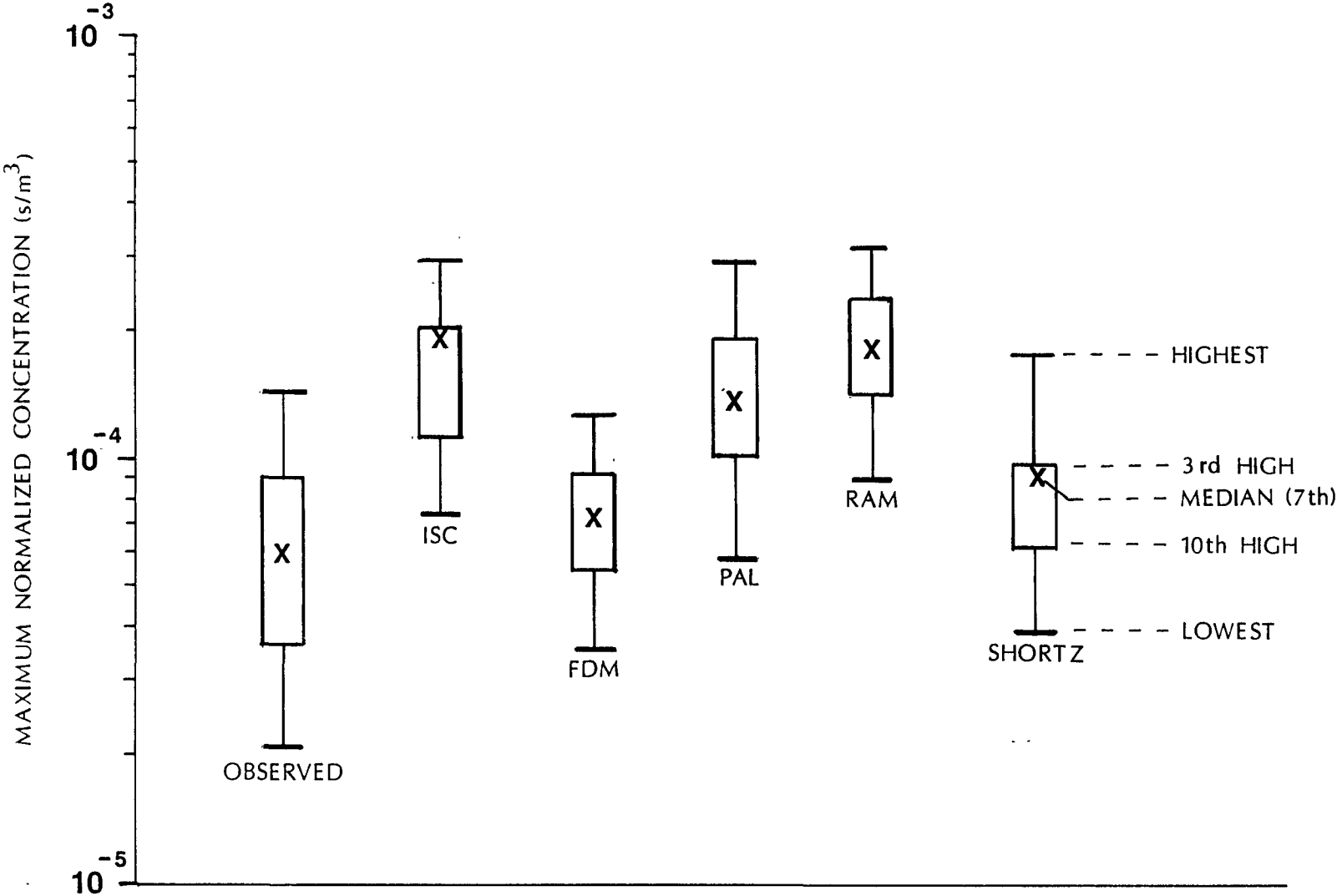

Figure 4-2. RANGE OF MAXIMUM PREDICTED AND OBSERVED CONCENTRATIONS FOR TRACER RELEASE EXPERIMENTS.

TABLE 4-2

MAXIMUM OBSERVED AND PREDICTED NORMALIZED
TRACER CONCENTRATION FOR EXPERIMENT

Test Number	Observed Concentration (10^{-6} s/m^3)	ISC	FDM	PAL	RAM	SHORTZ
1	24.5	292.	123.	295.	322.	163.
2	87.8	174.	88.	149.	232.	101.
3	33.7	101.	55.	89.	139.	64.
4	74.6	101.	53.	88.	135.	60.
5	88.5	109.	50.	102.	120.	38.
6	58.5	71.	36.	57.	91.	42.
7	67.1	172.	76.	169.	206.	98.
8	21.7	227.	94.	222.	304.	125.
9	37.0	190.	82.	186.	253.	103.
10	99.8	162.	70.	159.	182.	97.
11	151.9	143.	63.	140.	160.	86.
12	45.9	180.	81.	191.	187.	104.
13	42.8	181.	81.	157.	209.	102.
# Closest to Observed		0	8	3	1	1
# Closest to Observed and Greater		1	8	3	1	0

TABLE 4-3

SUMMARY OF RELATIVE DIFFERENCES BETWEEN
OBSERVED AND PREDICTED MAXIMUM VALUES

Ratio (R) of Predicted to Observed Maximum Concentration	ISC	FDM	PAL	RAM	SHORTZ
$R > 2$	7	3	7	8	5
$2 \geq R > 1.25$	3	4	2	4	2
$1.25 \geq R > 0.8$	3	1	4	1	2
$0.8 \geq R > 0.5$	-	4	-	-	3
$0.5 \geq R$	-	1	-	-	1

observed values for 9 of the 13 experiments. Three models overpredicted by more than a factor of 2.0 for the majority of events.

While maximum predicted values are closely tied to meteorological conditions, observed maximum values do not show a similar pattern. The highest observed values occurred for tests 10 and 11 (B stability, low wind speed), but tests 8 and 9 with similar meteorology have low observed maximum values. The Turner stability method (based on wind speed and cloud cover) does not provide an effective method of classifying the observed dispersion behavior for these experiments.

Summary - Comparisons of observed and predicted maximum concentrations for the 13 one-hour experiments demonstrate a general tendency towards systematic overprediction by all five short-term models. FDM showed the least bias, overpredicting the median maximum value by roughly a factor of 1.3. Maximum values predicted by FDM were within a factor of 2 of the observed maximum for 9 of 13 events. The median maximum predicted by SHORTZ was a factor of 1.7 higher than observed; predicted and observed maxima agreed within a factor of 2 for 7 events for SHORTZ. ISC, PAL and RAM all overpredicted the median maximum value by approximately a factor of 3. For these three models, predicted and observed values agreed within a factor of 2 for 5 or 6 events. RAM overpredicted for all 13 events.

geometry for all of the configurations analyzed. FDM produced small inconsistencies (generally 10 percent or less) for two tests sensitive to source geometry. Predictions by SHORTZ and ISCST in the near-field did not accurately reflect source-receptor geometry for one or more comparisons. RAM did not give physically reasonable results for either near-field or far-field predictions.

None of the three long-term average models consistently gave reasonable results. Comparisons of predictions for different scenarios indicated inaccuracies of 10 percent or more in calculated concentrations. Serious deficiencies in VALLEY were indicated by several tests. ISCLT and CDM gave reasonable results for most comparisons. ISCLT, however, predicted large differences for the subdivision comparison, while CDM gave erratic results for the far-field convergence test.

Comparison with Observed Concentrations. Observed and predicted concentrations were compared for a data base of thirteen one-hour experiments involving tracer releases within an isolated grove of trees. The release was modeled as a 1.5 ha area source. All five of the short-term models tend to predict higher maximum tracer concentrations than were measured roughly 100 m downwind of the source region (Table 4-2). FDM and SHORTZ overpredicted by a factor of 2 less than half of the test cases, while ISCST, PAL and RAM overpredicted more than half of the cases by a factor of 2 or more. All of the models showed poor correlation between observed and predicted maximum values, paired by event.

Recommendations. Overall, the short-term models which employ algorithms based on the line-source method (FDM, PAL) appear to provide an adequate treatment of near-source geometry and reasonable far-field behavior. Subject to further performance testing, either FDM or PAL is recommended for use with near-ground area sources. (The area source algorithm in FDM is not a separate modular component of the model. This algorithm is coupled to line source and

REFERENCES

Allwine, G., Lamb, B. and Westberg, H., Application of Atmospheric Tracer Techniques for Determining Biogenic Hydrocarbon Fluxes from an Oak Forest, The Forest - Atmosphere Interaction, Ed. Hutchison, B.A. and Hicks, B.B., D. Reidel Publishing Company, Boston, 1985.

Benson, P.E., CALINE3 - A Versatile Dispersion Model for Predicting Air Pollutant Levels Near Highways and Arterial Streets, PB80-220841, November 1979.

Bjorklund, J.R. and Bowers, J.F., User's Instructions for the SHORTZ and LONGZ Computer Programs, Volumes I and II, EPA-903/9-82-004a and 004b, March 1982.

Burt, E.W., Valley Model User's Guide, EPA-450/2-77-018, September 1977.

Chitgopekar, N.P., D.D. Reible and L.J. Thibodeaux, "Modeling Short Range Air Dispersion from Area Sources of Non-Buoyant Toxics", AWMA, August 1990, Vol. 40, #8.

Gschwandtner, G., Eldridge, K. and Zerbonia, R., "Sensitivity Analysis of Dispersion Models for Point and Area Sources," JAPCA, Vol. 32, #10, October 1982.

Guideline on Air Quality Models (Revised), EPA-450/2-78-027R, July 1986.

Hodanbosi, R.F. and Peters, L.K., "Evaluation of RAM Model for Cleveland, Ohio," JAPCA, Vol. 31, #3, March 1981.

Hwang, S.T., "Methods for Estimating On-Site Ambient Air Concentrations at Disposal Sites," Nuclear and Chemical Waste Management, Vol. 7, 1987.

Irwin, J.S. and Brown, T.M., "A Sensitivity Analysis of the Treatment of Area Sources by the Climatological Dispersion Model," JAPCA, Vol. 35, #4, April 1985.

Irwin, J.S., Chico, T. and Catalano, J., CDM 2.0 -- Climatological Dispersion Model, EPA/600/8-85/029, PB86-136546, November 1985.

Rao, K.S., User's Guide for PEM-2: Pollution Episodic Model (Version 2), EPA/600/8-86/040, PB 87-132 098, December 1986.

Schere, K.L. and Demerjian, K.L., User's Guide for the Photochemical Box Model (PBM), PB85-137164, November 1984.

Schulze, R., Practical Guide to Atmospheric Dispersion Modeling, Trinity Consultants, Inc., Dallas, 1989.

Schulze, R.H., Ed., "All Area Source Models Are Not Created Equal," Atmospheric Diffusion Notes, Trinity Consultants, Inc., Issue #7, July 1982.

Scire, J.S., Lurmann, F.W., Bass, A. and Hanna, S.R., User's Guide to the Mesopuff II Model and Related Processor Programs, EPA-600/8-84-013, April 1984.